EFFECT OF POLYMERS ON PHYSICAL AND KINETIC PROPERTIES OF GLUTAMATE DEHYDROGENASE FROM BOVINE LIVER

By

JAMES RICHARD APPLEMAN

Bachelor of Science

Oklahoma State University

Stillwater, Oklahoma

1978

Submitted to the Faculty of the Graduate College
of the Oklahoma State University
in partial fulfillment of the requirements
for the Degree of
DOCTOR OF PHILOSOPHY
July, 1983

EFFECT OF POLYMERS ON PHYSICAL AND KINETIC PROPERTIES OF GLUTAMATE DEHYDROGENASE FROM BOVINE LIVER

Thesis Approved

H. Olin Apsimon
Thesis Adviser

Andrew Mont

Richard C. Essenberg

Franklin R. Leach

Bruce J. Anderson

Norman N. Durham
Dean of the Graduate College

PREFACE

This study is concerned with the effects of polymers on several properties of the enzyme glutamate dehydrogenase. These properties include solubility, self-association, and regulation of the enzyme's activity by GDP. The primary objective of this study is to evaluate an excluded volume mechanism for the general action of polymers on proteins.

I wish to express my appreciation to my major thesis adviser, Dr. H. Olin Spivey, for both his professional guidance thoughout my graduate and undergraduate tenures at OSU and for my enjoyment of our professional and private relationship. I also wish to thank my other committee members, Dr. Richard Essenberg, Dr. Franklin Leach, and Dr. Chang-An Yu for their assistance during my graduate career. I am especially grateful to my final committee member, Dr. Bruce Ackerson, for making both his expertise and his laboratory facilities available to me without which the dynamic light scattering measurements reported in this thesis would not have been possible.

I also wish to thank Dr. Chuck Gardner, Dr. Jerry Merz, and Dr. Eric Manley for their wise counsel over the years, as well as Julie Ahern, Julja Burchard, and John Chmielesky for their technical assistance.

Finally, special gratitude is expressed to my wife, Evelyn, for her support, understanding, and encouragement, and to my son, Jeremy, just for being here.

TABLE OF CONTENTS

LIST OF TABLES

LIST OF FIGURES

NOMENCLATURE

AspAT	Aspartate aminotransaminase
ATP	Adenosine triphosphate
BSA	Bovine serum albumin
CS	Citrate synthase
D	Diffusion coefficient
EDTA	Ethylenediamine tetraacetate
E_i	GDH polymeric species consisting of i monomeric units
f	Frictional coefficient
G	Standard state free energy
$G(\Gamma)$	Distribution function of decay rates
$g(\tau)$	Autocorrelation function
G6PD	Glucose-6-phosphate dehydrogenase
GDH	Glutamate dehydrogenase
GDP	Guanosine diphosphate
GTP	Guanosine triphosphate
HSA	Human serum albumin
K	Equilibrium constant
k	Huggins coefficient
KP_i	Potassium phosphate
MDH	Malate dehydrogenase
MOPS	2-(N-morpholino)propane-sulfonic acid
n	Refractive index
NADH	Nicotinamide adenine dinucleotide, reduced form

P	Destructive interference factor in light scattering
PEG	Polyethylene glycol
PFK	Phosphofructokinase
PP	Parallelopiped
q	Light scattering vector
R_e	Radius of equivalent sphere
R_θ	Rayleigh's ratio
S	Solubility
s	Sedimentation coefficient
T	Temperature (degrees Kelvin)
$\overline{v}$	Partial specific volume
β	Constant reflecting the interaction of PEG with a protein
γ	Activity coefficient
Γ	With respect to excluded volume theory, a constant relecting solution nonideality With repect to quasielastic light scattering, the exponential decay constant
η	Viscosity
$[\eta]$	Intrinsic viscosity
θ	Angle of observation
λ	Wavelength of incident light
μ	Chemical potential
ξ	Ratio of major to minor axis
ρ	Density
τ	Autocorrelation time

CHAPTER I

INTRODUCTION

The concentrations of individual enzymes in both the mitochodrial matrix and cellular cytosol are 100 to 10,000 times greater in vivo than the concentrations normally used for in vitro enzyme kinetic studies (normally < 1 μg/ml) (1). These high individual enzyme concentrations promote enzyme associations by conventional "mass action" effects. Also, the total cellular concentration of proteins, nucleic acids, and other macromolecules is sufficiently great that a significant fraction of the intracellular volume is occupied by these biological polymers (1,2). This macromolecular crowding produces an excluded volume effect providing tens of kilocalories of excess free energy promoting further association of enzymes as well as transitions to and stabilization of compact macromolecular conformations (2) as discussed in more detail below. For this reason we chose to examine the effects of both physiological (BSA, dextrans) and synthetic (polyethylene glycols) polymers on the enzyme glutamate dehydrogenase. GDH was chosen because we thought that, due to its known ability to self-associate (see below), it would be a sensitive indicator of polymer effects. BSA and dextrans were chosen because they represent two different classes (proteins and polysaccharides) of physiological polymers. Polyethylene glycols (PEG's) were used as well as physiological polymers because PEG's offered us several experimental advantages, as described below.

Effects of Association on Enzyme Activity

At cellular concentrations, numerous enzymes self-associate, forming homologous enzyme complexes *in vitro*. In 1971, Frieden listed about 30 such enzymes. With the few of these enzymes studied by kinetic methods, significant catalytic changes have been shown to result from these self-associations. For example, erythrocyte G6PD undergoes a four-fold increase in specific activity upon association (3). As PFK associates, its response to the modifiers ATP and fructose-6-P are considerably altered. Similiarly, bovine liver glutamate dehydrogenase undergoes extensive changes in its regulation by purine nucleotides at cellular concentrations.

Several specific heterocomplexes of proteins are known. Those include PFK with FDPase, aspartate aminotransferase with glutamate dehydrogenase, ornithine aminotransferase with GDH, and malate dehydrogenase with GDH. For these heterologous enzyme complexes, significant catalytic differences were demonstrated when compared to the properties of either enzyme alone. Also, the formation of protein complexes of albumin with α_1-acid glycoprotein, albumin with lysozyme, ovalbumin with lysozyme, and transferrin with lysozyme has also been demonstrated, although possible kinetic consequences of these associations have not been examined. It is clear that both hetero- and homo-associations of enzymes are favored at physiological concentrations of enzymes, and that these associations can produce major changes in the kinetic properties of these enzymes.

Total Concentration of Proteins and Other Polymers *In Vivo*

A second important factor affecting the properties of enzymes *in vivo* is often overlooked. This is the high total polymer (macromolecular) concentration in the environment of an enzyme inside a cell. Among these polymers are other proteins, carbohydrates, and nucleic acids. For example, the matrix in a resting-state mitochondria is estimated to be 56% (w/w) protein (1). This concentration is even higher in a respiring mitochondria, since the volume of this organelle is reduced nearly two-fold (primarily through the removal of water) as it passes from the resting to the respiring state (1). An average protein crystal has approximately 40% of its total weight as water or solvent (4). Some crystals contain more than 90% solvent, while very few contain less than 20% (5). Thus, the matrix proteins are in an environment much more like that found in protein crystals than that in free solution. Although the cytosolic compartment is not as deprived of water as in the mitochondrial matrix, protein concentrations in cytosol are much higher than normally used for studies *in vitro*. Approximately 20% of the total weight of muscle cells is protein; red blood cells, 35%; actively growing cells, 17-26% (6). These concentrations, like those in the mitochondrial matrix, are very close to those found in protein crystals.

Such high total polymer concentrations and low water content are in part the cause of the high individual enzyme concentrations *in vivo* and the resulting mass action effect promoting enzyme associations. However, these high polymer concentrations provide additional factors strongly promoting further enzyme associations and effects on protein

conformations, as discussed next. In fact, these excluded volume and related effects can be much more potent in promoting enzyme associations than the more familiar mass action effects mentioned above.

Effects of Polymers on Proteins

Recently it has been recognized that the "macromolecular crowding" discussed above creates tens of kilocalories of excess free energy promoting enzyme associations as well as transition to and stabilization of compact macromolecular conformations (2). Several studies illustrate that both synthetic and physiological polymers can produce these effects in vitro. Herzog and Weber (7) found that either dextran or the synthetic polymer polyethylene glycol (PEG) could induce the formation of microtubles from tubulin, even in the absence of other proteins normally required for such formation. The same two polymers enhance the rate and extent of fibrin polymerization (8). Other water-soluble polymers known to increase the rate of fibrin polymerization include starch, polyvinyl alcohol, and ficol. PEG enhances the reversible self-association of MDH and CS[1], as well as hetero-association observed between these two enzymes (9). The association of AspAT with MDH in the presence of dextran and trimethylaminopolyethylene glycol or dextran and carboxymethyl-polyethylene glycol was observed in counter-current distribution measurements (10). Allosteric regulation of PFK at a physiological concentration of the enzyme in polyethylene glycol solutions is very similiar to that observed for concentrated solutions of PFK alone (11). This is probably due to enhancement of the

---

[1]Unpublished results, Dr. H. O. Spivey

self-association of the enzyme. Clark and Masters (12) observed complexes between glycolytic enzymes at physiological protein concentrations, whereas DeDuve (13) saw little or no association in dilute solution. PEG is able to induce specific hetero-precipitations between some of the Krebs cycle and related enzymes. These include AspAT with GDH (14), MDH with GDH (14), and MDH with CS (9). These enzymes are all closely related in metabolism, and important regulatory and kinetic consequences have been postulated for the interaction of these enzymes in vivo. Some evidence exists in all of these cases for association in solution phase prior to precipitation of protein by polymer.

Another property of high polymer concentrations is protein stabilization. The relative stability of many soluble enzymes at high protein concentrations as compared to that at low protein concentrations is enormous. Also, many enzymes are stabilized by the addition of even moderate quantities of PEG.

While some of the the polymers used in the above studies were natural cellular polymers (proteins, dextrans, and starch), in most instances synthetic polymers were used. We feel that changes in protein properties observed in vitro using these synthetic polymers are nonetheless likley to occur in vivo. The hetero-associations observed between mitochondrial matrix enzymes in the presence of synthetic polymers are highly specific. For example, the interactions observed by Backman and Johansson (10) between AspAT and MDH occurred only when the AspAT and MDH isozymes were from the same cellular compartment, cytosolic (c-) or mitochondrial (m-). Mixtures of m-AspAT with c-MDH or c-AspAT with m-MDH revealed no interactions. Similiarly, Halper and

Srere (9) demonstrated interactions between m-MDH and CS in PEG, whereas no interactions between CS and c-MDH or CS and any of nine other proteins were observed. The specificity of these polymer induced protein-protein interactions, as well as the fact that the interacting enzymes are adjacent in metabolic pathways, suggests that these associations also occur *in vivo*.

Possible Mechanisms of Polymer Action

The fact that different types of polymers have qualitatively the same associating effects on enzymes suggests that this effect is due to a common feature of polymers. One such common feature is their macromolecular nature; i.e. their large molecular size. The volume occupied by polymers at high concentrations impose limitations on the volume available to an enzyme. Because of this excluded volume, compact protein configurations are energetically favored over more extended ones. This may be the primary reason why polymers stabilize enzymes. If one considers that in most cases enzyme denaturation is nothing more than unfolding of the protein, then stabilizing a compact configuration tends to preserve enzymatic activity. It seems likely that stabilization of previously observed protein conformations, rather than the production of new ones, is to be expected in the majority of cases upon the addition of second polymer. This statement is supported by the results of studies on the effect of PEG's on proteins in solution. For a whole host of proteins, no change in protein secondary structure was observed upon addition of PEG.

The excluded volume effect is also predicted to produce hetero- or homo-associations among proteins. Such association (or the

conformational changes mentioned above) may result in extensive changes in enzyme catalytic properties. Promotion of enzyme associations by polymers may also explain the ability of PEG to precipitate proteins. The mechanism of this precipitation may be through increasing the size of protein aggregates until they become too large to stay in solution. The effects of PEG on proteins is discussed in greater detail in a subsequent secton.

The association and precipitation of proteins by the addition of a second polymer are probably due to the same forces that are involved in phase separation among a whole host of water-soluble polymers. The majority of aqueous-polymer solutions will separate into two aqueous phases upon mixing due to what Albertson (15) has termed "incompatibility" between the polymers. Let us consider two polymers, P1 and P2, that are mutually "incompatible" in solution. Furthermore, let P1 have very favorable solvent interactions so that it remains well solvated, even upon mixing with P2. If P2 also has very favorable polymer-solvent interactions, then aqueous phase separation may result. If the interaction of P2 with solvent is approximately equal to that of P2 with itself, then P2 may self-associate. If the solvation of P2 is poor and is made even poorer upon mixing with P1, then P2 may precipitate.

Let us consider a protein, P2, at a concentration far less than that of a second polymer, P1. Because of the low concentration of the protein it will exert very little effect on P1. However, P1 can have major repulsive effects on the protein. Since P1 is in such great excess, aqueous phase separation is highly unlikely. However, either precipitation of the protein or self-association of the protein tends to

increase the average distance between protein and P1, thus reducing the unfavorable interactions between the two polymers. In this treatment, no statement is made concerning the molecular sources or nature of the incompatibility of the two polymers. These molecular sources could include any of the following: direct repulsive forces, indirect repulsive forces mediated through the solvent, and the excluded volume effects discussed above.

In summary, the mechanisms of polymer effects on proteins are not clear. Excluded volume effects are likely to be extremely large under cellular conditions. Yet available data indicate that specific interactions between the macromolecules and between the macromolecules and water may play an equal or even greater role in some cases. These interactions depend on the chemical nature of the polymers in ways not understood. Therefore further studies are needed to clarify these mechanisms.

General Experimental Strategies

The above facts demonstrate the importance of studying enzymes at or near their cellular concentrations when practical. Enzyme reaction rates are generally proportional to total enzyme concentration, however. Thus, the cellular concentrations of many mitochondrial enzymes are too high for kinetic studies, even with fast kinetic methods. In these cases, addition of other synthetic or natural polymers is desirable to induce the enzyme associations at sufficiently low enzyme concentrations to permit kinetic (or other types of) measurements.

Relationship Between Protein Association and Precipitation by PEG

A major use of PEG by biochemists has been as a protein precipitating agent. This condensation may be considered to be protein association, with the extent of association being very large. The ability of PEG to precipitate proteins is then a consequence of a general mechanism of polymer enhancement of protein associations. I have discussed in this thesis how such associations can have significant consequences on the kinetic properties of enzymes.

Several lines of experimental evidence relate protein associations and precipitability by PEG. Miekka and Ingham (16) examined the correlation between conditions known to enhance the polymerization of certain self-associating proteins, and the solubility of these same proteins in PEG. The proteins studied were α-chymotrypsin, chymotrypsinogen, β-lactoglobulin, and glutamate dehydrogenase. They concluded that for these proteins, conditions which enhanced the extent of association in the absence of PEG also reduced the solubility in PEG. Miekka and Ingham (17) also investigated the relationship between hetero-association and hetero-precipitation by PEG among several of the proteins from human plasma. They concluded that conditions fostering enhanced precipitation of a given mixture also enhanced the formation of soluble hetero-complexes in the absence of the polymer. Conversely, enhanced precipitation was not observed under conditions where heterocomplexes were absent.

Miekka and Ingham (16,17) made two errors in these studies. The first involved the effect of PEG on soluble glutamate dehydrogenase. On the basis of sedimentation velocity measurements they concluded that

PEG-4000 actually inhibited GDH self-association (s = 19.9 S in buffer, s = 9.1 S in 8% PEG) even though the polymer drastically reduced the solubility of the enzyme. However, they failed to correct to standard conditions which, because of the extremely high viscosity of PEG solutions, could change their conclusions. Therefore, the effect of PEG on GDH self-association was uncertain. A second error occured in their interpretation of the effect of PEG on the hetero-protein systems. Here they concluded that PEG did not influence the associations between proteins in solution phase, but merely acted to lower the solubility of pre-existing protein complexes. However, if PEG was added to the hetero-associating system of albumin and lysozyme at a polymer concentration just below that leading to precipitation, then an increase in the size of the soluble protein aggregates was observed. This was the only measurement that they made on the effects of PEG on soluble complexes, and the results from this experiment are in disagreement with their overall conclusions.

Lee and Lee (18) studied the interaction of PEG with proteins by densitometric methods. They concluded that the interactions between the protein and polymer depended on a number of factors including the charge on and average hydrophobicity of the protein, as well as the molecular weight of both protein and PEG. Atha and Ingham (19) studied the same interactions using both solubility and equilibrium dialysis measurements. They concluded that with the possible exception of factors altering protein solubilities, the interaction between PEG and proteins in solution could be explained in terms of a simple excluded volume model consistent with their data and the data of Lee and Lee. The excluded volume model was not entirely consistent with PEG effects

on protein solubilities and they acknowledge the possibility of other factors contributing to this process. However, since this discrepancy could be rationalized in other ways, they do not believe it provides rigorous evidence for the importance of other factors.

Rationale for Investigations on GDH

Primarily I chose GDH because my adviser, Dr. Spivey, and I thought that its unusual open-ended association (see below) would be especially sensitive to polymer effects and therefore serve as an excellent detector and monitor of these interactions. This impression was based on the reasoning that a given pertubation from a polymer would shift an association equilibrium to a greater extent for proteins with a high affinity for association than for proteins with less affinity. That GDH has an unusually high affinity for enhanced association is demonstrated by its association even in the absence of other polymers. The extent of this association is altered by varying enzyme concentration or by allosteric modifiers. GDH also has the advantage of being very well studied, having been used as a model for enzymes undergoing self-association for a number of years (20). Therefore the mode of, as well as the regulation of GDH association is well-known. The enzyme undergoes reversible concentration dependent end-to-end polymerization involving the sequential addition of identical monomer units to a growing linear aggregate. An identical equilibrium constant governs each addition step, implying that no limits are placed on the extent of polymerization. The potential metabolic significance of the enzyme was also a factor in our decision. It is intriguing to consider an important regulatory role for the enzyme, since it has been shown to

hetero-associate with a number of other mitochondrial enzymes. Significant kinetic consequences have been demonstrated for both hetero- and homo-association.

Rationale for Use of PEG

PEG has been used more often than any other polymer in studying the effects of high polymer concentrations on proteins. PEG has the following advantages over other, more physiological polymers:

1. PEG is highly soluble in water.

2. The polymer is available in narrow distributions with respect to molecular weight for several different PEG molecular weights.

3. The polymer is in general much more potent than other polymers at equal weight concentrations in producing protein association, precipitation, etc.

4. PEG is nonionic. This simplifies interpretations of molecular mechanisms by excluding long range electrostatic interactions between protein and polymer.

5. PEG is an unbranched polymer which may permit a more realistic estimate of its configuration in solution.

6. More published data exist for PEG effects on proteins, which provides helpful reference data for planning and analyzing additional experiments.

Summary of Rationale, Objectives, and Results

At this time I wish to reiterate these points that constitute the motivation for these studies on the effects of polymers on GDH:

1. The concentration of individual enzymes in the cytosol and

mitochondrial matrix is very high, and the total protein concentration in these cellular compartments is comparable to that found in protein crystals.

2. As a consequence of the high cellular concentration of proteins and other polymers, significant differences between protein interactions (primarily associations) are to be expected in vivo when compared to those observed in dilute solutions in vitro.

3. Hetero- or homo-association of enzymes resulting from these high individual enzyme concentrations or polymer-induced protein interactions may cause major changes in the catalytic and regulatory properties of enzymes.

4. The mechanisms of polymer effects on proteins need further clarification.

Because of the potential significance of these polymer effects, I chose to further investigate them using GDH as a model self-associating protein. In particular, I wished to ask the following questions:

1. How is the precipitation of proteins by polymers, particularly PEG, related to the ability of proteins to associate?

2. Do polymers enhance protein association at polymer and protein concentrations at which the protein is soluble, and, if so, what is the relative potency of different polymers?

3. What are the mechanisms of polymer effects on proteins and how are these mechanisms related to the chemical nature of the polymer?

To these ends, I chose to examine the effects of several polymers (PEG's, protein, and dextrans) on the self-associating enzyme GDH. The polymers BSA and dextran were chosen for study because of their physiological nature. PEG's were used because of the previously stated

advantages offered by this polymer. Also, the polymer is used widely in biochemical applications, ranging from protein purifications to cell fusions. Yet the mechanism of PEG action is not understood. Therefore, the action of PEG on proteins is of interest for its own sake, as well as from the insight we hope to gain into the effects of polymers on proteins and the significance of these interactions in vivo.

The major findings of this work are:

1. Conditions which promote the self-association of GDH also lower the solubility of the enzyme in PEG. The onset of GDH insolubility is preceded by the formation in solution of large protein aggregates which are presumed to be the insoluble enzyme species.

2. All polymers examined enhanced the self-association of GDH.

3. Excluded volume effects alone are not sufficient to explain the extent of this enhanced association.

Additional discussion of these results as well as the experimental evidence leading to these conclusions are contained in the following chapters.

CHAPTER II

EXPERIMENTAL

Materials

Glutamate dehydrogenase was obtained as a suspension in ammonium sulfate from Boehringer-Mannheim. Lyophilized and crystalized globulin-free BSA was obtained from Sigma, as were NADH, ADP, GDP, MOPS, all PEG's, and all dextrans. PEG-200, -1000, -6000, and -20000 had molecular weights of 200, 1000, 8000, and 20,000, respectively. The substrate α-ketoglutarate was from Cal-Biochem. All other materials were reagent grade from either Baker Chemical Co. or Fischer Scientific Co.

Buffers

Only two buffers were used in this study. The first was 100 mM MOPS, 10 mM KP_i, 1 mM EDTA, pH 7.2 and is subsequently referred to as standard MOPS buffer. MOPS was used since the pH of MOPS buffer is insensitive to temperature. Also, MOPS buffer proved to be the only one of several buffers examined which did not undergo major shifts in pH upon the addition of PEG (see Appendix A for additional details). The second buffer, 10 mM KP_i, pH 7.2, was only used in an experiment measuring the dependence of GDH solubility in PEG-6000 on ionic strength. The ionic strength of the buffer was varied by the addition of KCl. The ratio of mono- and dibasic KP_i used was adjusted to

maintain a constant pH for each solution regardless of its ionic strength.

Methods

Standard Experimental Conditions

Except where noted, all experiments were performed at 5.0° C with solutions containing 1.00±0.05 mg/ml GDH in standard MOPS buffer with variable amounts of different polymers. Polymer concentrations are given as percent weight per volume (% w/v), which is equivalent to gm solute / 100 ml solution.

Enzyme Desalting

The ammonium sulfate was removed from the purchased GDH by the column centrifugation technique of Christopherson (21).

Enzyme Concentration Determination

The concentration of GDH was measured by A_{280} assuming a specific absorptivity of 0.97 ml/(mg-cm) (22).

Standard GDH Activity Assay

GDH activity was measured by spectrophotometrically monitoring the rate of oxidation of NADH to NAD^+ by absorbance changes at 340 nm. At this wavelength, the millimolar absorptivities ε are 6.22/(mM-cm) and 0 for NADH and NAD^+, respectively. Cell path length was 1 cm. The assay mixture contained 200 µM NADH, 7 mM α-ketoglutarate, 100 mM NH_4Cl, and 1 mM ADP in standard MOPS buffer. The reaction volume was two milliliters. The measurements were performed at room temperature. The

reaction was initiated by the addition of small volumes of GDH to the above mixture.

GDH Acetylation

GDH was acetylated by the method described by Frieden et al (23).

GDH Solubility

Triplicate samples of GDH or GDH with polymer were incubated overnight. Except where noted, these samples were 1 mg/ml in GDH and were incubated at 5° C. The samples were then centrifuged at 30,000 x g for 30 minutes at the same temperature as that at which the incubation was performed. The moderately high centrifugation force was required because of the large viscosity of some of the polymer-containing samples, particularly those with high PEG concentrations. After centrifugation, the supernatant was removed and the pellet dissolved in standard buffer. The activity in both pellet and supernatant was assayed. Total enzymatic activity was recovered within five percent or less. The solubility for each sample was calculated from the measured values for the activity in supernatant and pellet. The reported solubilities represent the average of the triplicate samples.

Sedimentation Velocity Measurements

These measurements were made at either 50,740 or 52,000 RPM in Beckman Model E Analytical Ultracentrifuges equipped with schlieren optics and RTIC temperature control. Temperature was maintained at 5.0° C. All measurements were made using the synthetic boundary technique as described by Chervenka (24). Schlieren peaks were recorded

on photographic plates and measured on a Nikon projector and micrometer. Sedimentation velocities were calculated by linear regression to log x versus time, where x is the radial position with respect to the center of the rotor of the maximum schlieren peak height. Sedimentation values were corrected to the standard conditions of 20° C and water by

$$\bar{s}_{20,w} = \bar{s}_{obs}[(1-(\bar{v}_2)_{20,w})/(1-\bar{v}_2\rho)]/[\eta_{T,sol'n}/\eta_{20,w}] \quad (1)$$

where $\bar{s}_{20,w}$ is the corrected average sedimentation coefficient,

$\bar{s}_{obs}$ is the observed average sedimentation coefficient,

$(\bar{v}_2)_{20,w}$ is the partial specific volume of the protein at standard conditions. For GDH, $(\bar{v}_2)_{20,w} = 0.74$.

$\bar{v}_2$ is the partial specific volume of the protein at the experimental conditions. Here, both values of $\bar{v}$ are considered to be equal.

ρ is the density of the solution,

$\eta_{T,sol'n}$ is the viscosity of the experimental solution at the experimental temperature, and

$\eta_{20,w}$ is 1.002 centipoise.

The solution density, ρ, for solutions containing polymers was calculated from the polymer density increments, which were 0.165, 0.255, and 0.422 gm/ml solution / (gm solute / ml solution) for PEG, BSA, and 9.4k dextran, repectively. The value of the increment for PEG is valid at all PEG's used (25). The value of the increment for BSA was calculated from its known $\bar{v}$ of 0.738 ml/mg (26). The value of the increment for the dextran was experimentally measured. Values for the kinematic viscosities, η_k, of the polymers in standard MOPS buffer at 5° C are contained in Appendix B. True viscosities are calculated from kinematic viscosities by the formula $\eta = \eta_k/\rho$. These viscosities were

measured using one of two Cannon capillary viscometers. The viscometer employed for any given measurement was chosen to give flow rates appropriate to avoid shear dependent viscosities.

Static Light Scattering Measurements

Measurements were made on a Brice-Phoenix Universal Light Scattering Photometer which was modified in our lab by replacement of the mercury lamp with a helium-neon laser light source (632.8 nm), the photomultiplier tube with a 1P28 photomultiplier tube, and detector with a Jarrell Ash 26-789 power supply/amplifer. This new detector was interfaced to an APPLE II+ microcomputer. Temperature was held at 5° C by the addition of a new cell holder with circulating chilled water. Values of R_θ for experimental samples were calculated by comparison of sample scattering intensity to that of a standard ludox solution of known turbidity (27). All sample components were mixed together and subsequently filtered through a pre-wetted Millex-HA 0.45 μm disposable filter unit. If several milliliters of a protein solution were filtered, the change in protein concentration upon filtration was negligible. Premixing of all components for solutions containg both polymer and protein was only practical at polymer concentrations no greater than a few percent.

Dynamic Light Scattering

Sample preparation was the same as for static light scattering. Temperature regulation was accomplished using the same cell holder as that employed for static measurements. The light scattering of a sample was monitered at 90° using an ITT FW photomultiplier. The light source

was an argon laser. Only the band with a wavelength of 514.5 nm was used. The autocorrelation function of the scattering intensity was calculated by a Langley-Ford autocorrelator interfaced to a PDP11/10 minicomputer. The data was stored on flexible disks for later analysis on a PDP11/40 minicomputer. See Appendix E for details of the analysis. Average diffusion coefficients $\overline{D}_{20,w}$ were corrected to standard conditions by

$$\overline{D}_{20,w} = \overline{D}_{obs}(\eta_k)_{sol'n,T}(293.1/T) \qquad (2)$$

where $\overline{D}_{obs}$ is the observed diffusion coefficient,

η_k is the kinematic viscosity of the solution, and

T is the experimental temperature (for all our measurements, T is 5^o C.).

GDH Inhibition by GDP

Transient-state kinetic parameters for the inhibition of GDH by GDP were measured with a Durrum-Gibson stopped-flow spectrophotometer. To reduce contributions from stray light, a 365 nm band-pass filter was placed between the light source and the sample. Under these conditions the measured absorbance was linear up to 200 μM NADH. The absorptivity coefficient for NADH at 365 nm was experimentally found to be 3.38/(mM-cm). A thermostated cell with a pathlength of 1.86 cm was used. Temperature was maintained at 5^o C. Detector output, representing the solution transmittance, was digitized by a Biomation 805 A/D converter and stored on an APPLE II+ microcomputer. The data were subsequently transfered to and analyzed on a PDP11/40 minicomputer. In these kinetic measurements, syringe 1 contained 1 mg/ml GDH. Syringe 2 contained 200 μM NADH, 14 mM α-ketoglutarate, 200 mM NH_4Cl, and 2 mM

GDP (for those measurements involving GDP). If PEG-6000 was included in the solutions, it was present at 2% w/v in both syringes. All solutions were prepared in standard MOPS buffer. The reaction was initiated by the rapid mixing of equal volumes of both solutions. Data were gathered over the complete time course of the reaction.

CHAPTER III

RESULTS AND DISCUSSION

Effect of Polymers on GDH Solubility

Solubility of GDH in Different Kinds of Polymers

Dextrans, PEG and protein (BSA) were tested for their ability to decrease GDH solubility. Of those tested, only the higher MW PEG's were shown to precipitate GDH at enzyme concentrations less than 1 mg/ml. At 5° C in standard MOPS buffer, GDH solubility exceeded 1 mg/ml in the following polymers (with polymer concentration given as percent polymer weight/ml solution):

37%, 9.4k dextran
37%, 18.4k dextran
18.5%, 500k dextran
10% (100 mg/ml) BSA
15% PEG-200

PEG-1000, -6000, and -20000 all significantly decreased the solubility of GDH under these conditions.

GDH Solubility in PEG Solutions

Effect of PEG Molecular Weight. At a given weight concentration of PEG, the solubility of GDH in PEG decreases in the following order: PEG-1000 >> PEG-20000 > PEG-6000 (Figure 1). Normally the solubility of a protein at a given concentration of PEG (w/v) decreases with increasing PEG molecular weight to an asymptotic limit with about

Figure 1. Solubility of GDH in Different Molecular Weight PEG's as a Function of PEG Concentration. Standard experimental conditions were used.

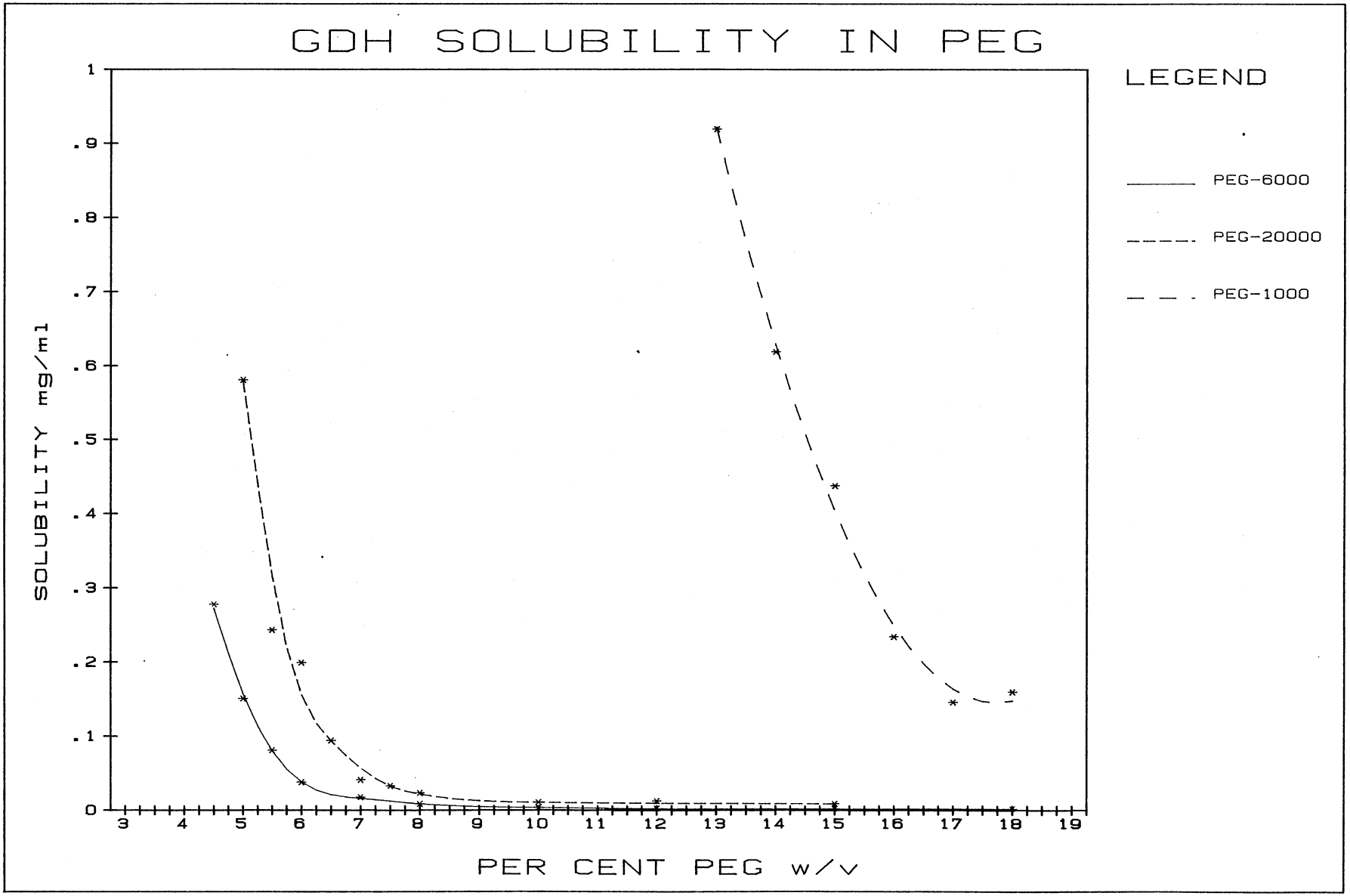
GDH SOLUBILITY IN PEG
LEGEND
PEG-6000
PEG-20000
PEG-1000
SOLUBILITY mg/ml
0
.1
.2
.3
.4
.5
.6
.7
.8
.9
1
3
4
5
6
7
8
9
10
11
12
13
14
15
16
17
18
19
PER CENT PEG w/v

PEG-6000. Atha and Ingham (19) demonstrated that PEG-6000 and -20000 were of similiar potency in precipitating human serum albumin at room temperature (22-24° C) with the solubility of the protein being slightly less in the higher molecular weight polymer at equal PEG concentrations (w/v). Their data were adequately fitted by a simple excluded volume model for HSA and these two PEG concentrations using R_e values of 2.65 and 4.65 nm (see Appendix C) for PEG-6000 and -20000, respectively. The solubility of HSA in low molecular weight PEG's did not fit such a model. This may be due to the treatment of them as hydrodynamic spheres. Such a treatment is valid for random coil polymers, but low molecular weights PEG's are not random coils. For instance, the number of polymer segments in PEG-1000 is only 20. Therefore attempts to analyze PEG effects in terms of excluded volumes should be confined to the higher molecular weight polymers or better models for the volume occupied by low molecular weight PEG's. While the effect of excluded volume alone is probably insufficient to explain the potency of PEG as a precipitating agent, it is certainly considered to be one of the more important factors involved.

One reason for the reversal in the relative potencies of PEG-6000 and PEG-20000 in these experiments with GDH relative to those with HSA mentioned above may be differences in buffer-PEG interactions. Atha and Ingham used 0.05 M potassium acetate buffer at pH 4.5, containing 0.1 M KCL at room temperature, while the buffer used with GDH studies was 100 mM MOPS, 10 mM potassium phosphate, 1 mM EDTA, pH 7.2 at 5° C. The effective excluded volume radius of a flexible polymer like PEG will increase or decrease depending on the relative magnitude of polymer segment-segment interactions and polymer segment-solvent interactions

(28). When segment-solvent interactions are greater than segment-segment interactions ("good solvent"), the polymer will swell from the size it occupies in the absence of intermolecular interactions. Similarly the polymer will shrink in a "poor solvent" where segment-segment interactions are greater than segment-solvent interactions. A pertinent measure of the intermolecular interactions can be obtained from viscosity data by calculating the Huggins constant k from

$$\eta_{sp}/c = [\eta] + k[\eta]^2 c \qquad (1)$$

where η_{sp}/c is the reduced viscosity,

$[\eta]$ is the intrinsic viscocity, and

c is the polymer concentration.

k was 0.53, 0.51, and 1.15 for PEG-1000, -6000, and -20000, respectively. For flexible polymer molecules in a good solvent, k is approximately 0.35 with higher values for poor solvents (29). Thus at 5° C the standard MOPS buffer is a poor solvent for PEG-20000, and a much better solvent for PEG-1000 and -6000. Although we don't have the data to calculate Huggins constants for PEG's and buffer used by Atha and Ingham, we can compare the apparent effective radii R_e as calculated from our viscosity data and the more limited viscosity data that they use. For PEG-6000 in our experiments, we obtain a R_e = 3.04 nm in comparison with 2.65 nm for their experiments. For PEG-20000 we obtain R_e = 4.56 (our experiments) and 4.65 (their experiments). These results support the view that PEG-6000 in our experiments is larger and therefore would be expected to provide a considerably larger excluded volume in our experiments than in those of Atha and Ingham. Remembering that the excluded volume is proportional to the cube of the radii (30)

and that equilibrium constants such as solubility constants are exponentially related to free energy changes, we should not be surprised at sizeable differences in solubility from these differences in solvent-polymer interactions.

It is possible that the values reported by Atha and Ingham for the R_e's of the two PEG's are erroneous, since they were based on intrinsic viscosities calculated from the interpolating formulas $[\eta] = a\bar{M}_2^{\,b}$ where a and b are 0.156 and 0.5 for the PEG molecular weight range $200 < \bar{M}_2 < 8000$ and 0.125 and 0.78 for $10^4 < \bar{M}_2 < 10^7$. We found these equations to be invalid at the temperature at which our measurements were made. However, the viscosity of polymer solutions is temperature dependent. Therefore, they may or may not be accurate for the system used by Atha and Ingham. In any case, it would require a rather large error in the calculated intrinsic viscosities to lead to a significant error in R_e, since R_e is proprotional to $\sqrt[3]{[\eta]}$ (Appendix C, Equation 1). It is important to remember that Atha and Ingham were able to correctly predict the constant reflecting interaction between the protein and PEG in the calculation of protein chemical potential (Equation 2, Page 28), on the basis of their values for the R_e's of the two PEG's and the known radius of HSA.

The system is complex, however, and other possible causes for the differences noted in relative potencies of PEG of different molecular weights exist. Factors other than exluded volume may be significant in determining precipitation. Indeed the relative hydrophobicities of GDH versus HSA may cause the difference in response to PEG. Alternatively the fact that GDH associates causes complex and atypical results (see next section). The observed behavior is probably the result of a number

of different factors which we are unable to differentiate at this time.

Effect of PEG Concentration. Studies with purified proteins indicate the dependence of protein solubility on PEG concentration generally conforms to the following equation:

$$\ln S = \beta c + \text{constant} \qquad (2)$$

where S is the protein solubility in grams/liter,

β is a constant reflecting PEG-protein interaction, and

c is concentration of PEG in percent weight/volume.

This equation is a consequence of Ogston's expression for the chemical potential of a macromolecule in a 2 macromolecule plus solvent (ternary component) system (31). As described in Appendix D one can demonstrate that the solubility of a self-associating enzyme like GDH would obey equation 2 only under very limited and unlikely conditions. Plots of ln S vs % (w/v) PEG are shown in Figure 2. As expected, they are not at all linear. The primary reason for this is that, at least in the solutions containing low concentrations of PEG, the insoluble form of GDH is not monomeric GDH, but is instead one of the polymeric forms. This is because at low PEG concentrations high GDH concentrations are required to reach the solubility limit. At these high GDH concentrations, polymerized GDH forms predominate. That the monomeric form of the enzyme is much more soluble than the polymeric forms was demonstrated by Miekka and Ingham (16), who showed that the addition of NADH and GTP to PEG-GDH solutions, which is known to drive the enzyme into its monomeric form, also vastly enhanced the solubility of the enzyme in PEG. Large proteins are generally less soluble in PEG solutions than are small ones. Therefore it is reasonable to expect that the solubility limit of one of the more highly polymerized forms

Figure 2. Ln of GDH Solubility in Different Molecular Weight PEG's as a Function of PEG Concentration. Standard experimental conditions were used.

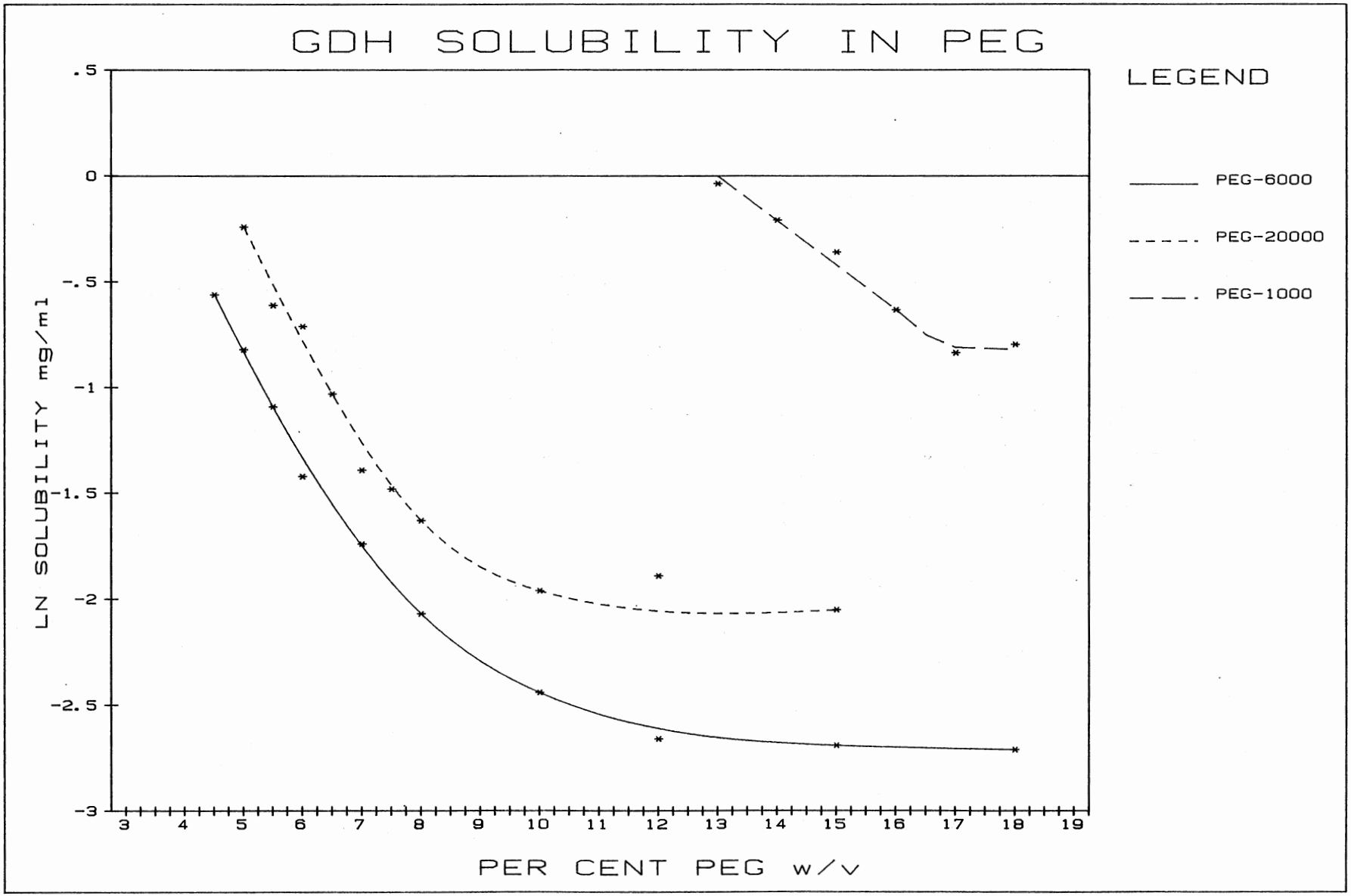
GDH SOLUBILITY IN PEG
LEGEND
PEG-6000
PEG-20000
PEG-1000
LN SOLUBILITY mg/ml
.5
0
-.5
-1
-1.5
-2
-2.5
-3
3
4
5
6
7
8
9
10
11
12
13
14
15
16
17
18
19
PER CENT PEG w/v

would be reached before that of a less polymerized form, even if the more polymerized form is at a lower concentration.

Effect of GDH Concentration. The solubility of an ideal solution should be independent of its initial concentration. However, when varying concentrations of GDH were incubated with 6% PEG-6000 under standard conditions, the measured solubility exhibited a dependence on [GDH] (Figure 3). Non-equilibrium conditions must be invoked in order to explain this. One can be mislead into concluding that, since it is one of the polymeric forms of GDH that is insoluble, and since the concentration of this form depends on the total GDH concentration, such a dependence is reasonable. However, such an argument is fallacious. If the form E_i is at its solubility limit, S (M), then the molar concentration of all other species E_j is given by

$$[E_j] = S^{j/i} K(j/i)-1 \qquad (3)$$

which is a constant independent of enzyme concentration. As explained in Appendix D for an equilibrium, only one of the polymeric species can reach its solubility limit. A constant distribution of species concentrations will be maintained as the total protein conentration is further increased and the excess protein precipitates. The enzyme form which first becomes saturated is a function of [PEG], however. We are therefore left with kinetic explanations for the observed behavior. The most likely explanation is very slow equilibration of enzyme forms, perhaps in the amorphous solid phase. We believe that the measured solubilities in 1 and 2 mg/ml GDH represent values very close to those at equilibrium, since there was no difference in observed solubility for these two concentrations, and the solubility measured in 0.5 mg/ml GDH appears to be approaching this same solubility limit. This implies that

Figure 3. Apparent Solubility of GDH in PEG-6000 as a Function of Initial GDH Concentration. Standard experimental conditions were used with the exception of varying the concentration of GDH. [PEG-6000] was 6% w/v for all GDH concentrations. At 0.1 mg/ml GDH, no precipitation of enzyme was observed.

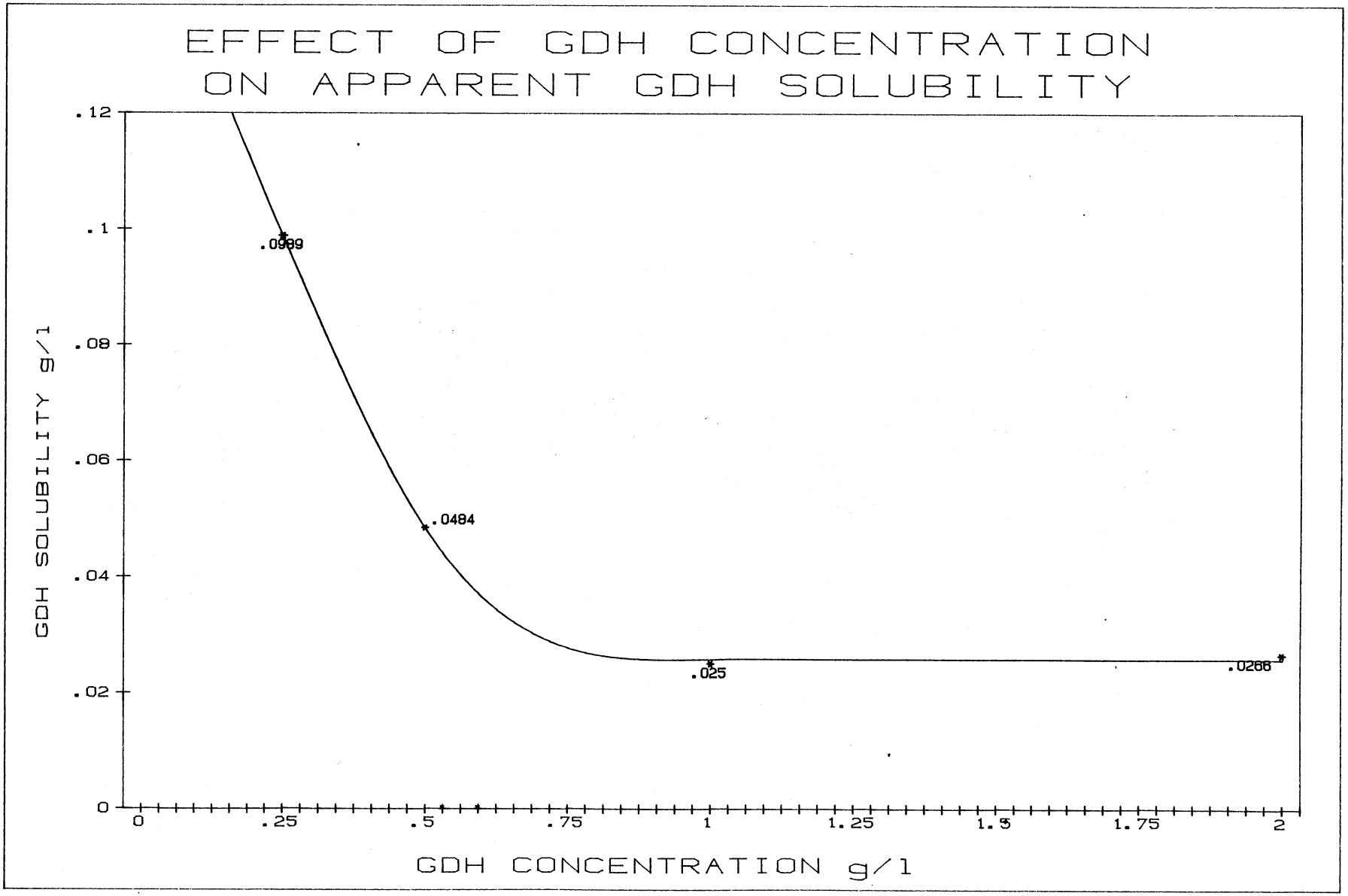
EFFECT OF GDH CONCENTRATION
ON APPARENT GDH SOLUBILITY
GDH SOLUBILITY g/l
.12
.1
.08
.06
.04
.02
0
.0989
.0484
.025
.0266
0
.25
.5
.75
1
1.25
1.5
1.75
2
GDH CONCENTRATION g/l

the rate of equilibration is a function of the total enzyme concentration. Therefore all other solubility measurements were performed using an initial enzyme concentration of 1 mg/ml.

Effect of pH and Ionic Strength. GDH solubility is fairly constant in the pH range 6 to 7.5, but increases a great deal between 7.5 and 8.0 in 5% PEG-6000 (Figure 4.). This correlates with the pH dependence of the association in solution of the protein in the absence of PEG. At an ionic strength of 115 mM (as compared to 121 mM for the measurements reported here on the effect of pH on GDH solubility), Sund et al (32) found the s_{20} of 4 mg/ml GDH to be constant (27S) from slightly below pH 6 to about pH 7.2. At pH 7.65, the s_{20} began decreasing. The authors ascribed this decrease to a lower extent of enzyme association rather than different hydrodynamic propertices solely due to changes in protein conformation. Unfortunately, they made no measurements above pH 7.65, citing reports of enzyme instability above pH 8 as the reason for not doing so.

Let us contrast the sedimentation behavior which Sund et al observed at moderate (115mM) ionic strength to that which they observed at low (40 mM) ionic strength. Whereas at μ = 121 mM the s_{20} of GDH was relatively constant over the pH range studied, at μ = 40 mM, s_{20} was highly pH dependent. At pH 7.2 (the pH at which we studied the effect of ionic strength on the PEG-induced insolubility of GDH), Sund measured s_{20} = 25 S for μ = 40 mM, and 27 S at 115 mM. Presumably the extent of GDH association increased upon raising the ionic strength at this pH.

If for GDH the forces involved in decreasing solubility are related to those involved in promoting protein association, we might expect that at pH 7.2 the solubility would decrease as the ionic strength is

Figure 4. Dependence on pH of GDH Solubility in PEG-6000. Standard conditions of temperature and enzyme concentration were employed. MOPS buffer was also used. KCl was added to all samples below pH 8.0 such that the ionic strength in all cases was 121 mM. The ionic strength of standard MOPS buffer at pH 7.2 is normally 79 mM. [PEG-6000] was 5% w/v.

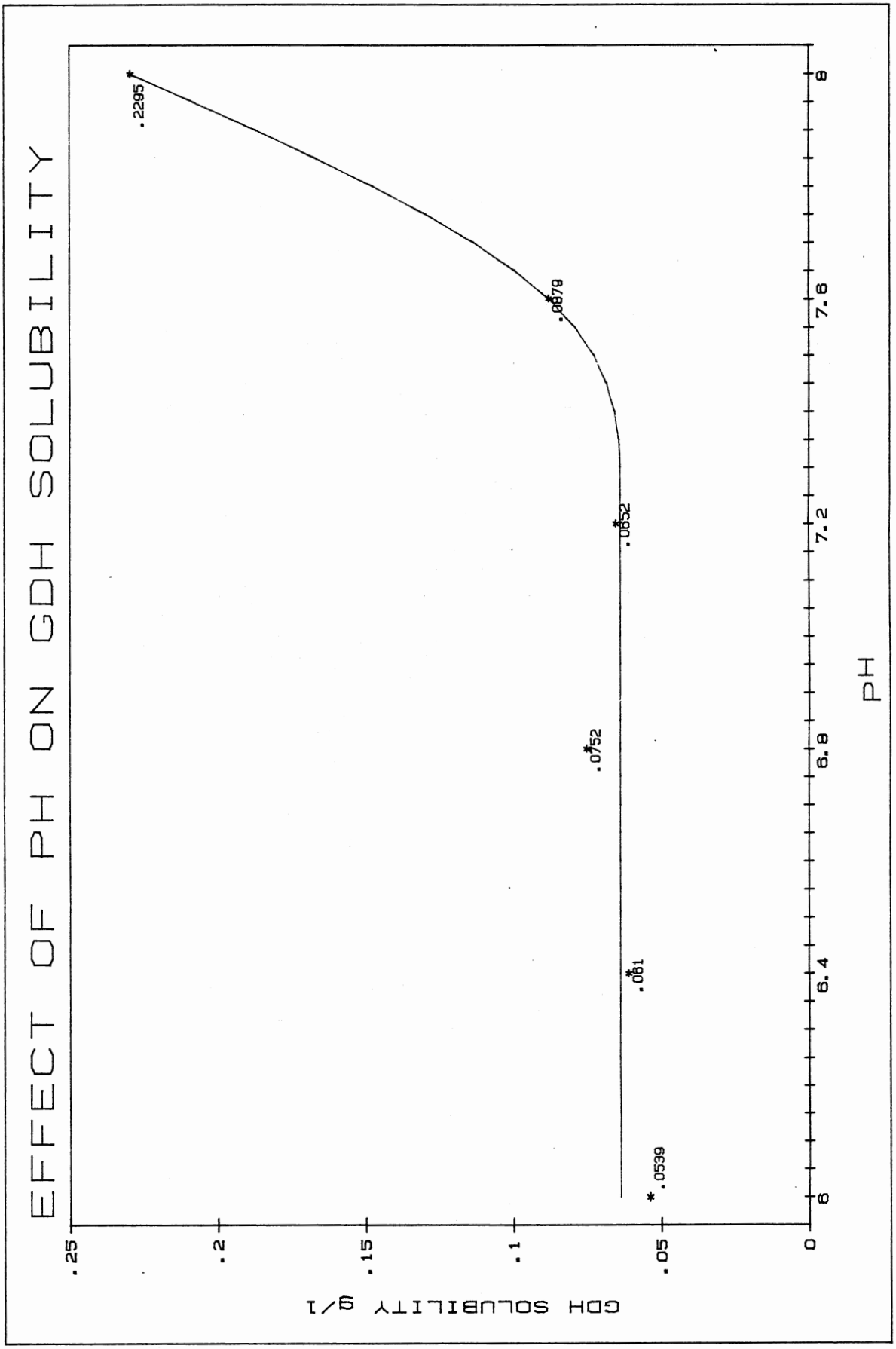
EFFECT OF PH ON GDH SOLUBILITY
GDH SOLUBILITY g/l
PH
.25
.2
.15
.1
.05
0
6
6.4
6.8
7.2
7.6
8
.2295
.0879
.0652
.0752
.061
.0539

Figure 5. Effect of Ionic Strength on GDH Solubility in PEG-6000 Solutions. Standard conditions of temperature and enzyme concentration were employed. [PEG-6000] was 6% w/v. The buffer used was 10 mM potassium phosphate, pH 7.2. The ionic strength was varied by the addition of potassium chloride. At ionic strengths of 25 and 37.5 mM, the enzyme solubility exceeded 1 mg/ml.

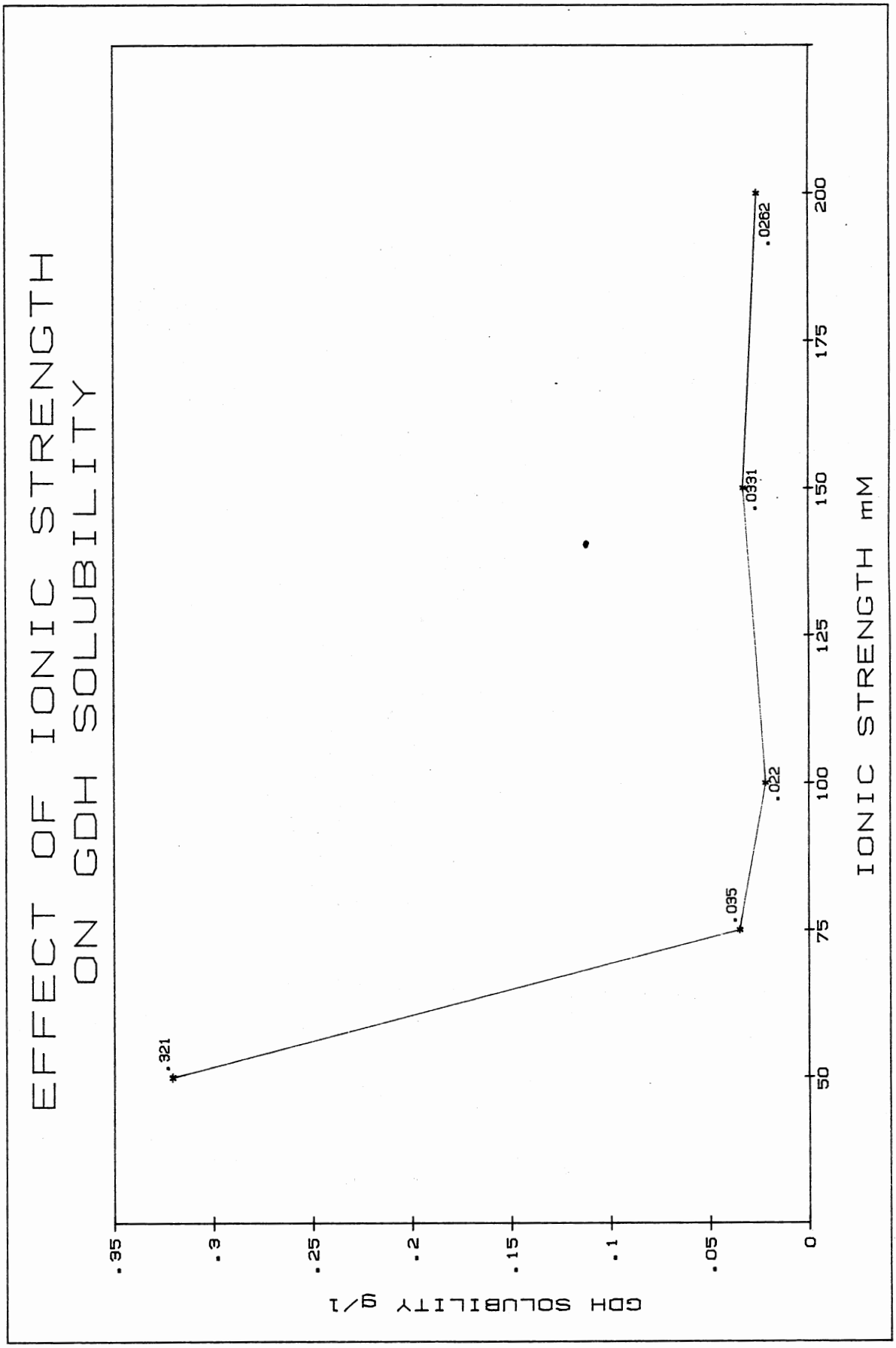
EFFECT OF IONIC STRENGTH
ON GDH SOLUBILITY
GDH SOLUBILITY g/l
.35
.3
.25
.2
.15
.1
.05
0
50
75
100
125
150
175
200
IONIC STRENGTH mM
.321
.035
.022
.0331
.0262

increased. This is indeed what is observed (Figure 5). For other proteins studied to date, the solubility of the protein in PEG has increased with increasing ionic strength. This has been attributed to a decrease in the size of the PEG coils in the higher ionic strength solutions. This effect could also be the "salting in" observed for proteins as the ionic strength is increased from very low levels to moderate ones. Studies examining the interaction of two proteins in polymer solutions have usually been done at very low ionic strengths. This is objectionable since at low ionic strengths nonspecific electrostatic interactions between proteins are high. With GDH, significant polymer-induced protein interactions occur without requiring low ionic strengths.

Effect of Temperature. The solubility of GDH in PEG increases with temperature (Figure 6). The apparent decrease in solubility at 25° C may be due to protein instability, especially in solution phase. The precipitated enzyme is thought to be less temperature sensitive than that in solution. The recovered activity in the sample at 25° was about 10% less than those at all other temperatures. Thus the solubility at this temperature could be as high as 0.19 mg/ml if this discrepency in activity was solely due to denaturation of soluble enzyme.

Polymer Effects on GDH Self-Association

We have just demonstrated that conditions which enhance the extent of GDH self-association also decrease its solubility in PEG solutions. Now we wish to examine the influence of polymers on GDH association in solution.

Figure 6. Temperature Dependence of GDH Solubility in PEG-6000. Standard MOPS buffer and the standard enzyme concentration were used. [PEG-6000] was 10% w/v.

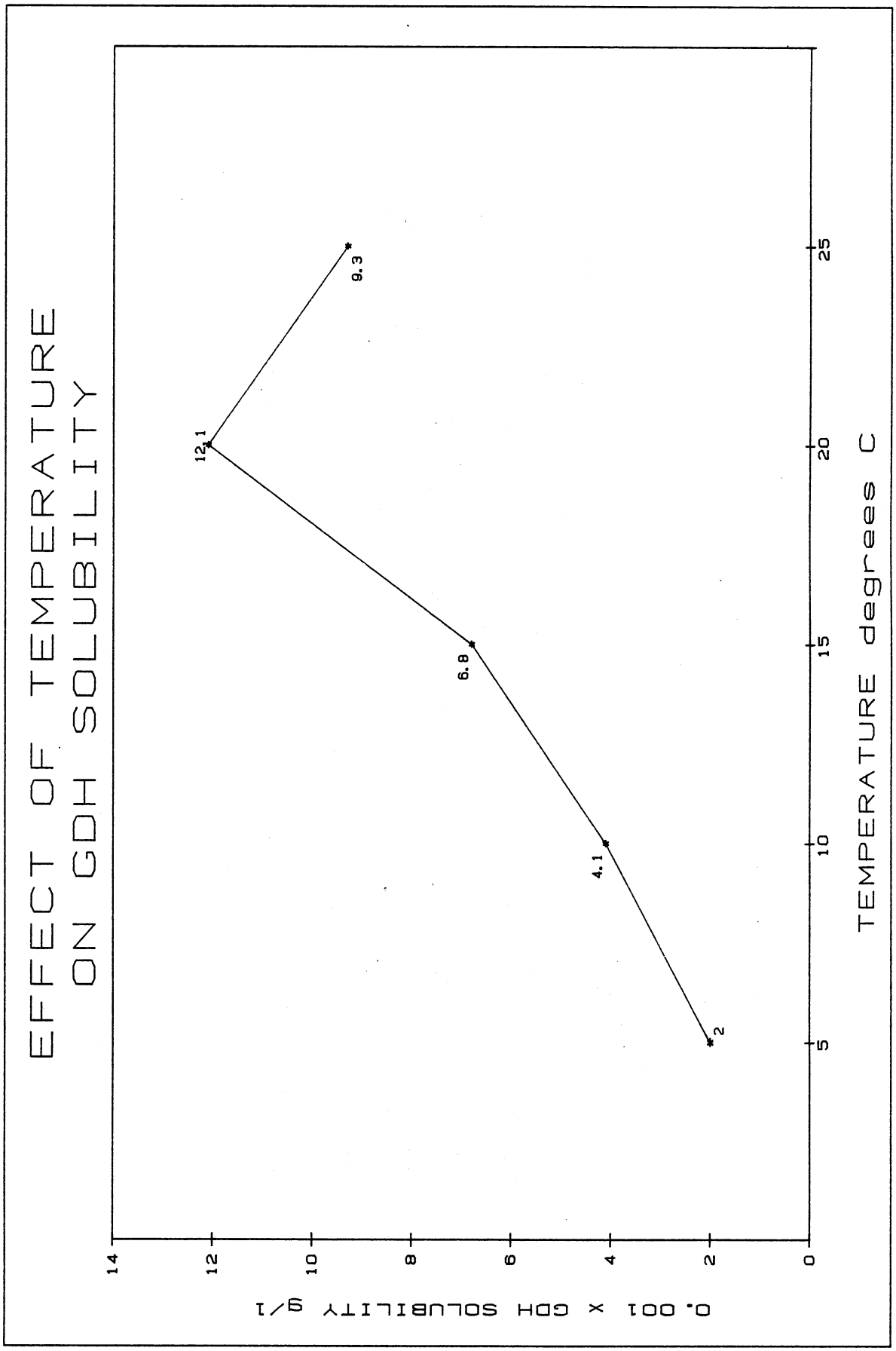
EFFECT OF TEMPERATURE
ON GDH SOLUBILITY
0.001 x GDH SOLUBILITY g/l
TEMPERATURE degrees C
0
2
4
6
8
10
12
14
0
5
10
15
20
25
2
4.1
6.8
12.1
9.3

Sedimentation Velocity Studies

The sedimentation coefficient of GDH in standard buffer containing various polymers was measured by analytical ultracentrifugation at 5° C. The polymers included PEG-1000, PEG-6000, PEG-20000, BSA, and 9.4 k dextran. The results are tabulated in Table I. If a sufficiently high polymer concentration was used, then the $s_{20,w}$ of GDH increased for all of the polymers examined. Two possible explanations (other than enhancement of GDH association) should be considered.

1. Binding of polymer to GDH. Several authors have demonstrated that PEG does not bind to proteins (18,19). In fact, the two tend to maximize the distance between each other in solution. It is possible that either dextran or BSA could bind to the protein. However, no evidence for such binding currently exists. As a test of binding of PEG the $s_{20,w}$ of acetylated GDH in varying concentrations of PEG-6000 was measured. Acetylation is known to greatly inhibit the self-association of the protein (23). Any changes in $s_{20,w}$ among the various solutions could only be ascribed to conformational changes in the protein or binding of polymer to the protein. However, the $s_{20,w}$ of acetylated GDH was independent of PEG-6000 concentration (Table II). This furthur supports the case against polymer binding to GDH.

2. Changes in the conformation of the associated protein. If polymeric GDH assumes a less extended conformation due to a change in the nature of its association (for instance, a shift from end-to-end association to a spherical form) then the protein will sediment faster than expected. However, analysis of the sedimentation and diffusion coefficient data as discussed below strongly support the view that PEG does not alter the axial ratio of associated GDH.

TABLE I

EFFECT OF ADDED POLYMER ON $\bar{s}_{20,W}$ OF GDH

[GDH] (mg/ml)	Polymer	[Polymer] (% w/v)	Number observations	$\bar{s}_{20,w}$ S
1	none		5	20.2
2	none		2	21.8
1	9.4k dextran	5	4	22.2
1	9.4k dextran	10	2	21.4
1	BSA	10	2	23.2
2.1	BSA	11.1	2	24.3
1	PEG-1000	5	2	22.0
1	PEG-1000	10	2	22.8
1	PEG-20000	2	2	20.4
1	PEG-20000	4	2	22.7
1	PEG-6000	1	2	22.9
1	PEG-6000	2	3	23.6
1	PEG-6000	3	2	25.3
2	PEG-6000	2	2	27.4

Values for $\bar{s}$ were measured at 5° C. in standard MOPS buffer containing polymer and corrected to standard conditions.

TABLE II

$s_{20,w}$ OF ACETYLATED GDH IN PEG-6000

[PEG] (% w/v)	$s_{20,w}$ S
0	13.7
1	13.5
2	13.7
3	13.5

Values for $s_{20,w}$ represent the average of two independent measurements. Experimental conditions were the same as in Table I.

Light Scattering by GDH in PEG-6000

Since PEG-6000 had the largest effect on GDH self-association at comparable weight concentrations, this system was chosen for further study by other methods. Initially, static light scattering intensity measurements were made on solutions containing 1 mg/ml GDH and varying concentrations of PEG-6000 at 5° C in standard MOPS buffer (Figure 7). The molecular weight of a protein can normally be evaluated from light scattering measurements by well-known equations relating the scattered intensity to both protein molecular weight and concentration. However, if two or more macromolecular solutes contribute comparable scattering intensities, additional terms may be needed in the equations (33). If such additional terms are significant, we would need considerably more data than we have to properly calculate GDH molecular weights. Since GDH is contributing greater than 90% of the total light scattering in our data however, it is probably safe to treat our system as if it contained only two components. In this case, calculation of M_w's only requires knowledge of the refractive index increment in the protein for the solvent system. However, experimental difficulties have so far prevented us from measuring these values for GDH in the PEG solutions.

What then can be learned from this experiment? The primary point of interest is the large increase in intensity with decreasing angle in 3% PEG. Such dependence is indicative of the existence of very large particles which at higher angles cause the destructive interference of some of the scattered light. To make detailed analysis of the static light scattering measurements on these particles requires either working at very low angles, or using very long wavelengths of light. Since

Figure 7. Angular Dependence of Light Scattering by 1 mg/ml GDH in Varying Concentrations of PEG-6000. Wavelength of incident light was 612.8 nm. Standard experimental conditions were employed.

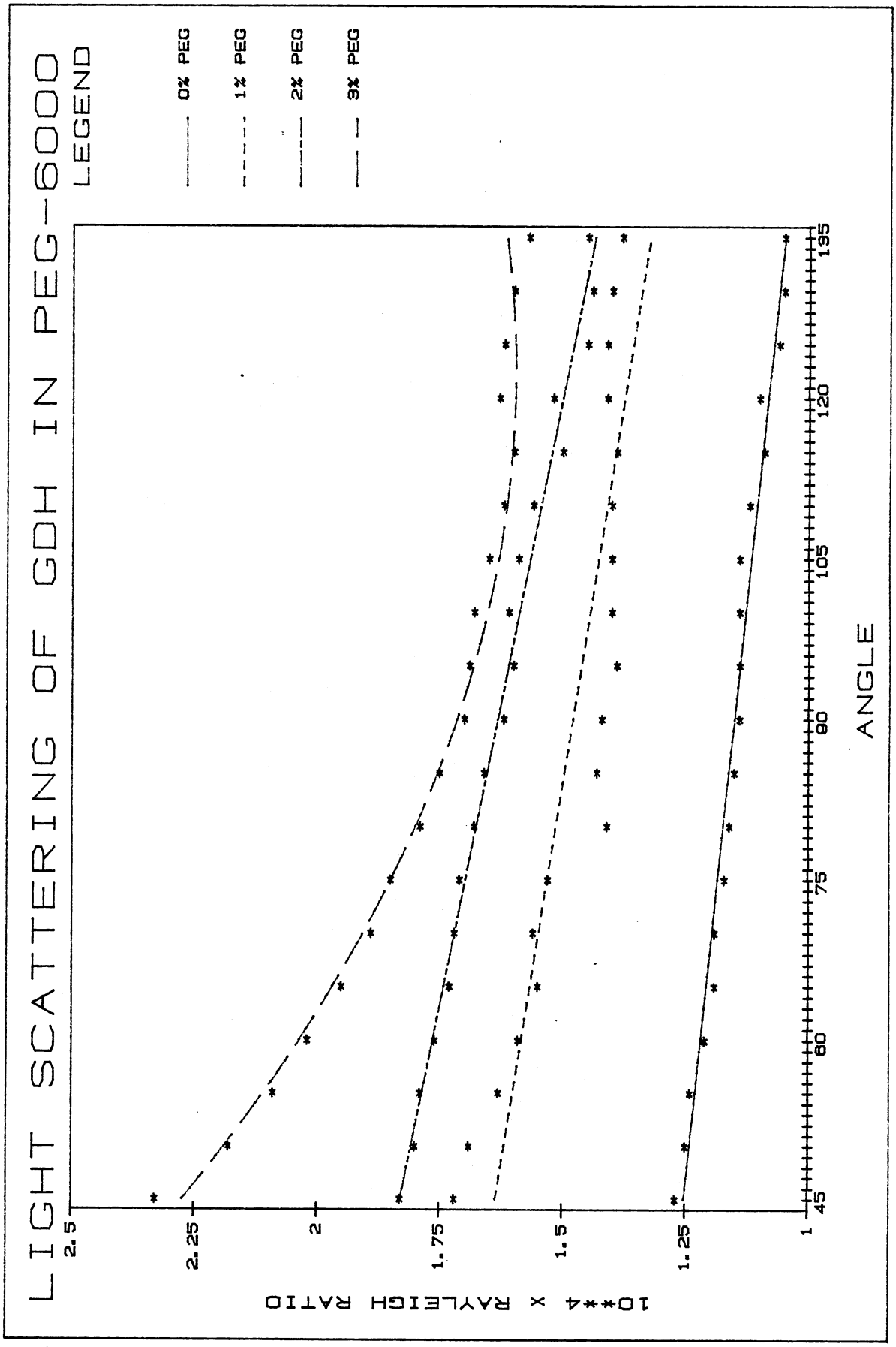
LIGHT SCATTERING OF GDH IN PEG-6000
LEGEND
0% PEG
1% PEG
2% PEG
3% PEG
10**4 X RAYLEIGH RATIO
2.5
2.25
2
1.75
1.5
1.25
1
45
60
75
90
105
120
135
ANGLE

these particles were not observed in sedimentation velocity studies, they must comprise a very small portion of the total protein. The fact that they are observed only as the solubility limit of the protein is approached is noteworthy. Similiar highly aggregated particles in solutions of MDH, CS, and PEG have been reported previously by this laboratory. We have also observed this recently with other proteins in PEG solutions. The observations together indicate that these PEG-induced protein associations are a general mechanism of protein precipitation by PEG. Further tests of this hypothesis are in progress in this laboratory.

Of greater interest is the distribution of particle sizes for the bulk of the protein in solution. To obtain more information about this, dynamic light scattering was employed. Samples like those used in the static measurements were characterized by this technique. Because of the wavelength of the light source employed (514.5 nm) and the angle at which the light scattering was observed (90^{o}), the large particles observed in the 3% PEG solution did not contribute significantly to the DLS signals. Data were analyzed by the delta function method of Pike, which is described in more detail in Appendix E. The advantage of this method is that the relative light scattering intensity of the enzyme particles in solution is measured as a function of their respective diffusion coefficients. The calculated distributions are shown in Figures 8 through 12. The delta function method lends itself to two methods of interpolation. The first involves shifting the position of the delta functions to be fitted. The second involves use of the explicit interpolating formula (Equation 8, Appendix E). The first method was employed for all samples. For the sample containing GDH

Figure 8. Light Scattering Intensity of GDH in Buffer as a Function of Diffusion Coefficient. These are the results of fits to combined DLS data sets with 2, 5, 10, 20, and 50 μs coherence times by the delta function method of analysis. The smooth curve represents interpolation to data indicated by the solid bars using of Equation 9, Appendix E. Standard experimental conditions were employed.

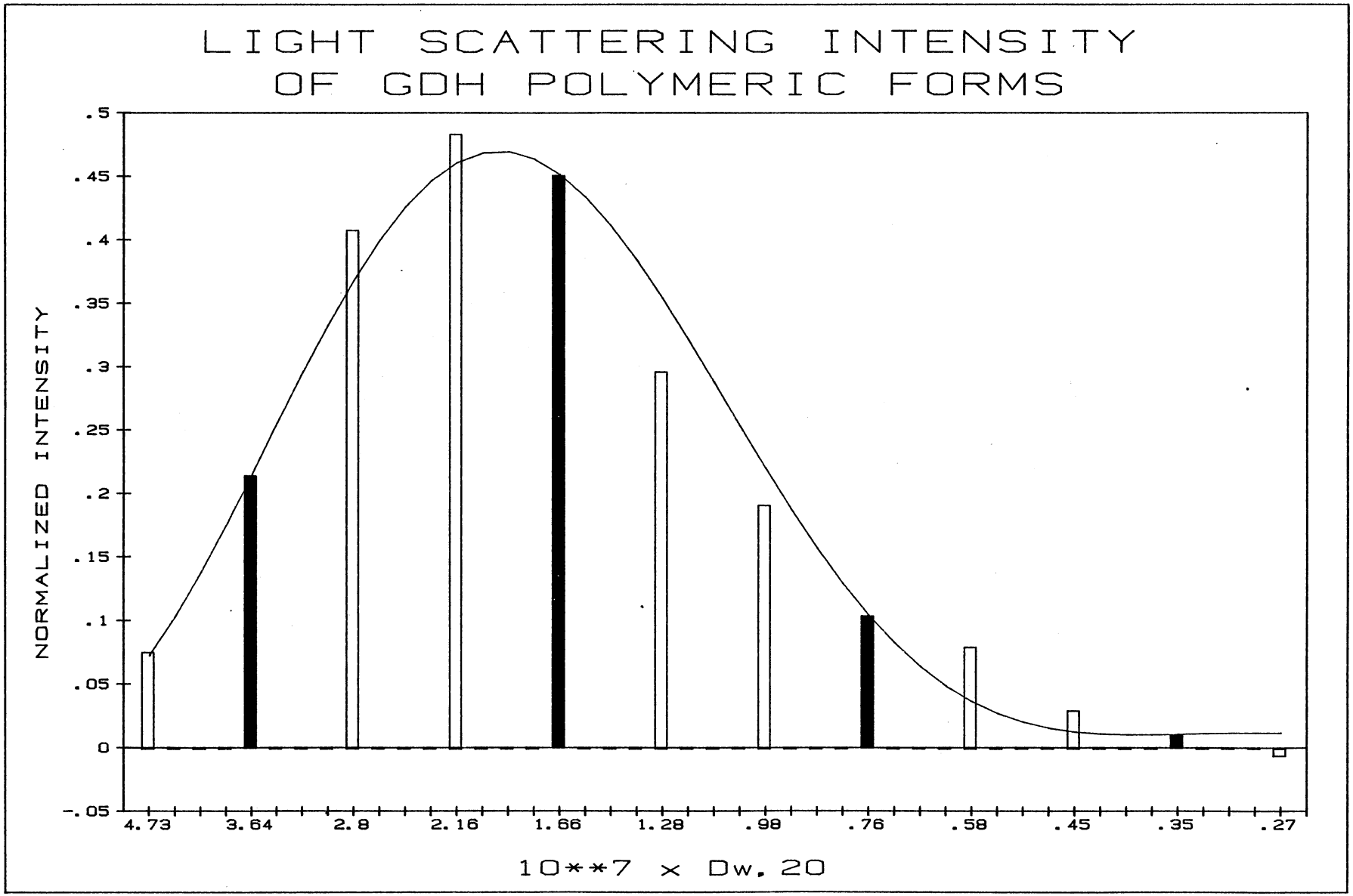
LIGHT SCATTERING INTENSITY
OF GDH POLYMERIC FORMS
NORMALIZED INTENSITY
.5
.45
.4
.35
.3
.25
.2
.15
.1
.05
0
-.05
4.73
3.64
2.8
2.16
1.66
1.28
.98
.76
.58
.45
.35
.27
10**7 x Dw, 20

Figure 9. Light Scattering Intensity of GDH in Buffer as a Function of Diffusion Coefficient. Data sets with coherence times of 2, 5, 10, and 20 μs were simultaneously fit. No interpolation was performed on the resulting fits. Density of fitted intensity values corresponding to the diffusion coefficients was greater than in Figure 8. Standard experimental conditions were employed.

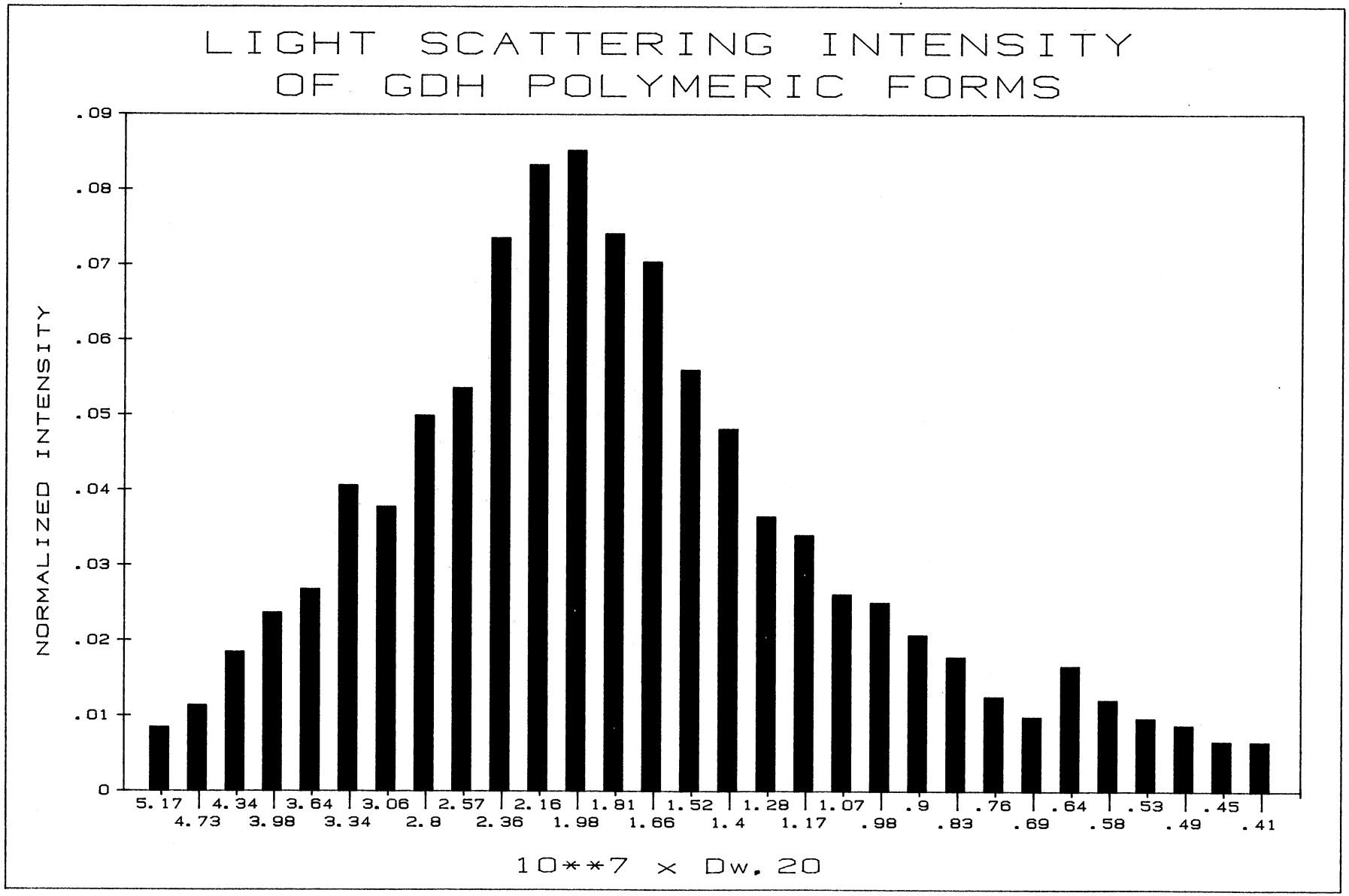
LIGHT SCATTERING INTENSITY
OF GDH POLYMERIC FORMS
NORMALIZED INTENSITY
.09
.08
.07
.06
.05
.04
.03
.02
.01
0
5.17
4.73
4.34
3.98
3.64
3.34
3.06
2.8
2.57
2.36
2.16
1.98
1.81
1.66
1.52
1.4
1.28
1.17
1.07
.98
.9
.83
.76
.69
.64
.58
.53
.49
.45
.41
10**7 x Dw, 20

Figure 10. Light Scattering Intensity of GDH in 1% PEG-6000 as a Function of Diffusion Coefficient. Intensity contributions at values of D greater than approximately 4×10^{-7} cm^2/s are due to PEG contributions. Other experimental details are identical to those in Figure 9.

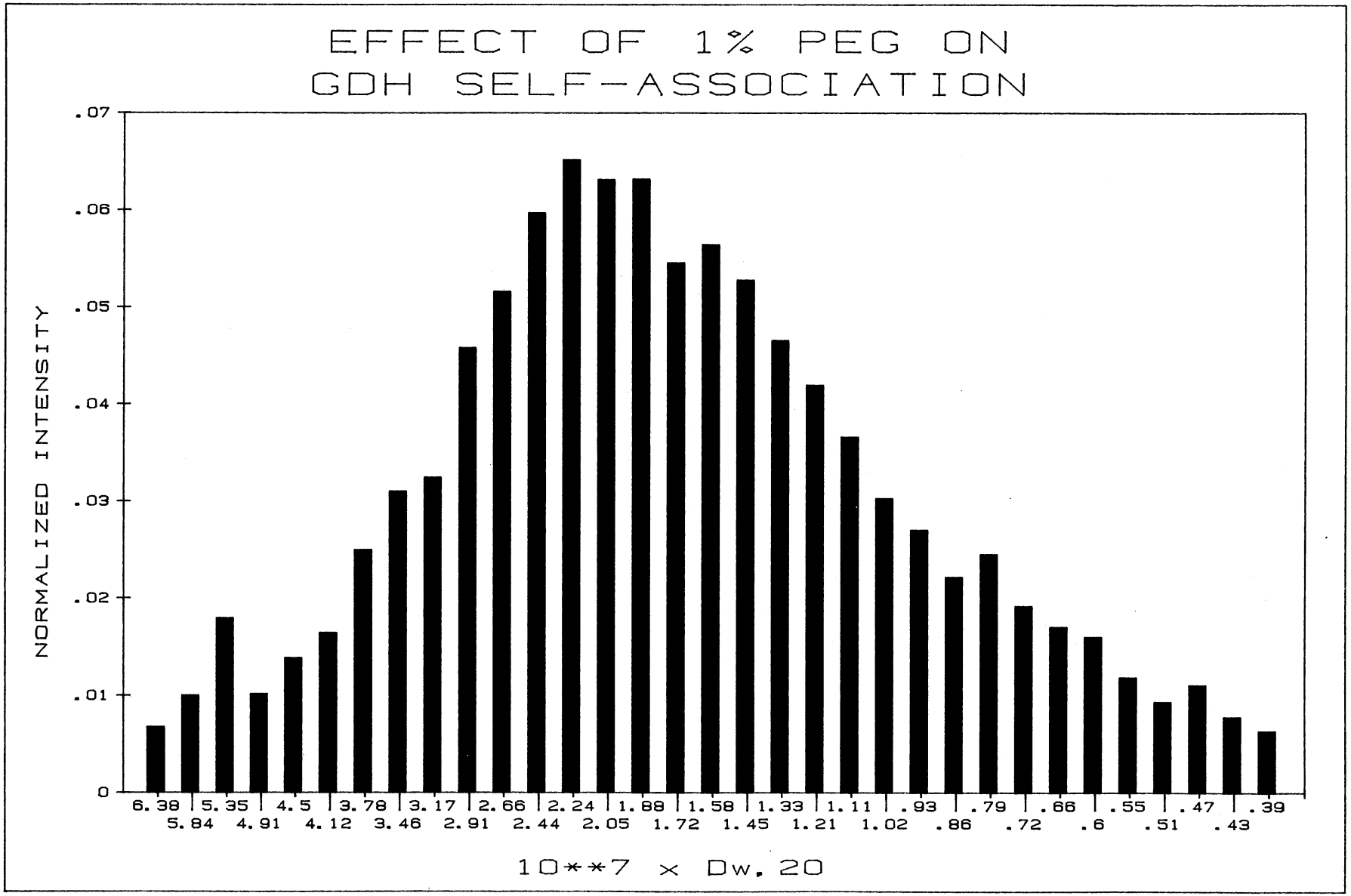
EFFECT OF 1% PEG ON
GDH SELF-ASSOCIATION
NORMALIZED INTENSITY
.07
.06
.05
.04
.03
.02
.01
0
6.38 5.35 4.5 3.78 3.17 2.66 2.24 1.88 1.58 1.33 1.11 .93 .79 .66 .55 .47 .39
5.84 4.91 4.12 3.46 2.91 2.44 2.05 1.72 1.45 1.21 1.02 .86 .72 .6 .51 .43
10**7 x Dw, 20

Figure 11. Light Scattering Intensity of GDH in 2% PEG-6000 as a Function of Diffusion Coefficient. Intensity contributions at values of D greater than approximately 4×10^{-7} cm^2/s are due to PEG contributions. Other experimental details are identical to those in Figure 9.

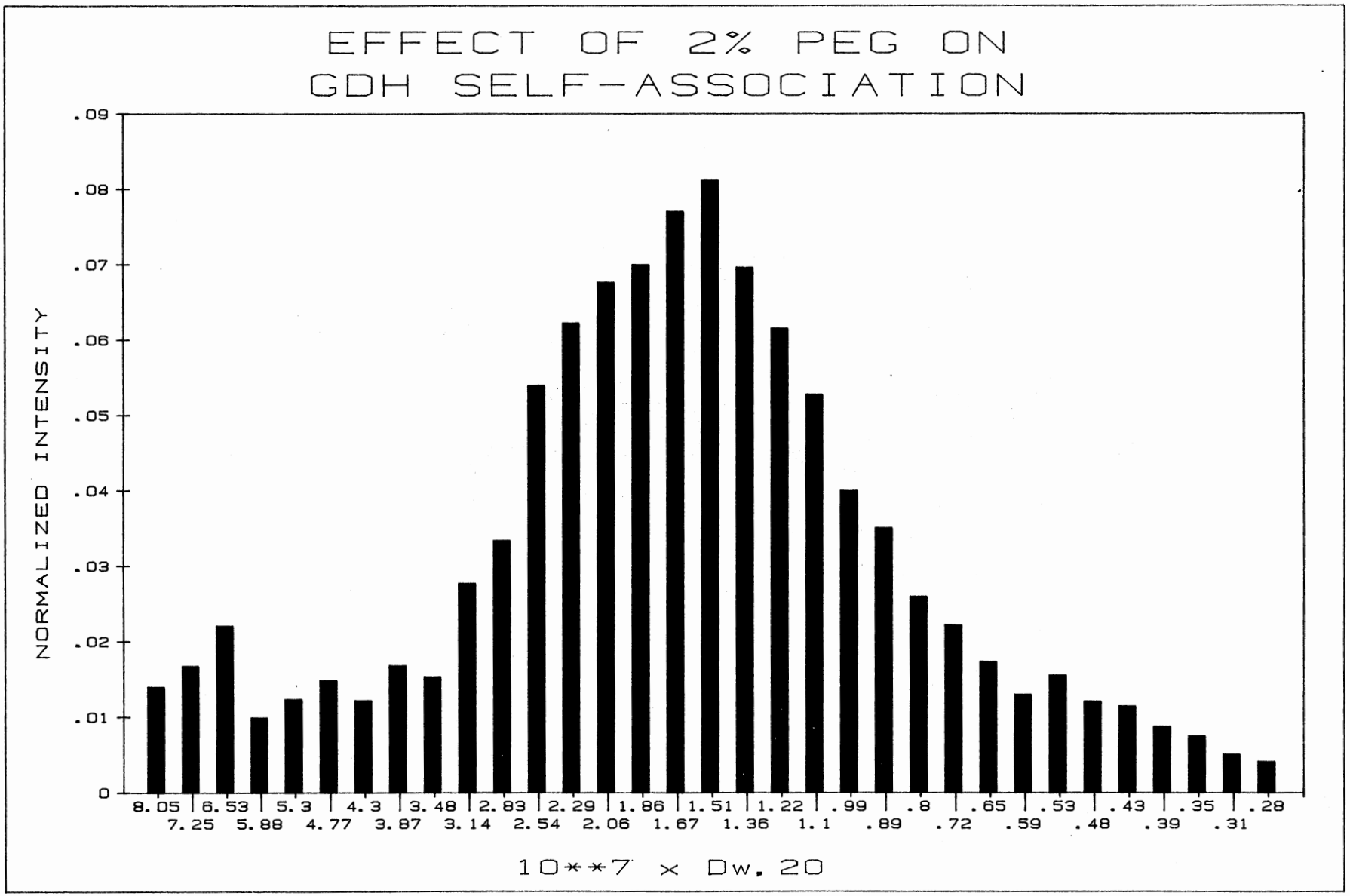
EFFECT OF 2% PEG ON
GDH SELF-ASSOCIATION
NORMALIZED INTENSITY
.09
.08
.07
.06
.05
.04
.03
.02
.01
0
8.05 6.53 5.3 4.3 3.48 2.83 2.29 1.86 1.51 1.22 .99 .8 .65 .53 .43 .35 .28
7.25 5.88 4.77 3.87 3.14 2.54 2.06 1.67 1.36 1.1 .89 .72 .59 .48 .39 .31
10**7 x Dw, 20

Figure 12. Light Scattering Intensity of GDH in 3% PEG-6000 as a Function of Diffusion Coefficient. Intensity contributions at values of D greater than approximately 4×10^{-7} cm^2/s are due to PEG contributions. Other experimental details are identical to those in Figure 9.

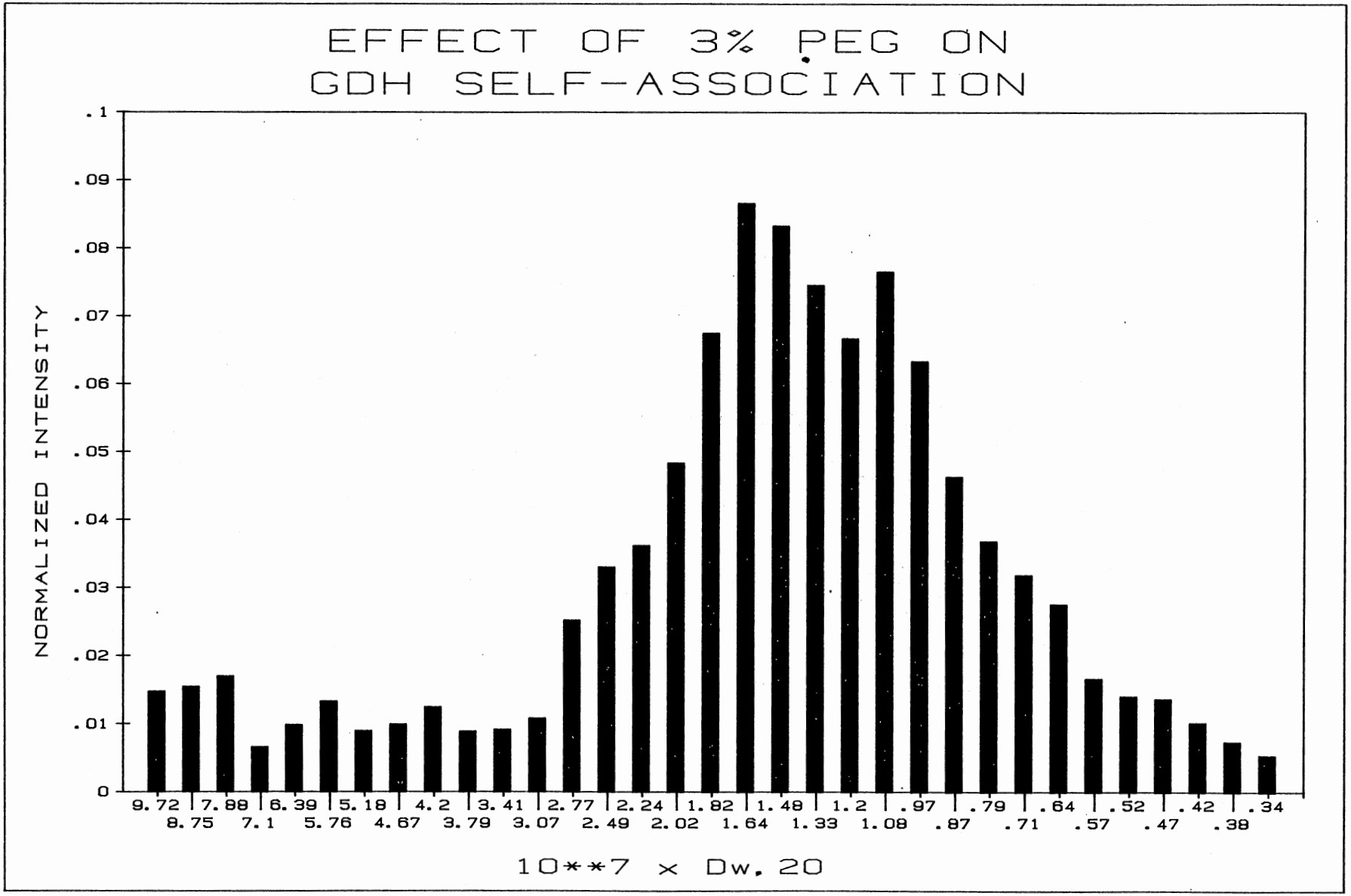
EFFECT OF 3% PEG ON
GDH SELF-ASSOCIATION
NORMALIZED INTENSITY
.1
.09
.08
.07
.06
.05
.04
.03
.02
.01
0
9.72 7.88 6.39 5.18 4.2 3.41 2.77 2.24 1.82 1.48 1.2 .97 .79 .64 .52 .42 .34
8.75 7.1 5.76 4.67 3.79 3.07 2.49 2.02 1.64 1.33 1.08 .87 .71 .57 .47 .38
10**7 x Dw, 20

without PEG, the second method was also used in order to provide a comparison of the two methods. Some details of the parameters used for and obtained from fitting to the data are contained in Table III. It is likely that the density of delta functions fit is somewhat too high. This explains the deviation from a smooth distribution observed in some sets. However, this does not significantly affect the average values subsequently calculated from these distributions.

The raw data and fitted autocorrelation function curves measured on the sample containing GDH and 3% PEG at different correlation ("delay") times are shown in Figures 13-16. The curves fit by the cumulant method deviate far more from the experimental data than do those from the delta function method. The weight-average diffusion coefficient, $\bar{D}$, and several other moments of the distribution function were calculated from the delta function fits (results in Table III). Most of the light scattering by particles with apparent diffusion coefficients greater than 4×10^{-7} cm^2/s was due to PEG. These terms were not included in the summations used to calculate the average diffusion constants. The delta functions included are specified in column 6 of Table III.

Computer Simulations of GDH Properties

Self-Association of GDH.

Glutamate dehydrogenase undergoes end-to-end self-association. This assembly follows the simple model in which the equilibrium constants for all association-dissociation steps are equal, i.e.

$$E_1 + E_i \overset{K}{\rightleftharpoons} E_{i+1};\ i=1,2,\ldots,\infty \tag{4}$$

$$K = [E_{i+1}]/([E_i][E_1]) \tag{5}$$

where the index i denotes the number of monomer units per polymer chain.

Figure 13. Autocorrelation Function of GDH in 3% PEG-6000. Correlation time is 2 μs. The solid and broken lines are calculated from the simultanous fitting of data with correlation times of 2, 5, 10, and 20 μs to the delta and cumulant functions, respectively. The fitted delta function values for these data sets are plotted in Figure 12. Standard experimental conditions were used.

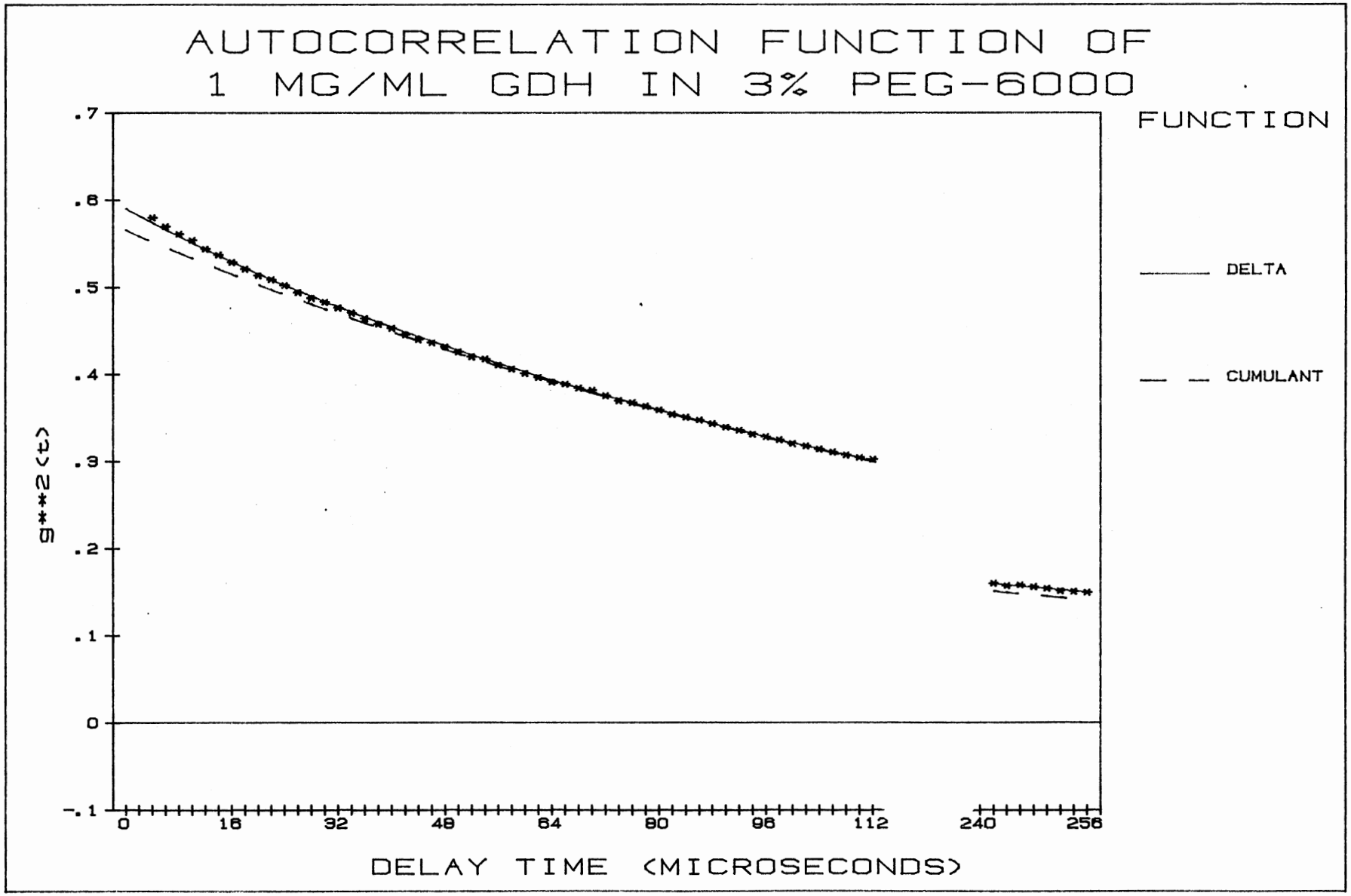
AUTOCORRELATION FUNCTION OF
1 MG/ML GDH IN 3% PEG-6000
FUNCTION
DELTA
CUMULANT
g**2(t)
.7
.6
.5
.4
.3
.2
.1
0
-.1
0
16
32
48
64
80
96
112
240
256
DELAY TIME (MICROSECONDS)

Figure 14. Autocorrelation Function of GDH in 3% PEG-6000. Correlation time is 5 μs. Details are identical to those in Figure 14.

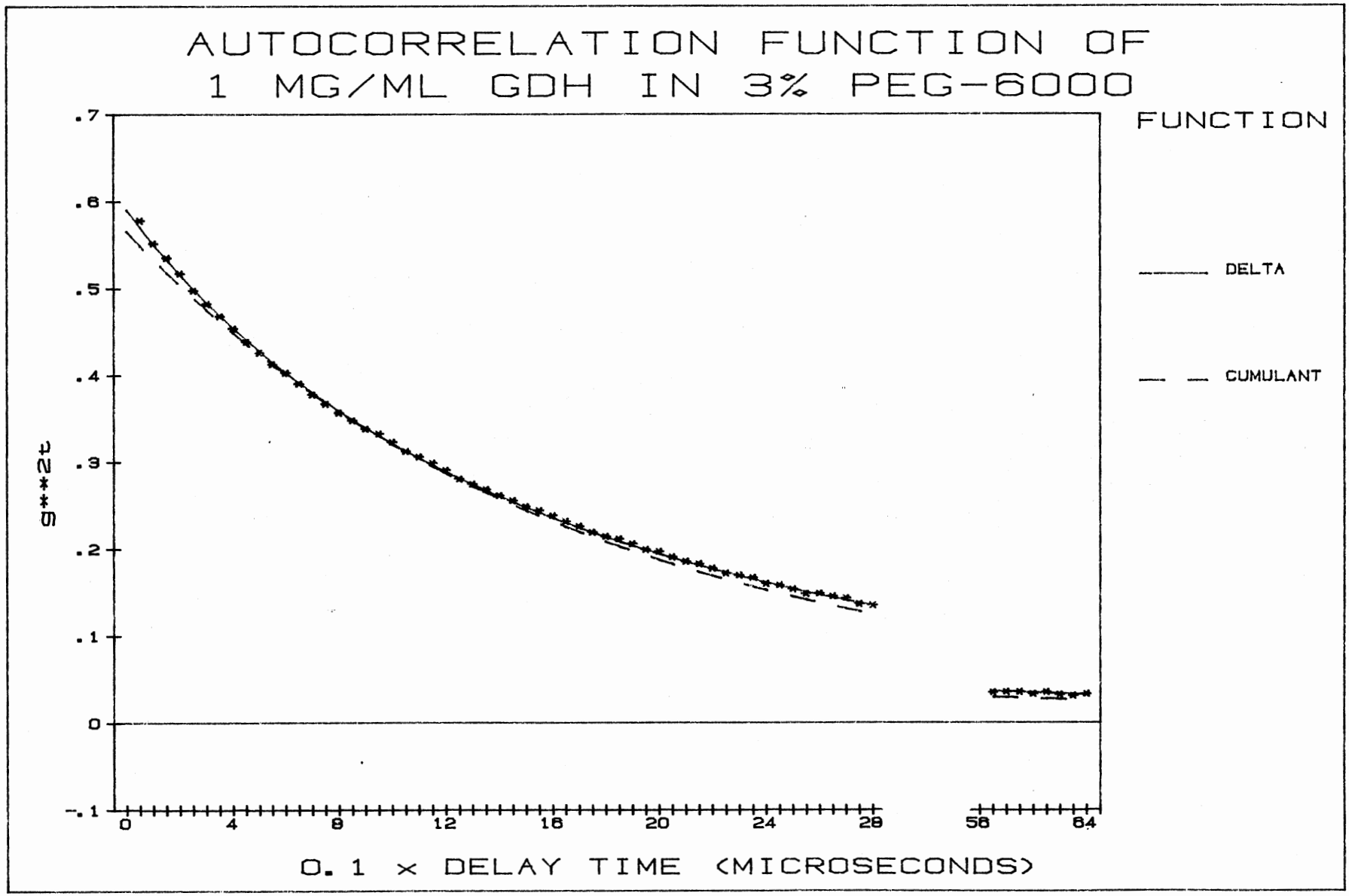
AUTOCORRELATION FUNCTION OF
1 MG/ML GDH IN 3% PEG-6000
FUNCTION
DELTA
CUMULANT
g**2t
.7
.6
.5
.4
.3
.2
.1
0
-.1
0
4
8
12
16
20
24
28
56
64
0.1 x DELAY TIME (MICROSECONDS)

Figure 15. Autocorrelation Function of GDH in 3% PEG-6000. Correlation time is 10 μs. Details are identical to those in Figure 14.

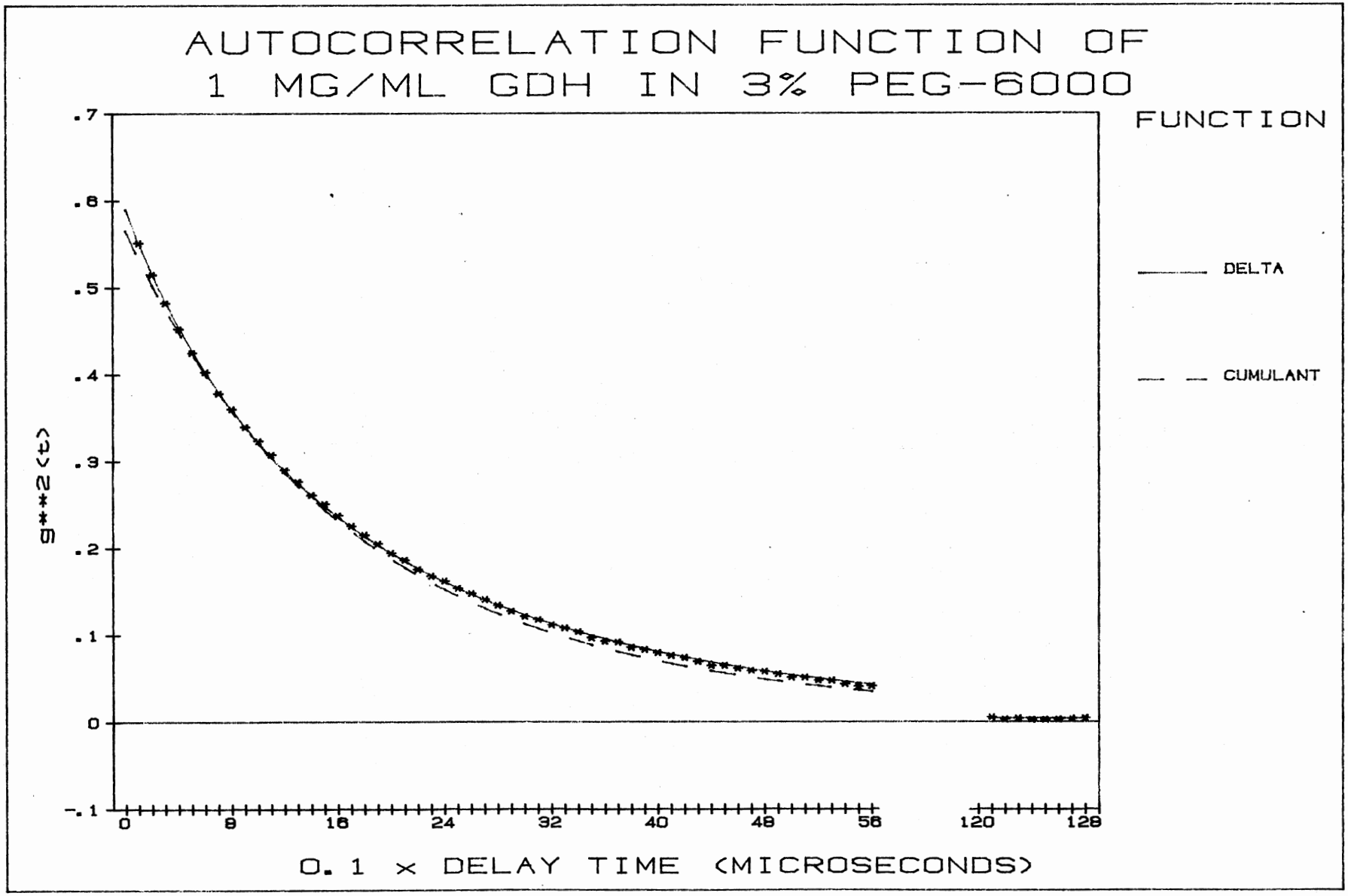
AUTOCORRELATION FUNCTION OF
1 MG/ML GDH IN 3% PEG-6000
FUNCTION
DELTA
CUMULANT
g**2 (t)
.7
.6
.5
.4
.3
.2
.1
0
-.1
0
8
16
24
32
40
48
56
120
128
0.1 x DELAY TIME (MICROSECONDS)

Figure 16. Autocorrelation Function of GDH in 3% PEG-6000. Correlation time is 20 μs. Details are identical to those in Figure 14.

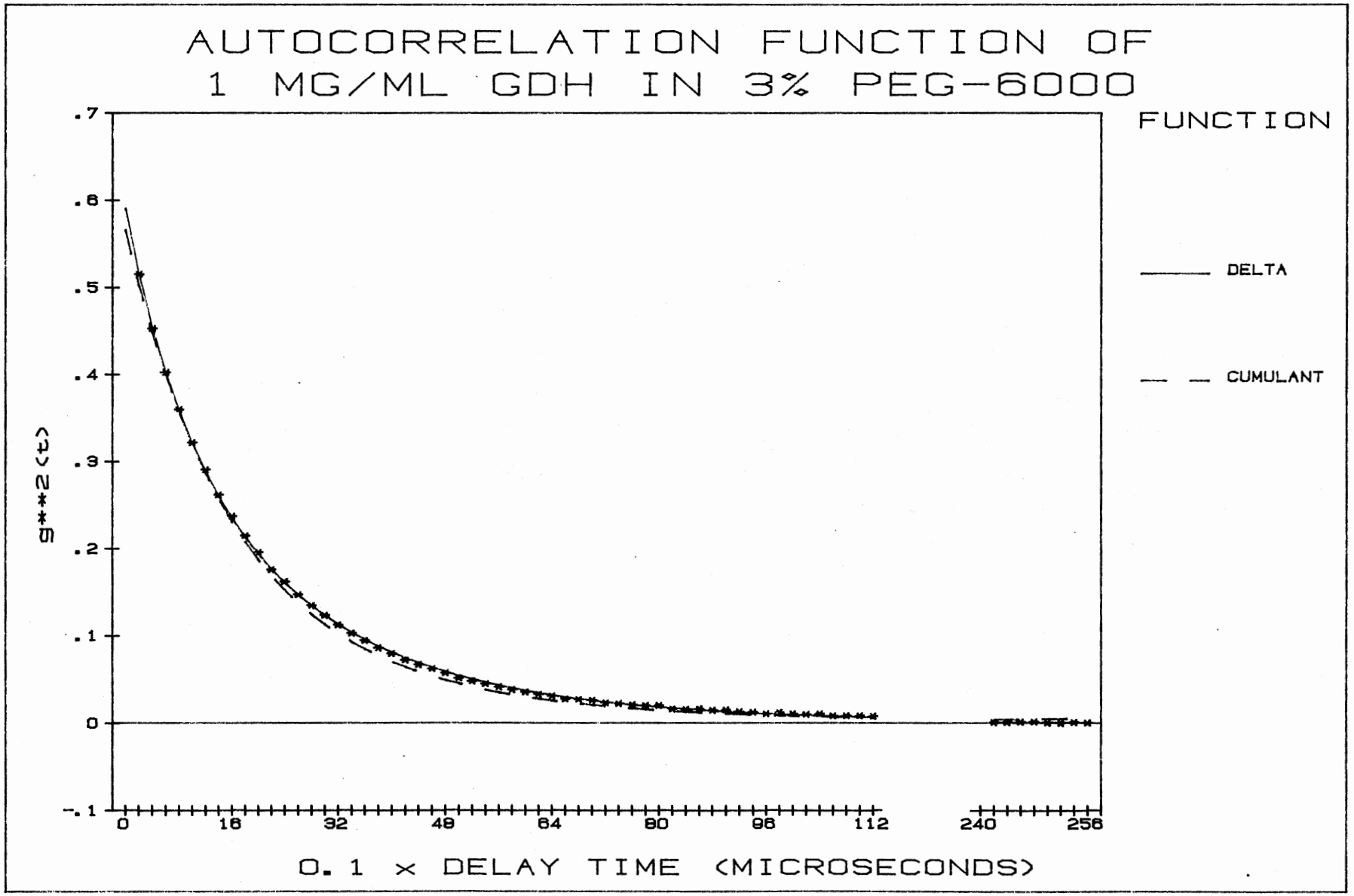
AUTOCORRELATION FUNCTION OF
1 MG/ML GDH IN 3% PEG-6000
FUNCTION
DELTA
CUMULANT
g**2(t)
.7
.6
.5
.4
.3
.2
.1
0
-.1
0
16
32
48
64
80
96
112
240
256
0.1 x DELAY TIME (MICROSECONDS)

TABLE III

$\overline{D}_{20,w}$ FROM DYNAMIC LIGHT SCATTERING

[PEG]-6000 (% w/v)	Γ_{max}	$10^7 D^{max}_{20,w}$ cm^2/s	w_{max}	N	Delta Values Included	$10^7 \overline{D}$ cm^2/s	$10^{14}\mu_2$	$10^{20}\mu_3$	$10^{26}\mu_4$
3	16656	9.72	10	11	9 - 33	1.42	4.47	2.68	1.86
	15000	8.75							
	13509	7.88							
2	16656	8.05	10	11	7 - 33	1.63	3.08	1.29	0.68
	15000	7.25							
	13509	6.53							
1	16368	6.38	12	11	6 - 33	1.81	1.60	0.34	0.13
	15000	5.84							
	13746	5.35							
0	16368	5.17	12	10	3 - 30	1.93	1.01	0.11	0.04
	15000	4.73							
	13746	4.33							
0	15000	4.73	4	4	1 - 12	1.96	0.99	0.09	0.03
	11545	3.64							
	8886	2.80							

Description of fitting parameters and resulting calculated mean values. For an interpretation of each column, see Appendix E.

For such a scheme the concentration of all species is given by

$$[E_i] = [E_1]([E_1]K)^{i-1} \qquad (6)$$

as can be demonstrated by recursive substitution in Equation 5. Using the conservation equation, $c_t = \sum_{i=1}^{M} i[E_i]$, and since $\sum ix^{i-1} = 1/(1-x)^2$ we find that

$$[E_1] = [1+2c_tK/M_1 - (1+4c_tK/M_1)^{1/2}]/(2c_tK^2/M_1) \qquad (7)$$

where K is the equilibrium constant,

c_t is the total weight concentration of E, and

M_1 is the molecular weight of E_1.

The association constant is dependent upon temperature, ionic strength, and allosteric effectors. In addition, saturation of a GDH solution with toluene greatly enhances the extent of association.

By defining a new constant, $K' = c_tK/M_1$, the normalized distribution of enzyme species, c_i/c_t, becomes a function of only K'. The weight concentration of E_i is c_i. This distribution is shown for various values of K' in Figure 17.

The number average molecular weight, M_n, equals $\Sigma c_i/\Sigma(c_i/M_i)$ for polydisperse distributions of species. For GDH, $M_i = iM_1$. Therefore

$$M_n/M_1 = \Sigma c_i/\Sigma(c_i/i) \qquad (8)$$

and is strictly a function of K'. Similiarly, the normalized weight average molecular weight, M_w/M_1, equals $\Sigma(ic_i)/\Sigma c_i$, and the normalized z average molecular weight, M_z/M_1, equals $\Sigma(i^2c_i)/\Sigma(ic_i)$.

Translational Diffusion and Sedimentation Coefficients. Thusius et. al. (34) have shown that the ratio of the diffusion coefficient between polymer, D_i, and monomer, D_1, for GDH is given by assuming frictional coefficients appropriate for a prolate ellipsoids for both polymeric and monomeric GDH.

Figure 17. Normalized Distribution of GDH Polymeric Forms, c_i/c_t, as a Function of K' (= Kc_t/M_1). Molar concentrations corresponding to these weight concentrations were calculated from Equations 6 and 7 of this chapter. A) K'=0.1 B) K'=1.0 C) K'=5.0

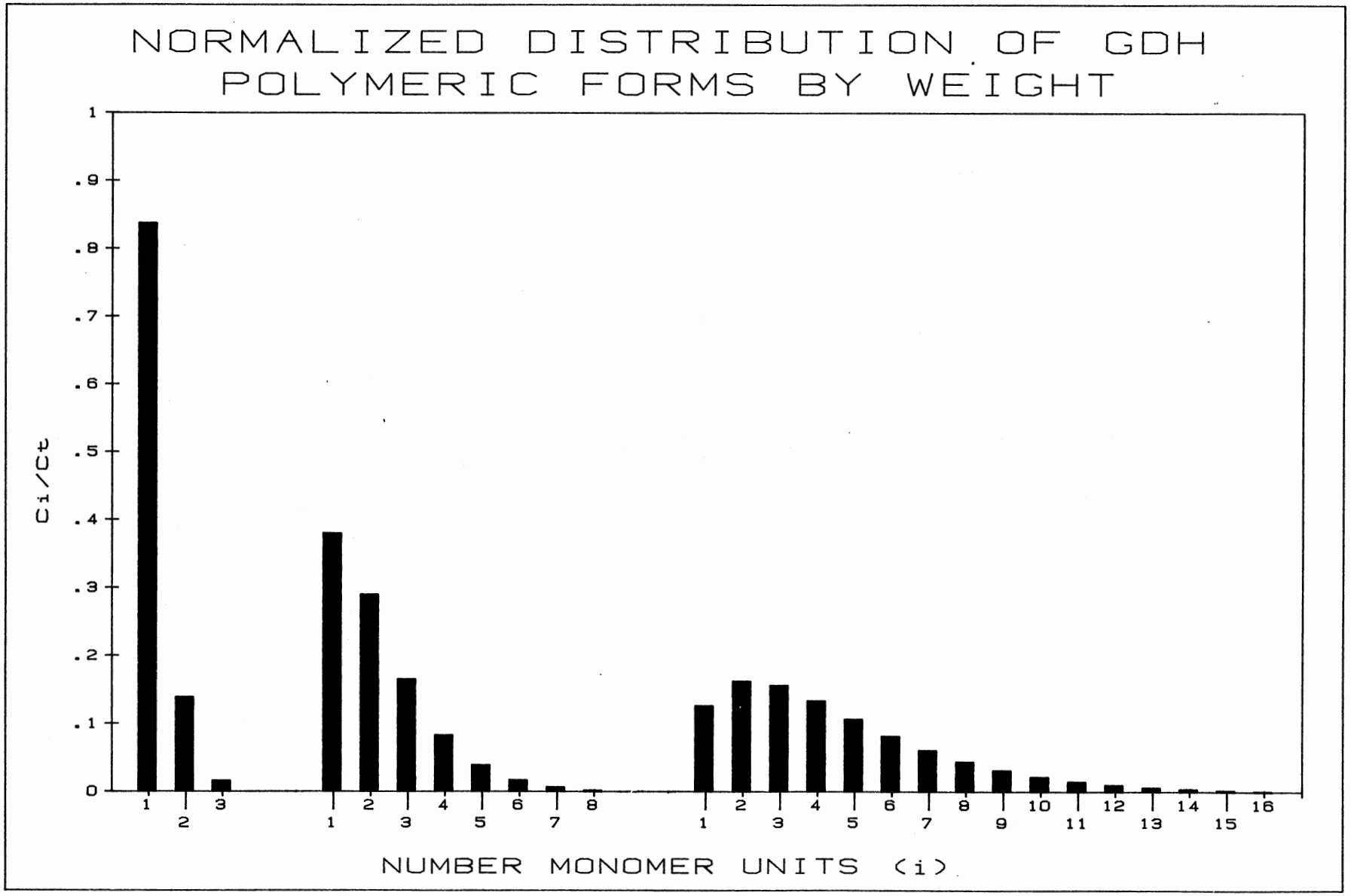
NORMALIZED DISTRIBUTION OF GDH
POLYMERIC FORMS BY WEIGHT
Ci/Ct
1
.9
.8
.7
.6
.5
.4
.3
.2
.1
0
1 2 3
1 2 3 4 5 6 7 8
1 2 3 4 5 6 7 8 9 10 11 12 13 14 15 16
NUMBER MONOMER UNITS (i)

$$\frac{D_i}{D_1} = \frac{(1-\xi_1^{-2})^{0.5}\ln[(1+(1-i^{-2}\xi_1^{-2})^{0.5})i\xi_1]}{i(1-i^{-2}\xi_1^{-2})^{0.5}\ln[(1+(1-\xi_1^{-2})^{0.5})\xi_1]}$$

where ξ_1 = b/a; the equivalent ratio for $E_i = i\xi_1$.

b = major axis of monomer unit, and

a = minor axis of monomer unit

Since

$$M_i = (s_i/D_i)\,(1-\bar{v}\rho)/RT \tag{10}$$

where $\bar{v}$ is the partial specific volume of the protein, and

ρ is the density of the solution, then

$$M_i/M_1 = (s_i/D_i) \,/\, (s_1/D_1) \tag{11}$$

But

$$M_i = iM_1 \tag{12}$$

Therefore,

$$s_i/s_1 = iD_i/D_1 \tag{13}$$

Thusius (34) initially assumed $\xi_1 = 1.5$. This proved to be too large to fit experimentally determined values of $\bar{D}/D_1$. Rather than use different dimensions for monomeric GDH, Thusius postulated that, with respect to its hydrodynamic properties, the enzyme could be more closely modelled as a rod with a length to diameter ratio of L/d than as a prolate ellipsoid with axial ratio b/a. Tanford (35) has shown that the hydrodynamic properties of such a rod are the same as those of a prolate ellipsoid with axial ratios given by

$$(b/a)' = (2/3)^{0.5}L/d \tag{14}$$

Let ξ' be equal to $(b/a)'$. If L/d is 1.5 for monomeric GDH, then ξ' is 1.21. $(\xi_i)'$ is now substituted for ξ_i in equation 9, and values of s_i/s_1 and D_i/D_1 are calculated as before. Given these results, Thusius

was able to adequately fit the experimentally measured values of $\overline{D}/D_1$ with a single constant K' using the results of equations 6 above and 19 and 20 below. However, it was probably not necessary to treat GDH as a rod. Thusius appears to have used incorrect dimensions for GDH and obtained an erroneouly high value for ξ_1. Electron micrographs of GDH indicate axes of 11.0 nm by 8.5 nm, or $\xi_1 = 1.294$ (36). This is not unlike the value of $(\xi_1)'$ used by Thusius with acceptable results. For $\xi_1 = 1.294$, D_i/D_1 and s_i/s_1 are presented in Figures 18 and 19, respectively.

Since at even moderate concentrations many different polymeric species of GDH are present, we will define the mean sedimentation coefficient, $\overline{s}$, as follows:

$$\overline{s} = \Sigma c_i s_i / c_t \tag{15}$$

Since c_i/c_t is fixed by K' for GDH, then $\overline{s}/s_1$ is a function solely of ξ_1 and K'. This dependence is shown in Figure 20.

If particle diffusion is measured by quasielastic light scattering, then the D_i's are weighted by the average light scattering intensity $\langle I \rangle_i$ of each species present. That is,

$$\overline{D} = \Sigma \langle I_i \rangle D_i / \langle I \rangle_{tot} \tag{16}$$

$\langle I_i \rangle$ is proportional to $M_i c_i$ $(= iM_1 c_i)$. However, as the length of the rod exceeds $\lambda/20$ where λ is the wavelength of the light in solution, then there is some loss due to destructive interference.

$$\langle I_i \rangle \propto iP_i M_1 c_i \tag{17}$$

where P is the ratio of scattering intensity in the presence of destructive interference to that in its absence. For a long thin rod,

$$P = (2/qL) \int_0^{qL} (\sin u/u)du - [\sin(qL/2)/(qL/2)]^2 \tag{18}$$

Figure 18. Relative Diffusion Coefficients, D_i/D_1, for GDH. This is shown as a function of both polymer size in monomer units (i) and for three different presumed monomer axial ratios, ξ_1. The results were calculated from Equation 9 of this chapter.

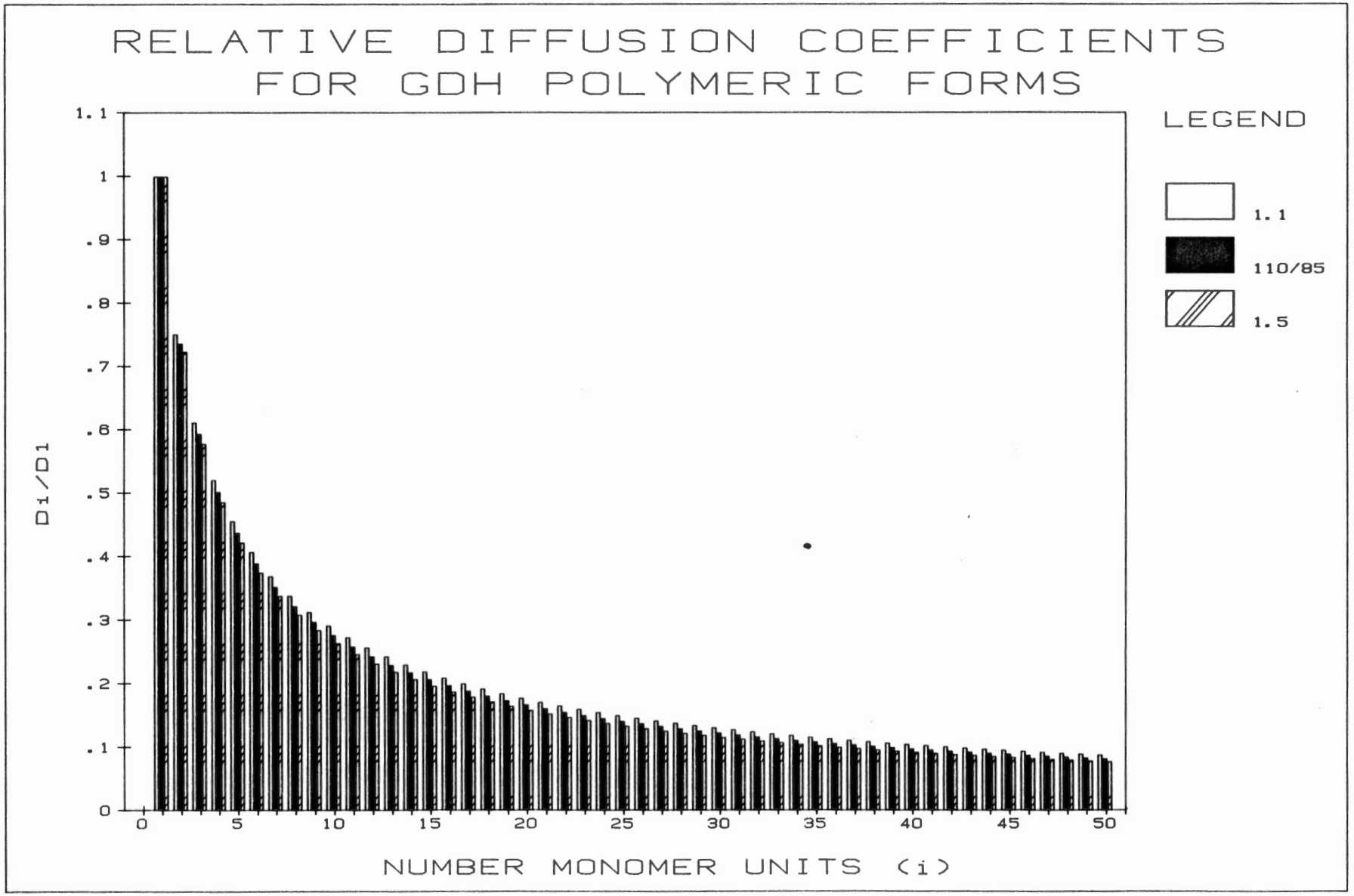
RELATIVE DIFFUSION COEFFICIENTS
FOR GDH POLYMERIC FORMS
LEGEND
1.1
110/85
1.5
Di/D1
1.1
1
.9
.8
.7
.6
.5
.4
.3
.2
.1
0
0
5
10
15
20
25
30
35
40
45
50
NUMBER MONOMER UNITS (i)

Figure 19. Relative Sedimentation Coefficients, s_i/s_1, for GDH. This ratio was calculated from Equations 13 and 19. The results are shown as a function of both polymer size in monomer units (i) and for three different assumed values of the monomer axial ratios, ξ_1.

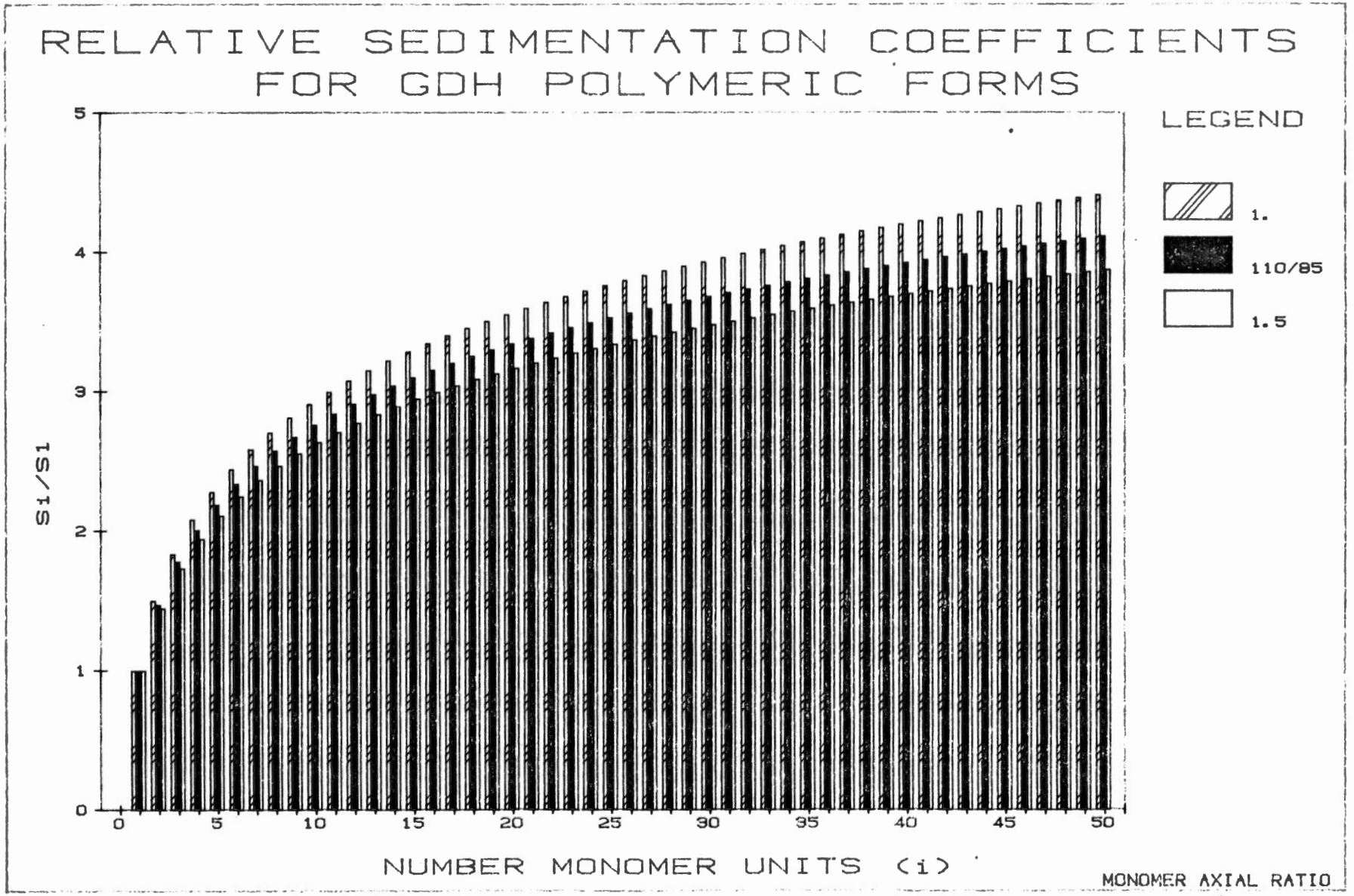
RELATIVE SEDIMENTATION COEFFICIENTS
FOR GDH POLYMERIC FORMS
LEGEND
1.
110/85
1.5
Si/S1
0
1
2
3
4
5
0
5
10
15
20
25
30
35
40
45
50
NUMBER MONOMER UNITS (i)
MONOMER AXIAL RATIO

Figure 20. Normalized Average Sedimentation Coefficients, $\bar{s}/s_1$, for GDH as a Function of K' ($= Kc_tM_1$). Results were calculated from Equation 15 and are shown for three different presumed values of the monomer axial ratio, ξ_1.

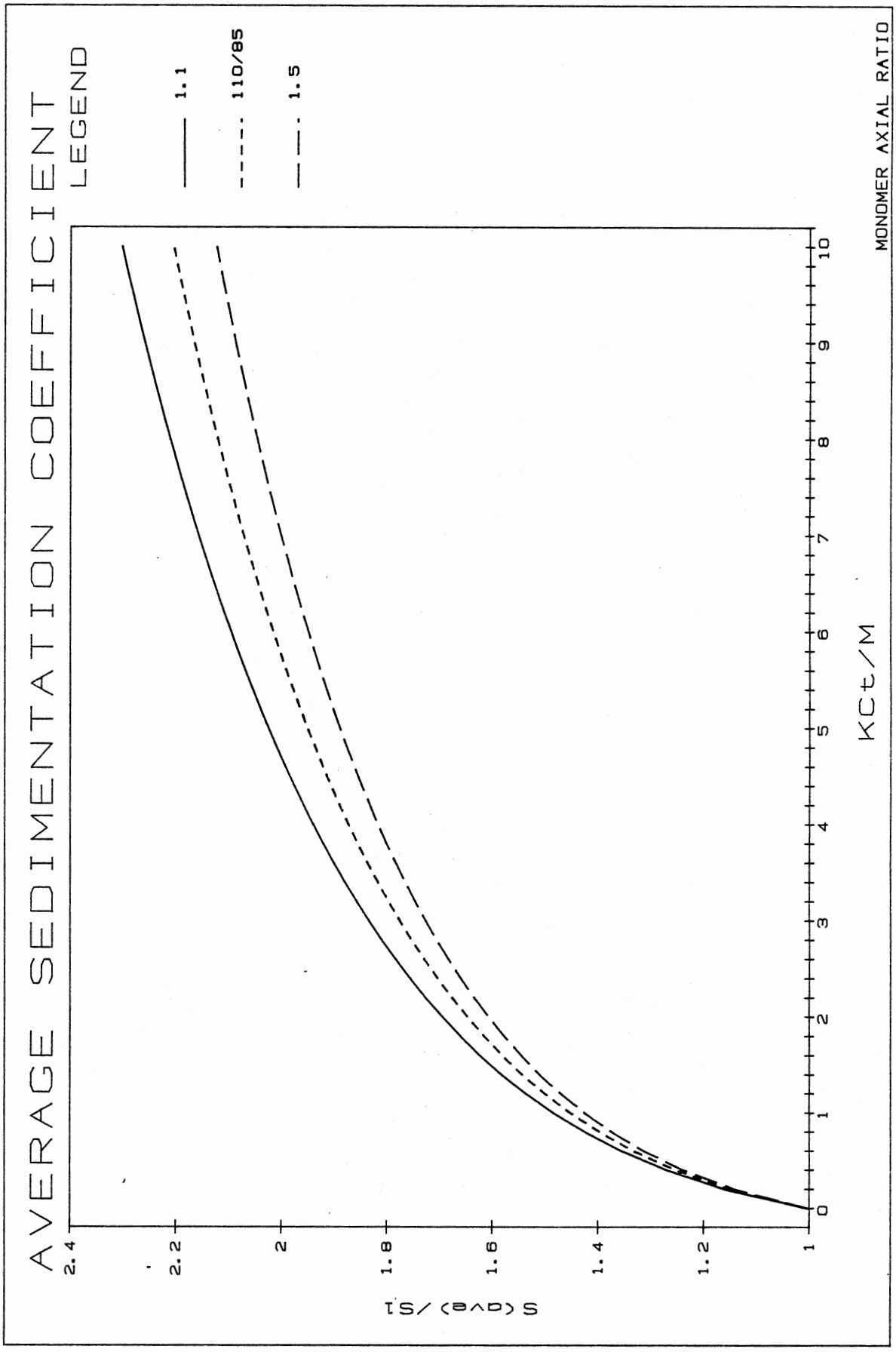
AVERAGE SEDIMENTATION COEFFICIENT
LEGEND
1.1
110/85
1.5
S <Q v e> /S1
2.4
2.2
2
1.8
1.6
1.4
1.2
1
0
1
2
3
4
5
6
7
8
9
10
KCt/M
MONOMER AXIAL RATIO

where L = length of rod,

$q = 4\pi n \lambda_0 \sin(\theta/2)/\lambda_0$.

n = refracive index of the solution,

λ_0 = wavelength of incident light in vacuo, and

θ = angle of observation.

The ratio of scattering intensity of the translational component of the diffusion coefficient to the total is given by

$$P_{trans} = [(2/qL)\int_0^{qL/2}(\sin u/u)du]^2 \quad (19)$$

Figure 21 presents these values for various polymeric forms of GDH, assuming the length of E_i = i * length of monomer (11.0 nm). P is approximately equal to P_{trans} for forms containing up to 20 monomeric units for λ of 514.5 nm, n of 1.33, and θ of $\pi/2$ radians. Thus the contribution of all other terms including those for rotational diffusion are insignificant for the GDH forms in solution under the experimental conditions used. Then

$$\overline{D} = \Sigma iP_i c_i D_i \; / \; \Sigma iP_i c_i \quad (20)$$

and, as for $\overline{s}$, $\overline{D}/D_i$ is solely a function of K' and ξ_1. Figure 22 shows this dependence.

Relationship between $\overline{s}$,$\overline{D}$, and Mw. Let us first consider the case in which P_i is 1 for all species present. Then

$$\overline{s} = \Sigma c_i s_i / c_t \quad (21)$$

$$\overline{D} = \Sigma ic_i D_i / \Sigma ic_i \quad (22)$$

$$M_w/M_i = \Sigma ic_i / \Sigma c_i = \Sigma ic_i / c_t \quad (23)$$

$$\overline{s}/\overline{D} = \Sigma c_i s_i / c_t * \Sigma ic_i / \Sigma ic_i D_i \quad (24)$$

$$\overline{s}/\overline{D} = M_w/M_1 * \Sigma c_i s_i / \Sigma ic_i D_i \quad (25)$$

But

Figure 21. Total and Translational P Factors for GDH Polymeric Forms. Values for the total P factor and the translational component of this factor were calculated from Equations 18 and 19, respectively, assuming a light source with a wavelength of 514.5 nm, an observation angle of 90°, and a GDH monomer length of 11.0 nm.

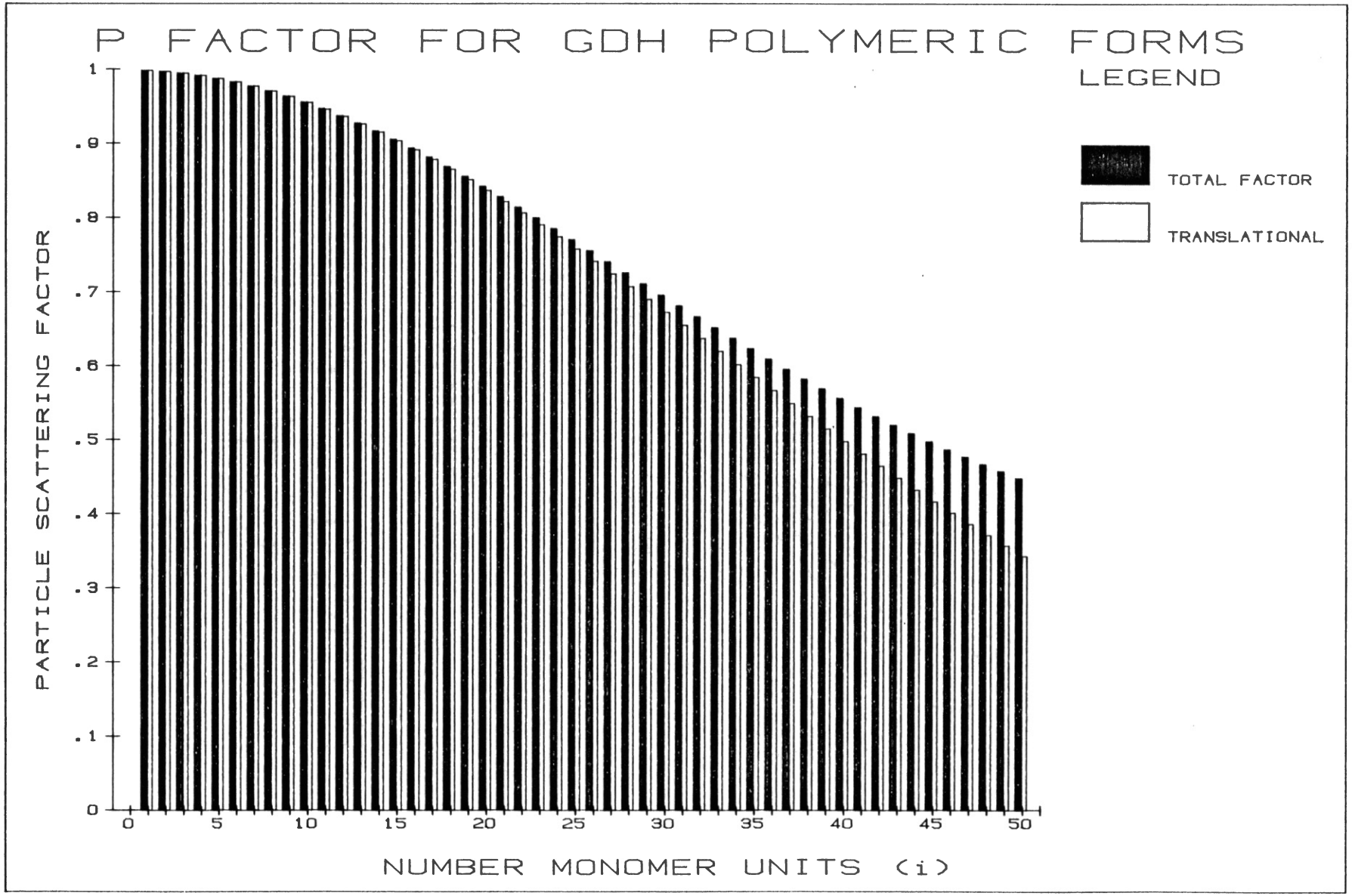
P FACTOR FOR GDH POLYMERIC FORMS
LEGEND
TOTAL FACTOR
TRANSLATIONAL
PARTICLE SCATTERING FACTOR
0
.1
.2
.3
.4
.5
.6
.7
.8
.9
1
0
5
10
15
20
25
30
35
40
45
50
NUMBER MONOMER UNITS (i)

Figure 22. Normalized Average Diffusion Coefficients, $\bar{D}/D_1$, for GDH as a Function of K' ($= Kc_tM_1$). Results were calculated from Equation 20 and are shown assuming three different values for the monomer axial ratio, ξ_1. The P factors used in Equation 20 are those shown for the total P factor as a function of polymer size in Figure 21.

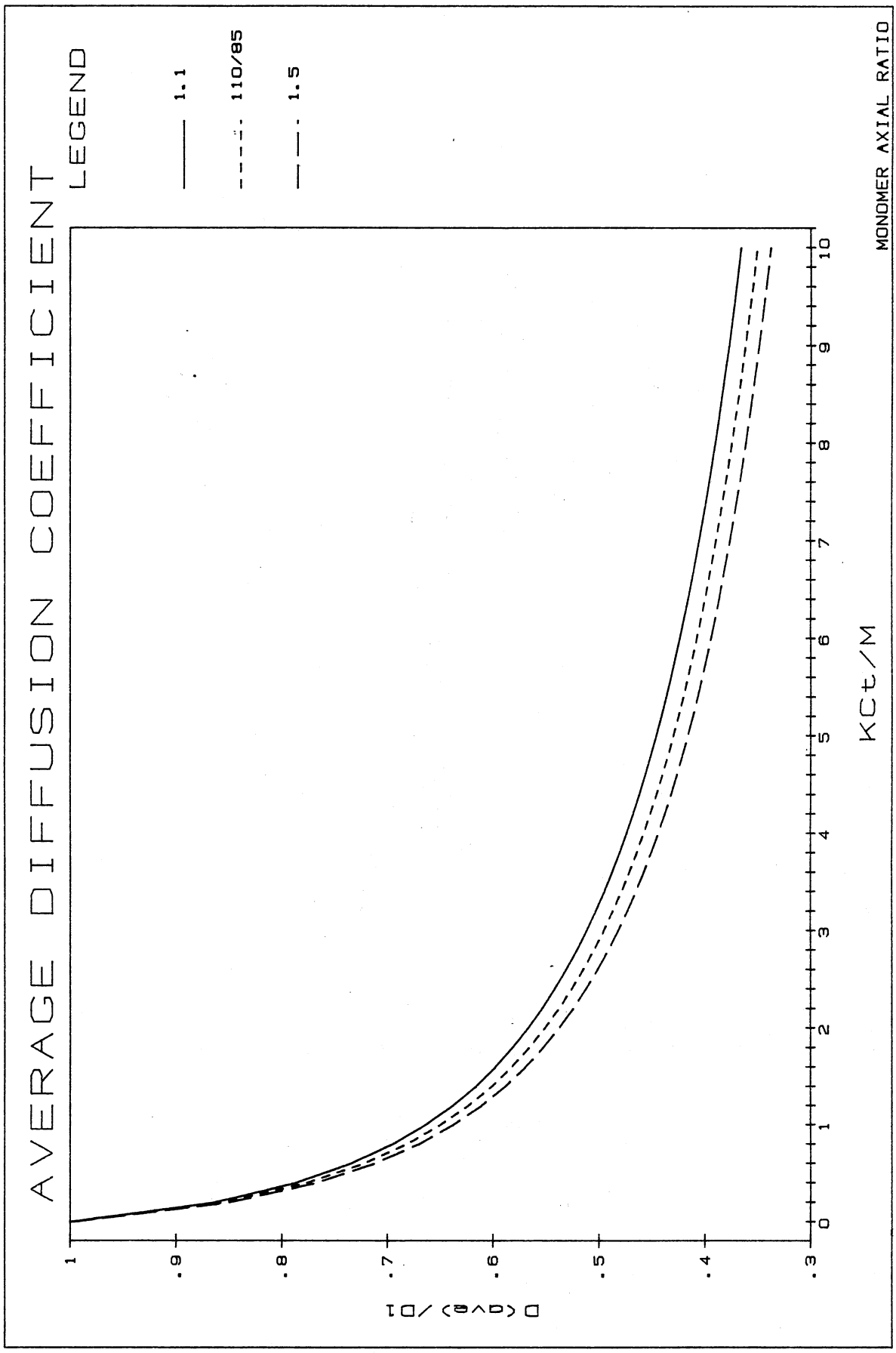
AVERAGE DIFFUSION COEFFICIENT
LEGEND
1.1
110/85
1.5
D (Qv@) /D1
1
.9
.8
.7
.6
.5
.4
.3
0
1
2
3
4
5
6
7
8
9
10
KCt/M
MONOMER AXIAL RATIO

$$s_i = iD_i s_1/D_1 \tag{26}$$

$$\overline{s/D} = M_w/M_1 * \Sigma c_i(iD_i s_1/D_1)/\Sigma ic_i D_i \tag{27}$$

$$\overline{s}/\overline{D} = M_w/M_1 * s_1/D_1 \tag{28}$$

Therefore

$$M_w = \overline{s/D} * D_1/s_1 * M_1 \qquad P_i = 1 \tag{29}$$

However, P_i is not equal to 1. In this case, it may be shown that

$$M_w = \overline{s/D} * D_1/s_1 * M_1 * (\Sigma ic_i/\Sigma ic_i D_i) * (\Sigma ic_i P_i D_i/\Sigma ic_i P_i) \tag{30}$$

The product of the last two terms is very close to, but slightly greater than, one. This product is less sensitive to the axial ratio than either s or D alone, and is essentially constant for $0.1<\xi_1<1.5$. Thus M_w can be estimated quite accurately from $\overline{s}$ and $\overline{D}$. The dependence of M_z/M_1, M_w/M_1, M_n/M_1, and $(\overline{s}/\overline{D})$ / (s_1/D_1) on K' $(=Kc_t/M_1)$ are presented in Figure 23.

Effect of PEG on K

The dependence of the GDH self-association constant K on [PEG-6000] was calculated from the experimentally measured values of $\overline{s}$ and $\overline{D}$ and literature values for s_1 and D_1 using the results of the previous section. This dependence is shown in Figure 24 for K values calculated from $\overline{s}/s_1$, $\overline{D}/D_1$, and the ratio of these two values. For the curves shown, axial ratios ξ_1 of 1.5, 110/85 (≃ 1.3), and 1.1 were used for monomeric GDH, where the 110/85 ratio corresponds to that determined by electron microscopy (36). For a given PEG concentration, the value of K estimated from $\overline{s}/s_1$ is always less than that estimated from $\overline{D}/D_1$, although the difference decreases as the axial ratio used in the calculations is increased. At an axial ratio of 1.7, the two different methods give approximately the same values for K for all PEG

Figure 23. Normalized Average Molecular Weights, $\bar{M}/M_1$, as a Function of K' (= Kc_tM_1). Values of $(\bar{s}/D)/(s_1/D_1)$ were calculated from the results shown in Figures 20 and 22. The calculation of the average molecular weights is discussed in the text.

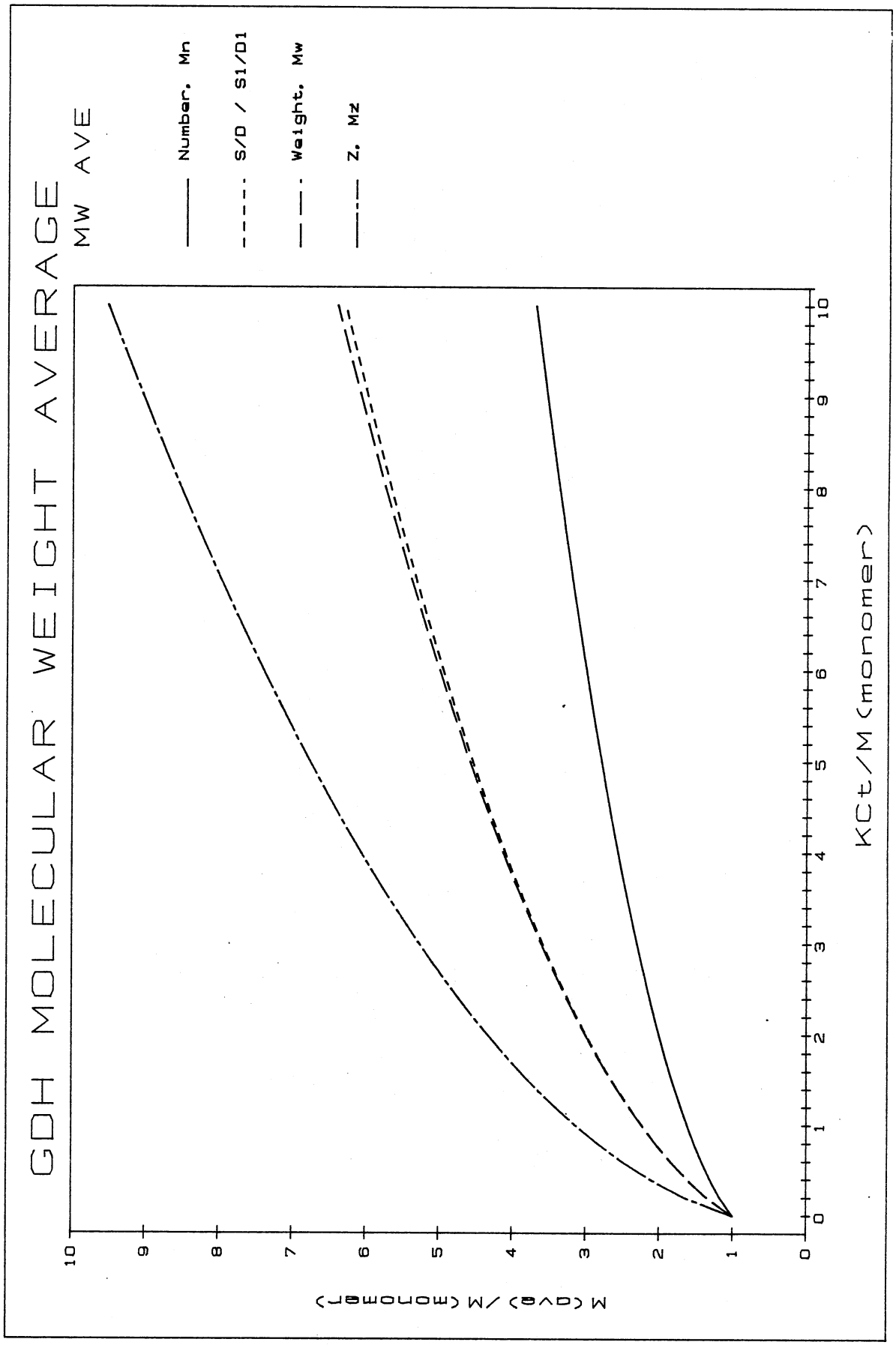
GDH MOLECULAR WEIGHT AVERAGE
MW AVE
Number, Mn
S/D / S1/D1
Weight, Mw
Z, Mz
M (Dv0) /M (monomer)
KCt/M (monomer)
0
1
2
3
4
5
6
7
8
9
10

Figure 24. GDH Association Constant, K, as a Function of [PEG-6000]. K was calculated from s/s_1, D/D_1, and $(s/D)/(s_1/D_1)$. The first two results depend on the monomer axial ratio assumed for GDH. Therefore the calculated values of K are shown for three different ratios.

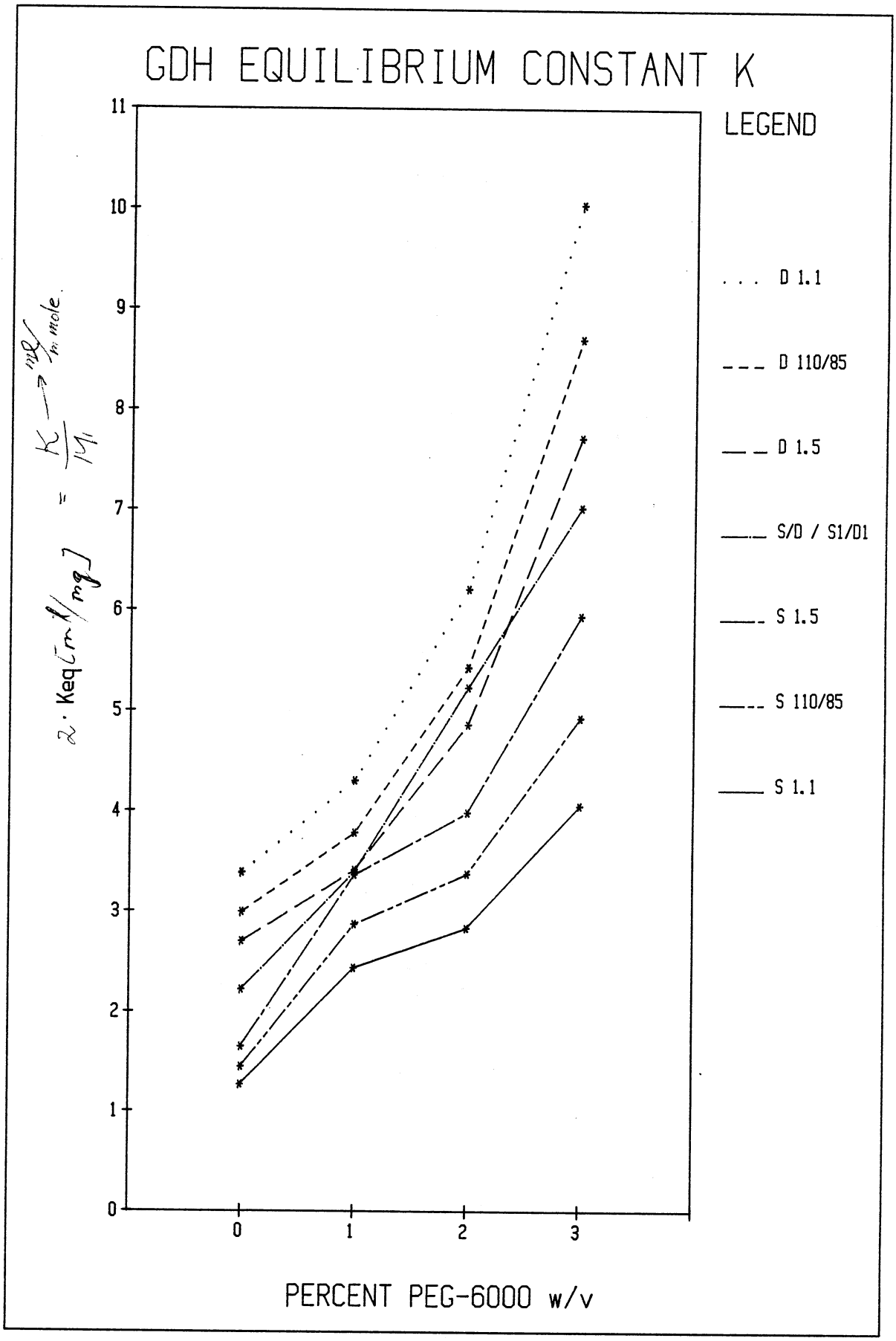
GDH EQUILIBRIUM CONSTANT K
LEGEND
D 1.1
D 110/85
D 1.5
S/D / S1/D1
S 1.5
S 110/85
S 1.1
11
10
9
8
7
6
5
4
3
2
1
0
0
1
2
3
PERCENT PEG-6000 w/v

concentrations employed. However, such an axial ratio for monomeric GDH is much larger than expected on the basis of known monomer dimensions. A likely cause for this is the nonideal contributions to experimental s values. Such nonideality causes s to vary with protein concentration and Equations 9 ff become inaccurate. Empirically, the variation is adequately described in most cases (37) by

$$s = s_0 - bc \tag{31}$$

where s_o is the true sedimentation coefficient obtained by extrapolation of experimental s values to zero protein concentration c.
Equations 9 ff require the true coefficients s_0. For a polymerizing enzyme like GDH, we will use Equation 31 to describe the average values of $\bar{s}$ and $\bar{s}_o$ as well. However, in this case it is not possible to obtain $\bar{s}_o$ by varying c since this will alter the distribution of enzyme forms. Only s_0 for the monomeric enzyme can be determined by extrapolation to zero concentration.

To determine $\bar{s}_o$ for the finite GDH concentrations used in our experiments (1 and 2 mg/ml), we will make use of the fact that nonideality causes much less variation (concentration dependence) in D values determined by DLS than in s values (34). For example, with GDH, strong deviations in $\bar{s}$ are noted at GDH concentrations c at 3-5 mg/ml (38). Similarly large deviations in static light scattering are not observed until about 10 mg/ml (39), and DLS data are considered to be even less sensitive to nonideality. Thus we will use equations 6, 7, 9, 13, 15, 18, and 20 of this chapter to calculate a true $\bar{s}_o$ from DLS data. From this calculated $\bar{s}_0$ value and the experimental $\bar{s}$ value on the same system (e.g., GDH at 2 mg/ml), the magnitude of the b coefficient can be calculated from equation 31. An average b value may also be calculated

from several such calculations. We then use this estimate of b to correct all experimental $\overline{s}$ values to the true constants $\overline{s}_o$ needed in Equations 9 ff for calculating the GDH association constants from sedimentation velocity data. I have chosen to use the $\overline{s}$ values for 1 and 2 mg/ml GDH in buffer (no PEG, Table I) and the corresponding value of $\overline{D}$ for 1 mg/ml GDH to estimate b values in this way. The resulting value for b is 2.55. When the $\overline{s}$ values of Table I are corrected in this way, the K values calculated by all three methods (s, s/D, and D) agree quite well for each PEG concentraion as shown in Figure 25.

The good agreement among GDH association constants calculated in these three ways suggests two useful conclusions. Since the value of K calculated from the s/D ratio depends very little on the axial ratio values in contrast to the other two methods of calculation, the agreement indicates that the correct values of axial ratios are used. Thus we conclude that GDH polymers are linear end-to-end associations of monomer units in the presence or absence of PEG. Since PEG can provide considerable free energy favoring conformational transitions to compact spherical protein forms (2), it would not have been surprising to find a different structure of polymerized GDH in the presence of PEG. Another conclusion from our results is that the coefficient b in Equation 31 is reasonably constant and independent of GDH and PEG concentrations. This technique of using DLS data to correct s values for non-ideal effects may be useful for characterizing other associating macromolecules.

Evaluation of Possible Mechanism for the Effects of PEG on GDH

Clearly, PEG enhances GDH self-association. A possible mechanism

Figure 25. The Association Constant, K, for GDH as a Function of [PEG-6000]. The assumed monomer axial ratio is 110/85. The average sedimentation coefficents were corrected for nonideality as discussed in the text.

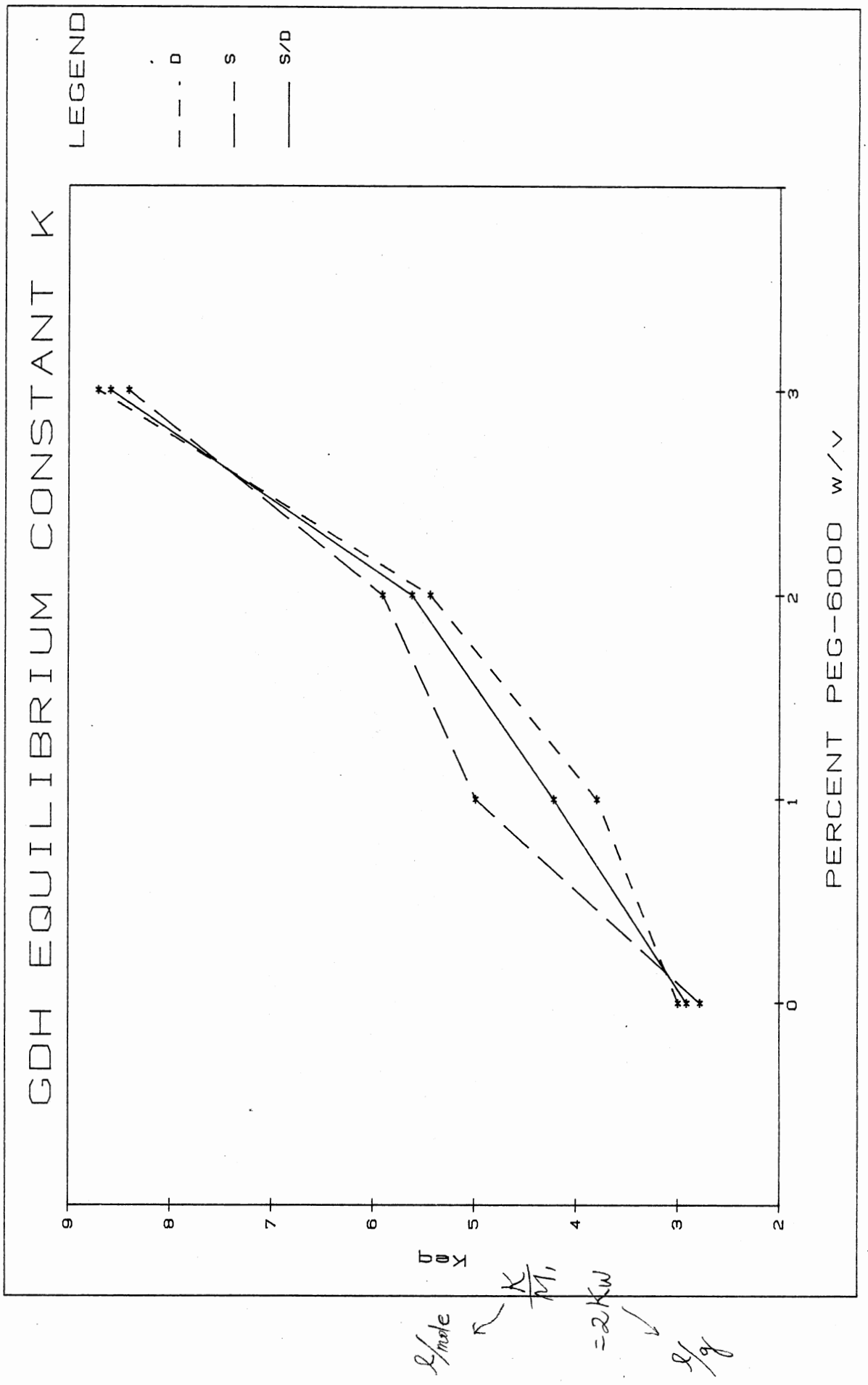
GDH EQUILIBRIUM CONSTANT K
LEGEND
D
S
S/D
K_{av}
PERCENT PEG-6000 w/v
9
8
7
6
5
4
3
2
0
1
2
3
l/mole
$\frac{K}{M_1}$
$=2K_W$
l/g

is through excluded volume effects, which alter chemical potentials and free energies promoting protein associations and transitions to more compact comformations. Minton has described calculations of these free energies contributed by excluded volumes (2). Similiar calculations applied to the PEG-GDH system are described in the following paragraphs. We wish to decide whether the PEG effects on the association of GDH can be explained by an excluded volume mechanism.

Consider a system containing N molecular species in thermodynamic equilibrium as indicated by equation 4:

$$n_1X_1 + n_2X_2 + \ldots + n_iX_i \rightleftharpoons n_{i+1}X_{i+1} + n_{i+2}X_{i+2} + \ldots + n_NX_N \quad (32)$$

The chemical potential of any one of the species is given by

$$\mu_j = \mu_j^o + RT\ln\gamma_jC_j \quad (33)$$

where C_j and γ_j are the molar concentration and activity coefficients for the j^{th} species.

This is equivalent to

$$\mu_j = \mu_j^o + RT\ln C_j + \mu_{NI,j} \quad (34)$$

where the nonideal component of the chemical potential for the j^{th} species, $\mu_{NI,j}$, equals $RT\ln\gamma_j$. When applied to reactions, Equation 6 gives the total standard free energy change of the reaction, ΔG_T, which, therefore, is also a sum of the ideal (ΔG_I) and nonideal (ΔG_{NI}^o) contributions:

$$\Delta G_T^o = \Delta G_I^o + \Delta G_{NI}^o \quad (35)$$

These terms are related to equilibrium constants and activity coefficient ratios Γ as follows,

$$\Delta G_T^o = -RT\ln K_c \quad (36)$$

$$\Delta G_I^o = -RT\ln K_c^o \quad (37)$$

and

$$\Delta G_{NI}^o = -RT\ln\Gamma \quad (38)$$

where the apparent equilibrium constant K_c is the familiar ratio of equilibrium concentrations, the thermodynamic equilibrium constant K_c^o is the corresponding ratio of thermodynamic activities, $a_j = \gamma_j C_j$, and thus

$$\Gamma = \prod_{j=i+1}^{N} \gamma_j^{(n_j)} \Big/ \prod_{j=1}^{i} \gamma_j^{(n_j)} \qquad (39)$$

Two approximate methods for the calculation of μ_{NI} were described by Minton (2). Both methods assume that the protein and polymer may be treated as hard particles of molecular dimensions with no long-range interactions between the particles. Therefore all nonideal contributions to the chemical potential come from excluded volume effects. Since PEG is flexible, the hard particle model should give an estimate of the maximum excluded volume effect. The first method of calculation uses the scaled particle theory, in which all particles have the same shape but may be of different sizes. The second method is a lattice treatment in which the chemical potential is calculated by representing all hard particles as rectangular parallelopipeds (PP) located in an environment of background cubes of arbitrary sizes. This lattice treatment constrains all surfaces to be parallel or perpendicular to one another. It therefore typically yields lower values for μ_{NI} than those calculated from the scaled particle treatment. However, this technique allows calculation of chemical potentials for particles of different shapes, whereas the scaled particle theory does not. Different shapes are needed in modelling GDH, which forms long rods, and PEG, which is assumed to be more nearly spherical in conformation. Minton suggests (2) that a partial correction for this underestimation may be achieved by calibrating the results from the lattice method with that from the scaled particle method using a system

Figure 26. Ratio of Ln of Activity Coefficients Calulated From Parallelopiped (PP) and Scaled Particle (SP) Models. The correction factor for the lattice model using PP's is the reciprocol of ln gamma(PP) / ln gamma(SP) for the values of phi and v/v_b employed in the calculations, where v is the volume of "dilute" macromolecules in a background of "concentrated" macromolecules of volume v_b.

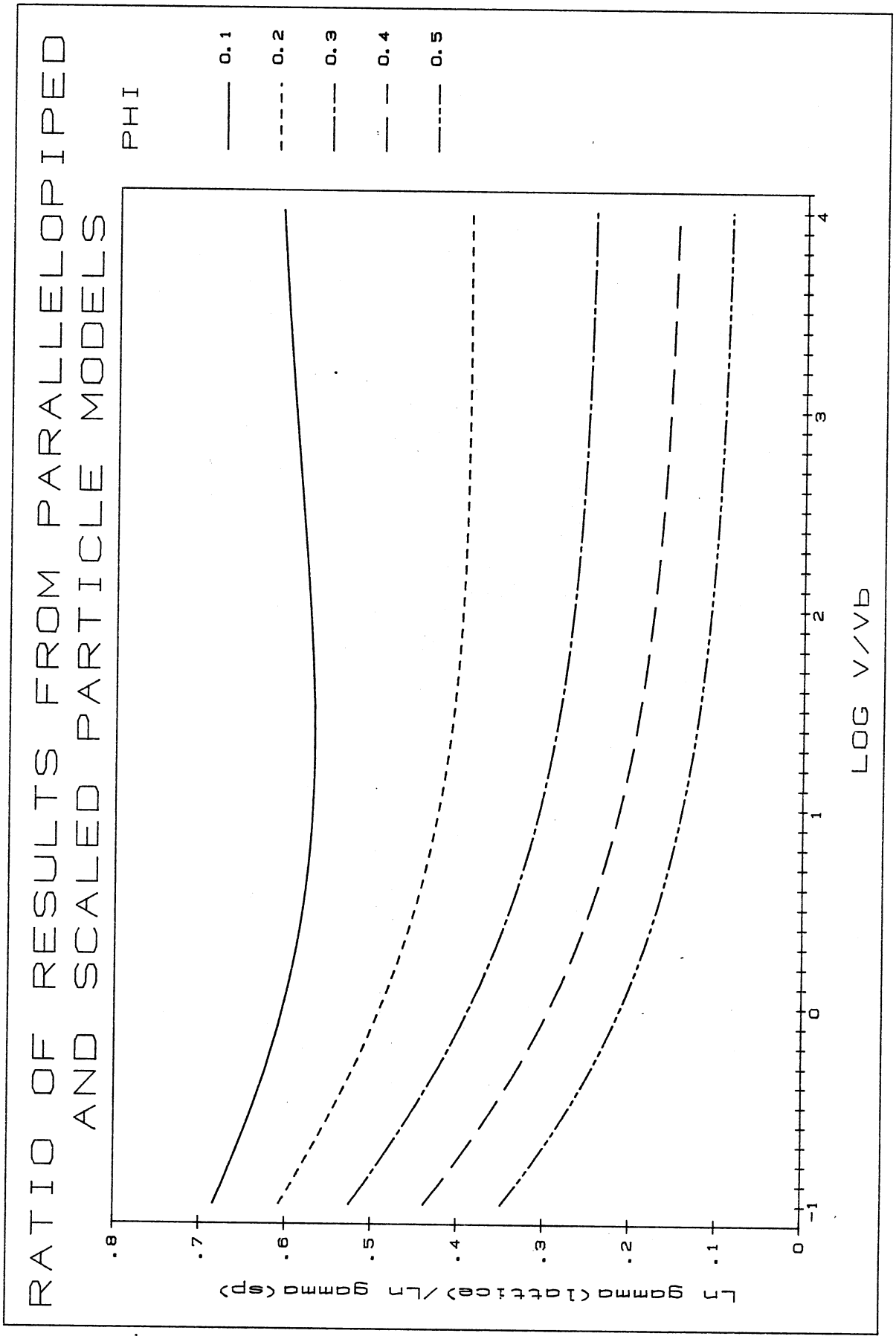
RATIO OF RESULTS FROM PARALLELOPIPED
AND SCALED PARTICLE MODELS
PHI
0.1
0.2
0.3
0.4
0.5
Ln gamma(lattice) /Ln gamma(sp)
LOG V/Vb
.8
.7
.6
.5
.4
.3
.2
.1
0
-1
0
1
2
3
4

that can be analyzed by both techniques. Figure 26 shows the results of such a calibration. All subsequent calculations for μ_{NI}(GDH) have been scaled accordingly.

For our calculations, we model PEG-6000 as cubes of 4.0 nm. Such a cube has approximately the same volume as a sphere with radius 3.04 nm, the same radius calculated for PEG-6000 from the intrinsic viscosity of the polymer (see Appendix C). GDH is considered as either a PP of dimensions 7.5 nm x 7.5 nm x (i*11.0 nm) or as a cube of sides $\sqrt[3]{i}$ x 8.5 nm, where i is the number of enzyme monomer units in the GDH polymer. We first calculate the excluded volume contribution (μ_{NI}) to the chemical potential of each polymer form. The results are shown in Figure 27 for varying values of ϕ, where ϕ is the fraction of the total volume occupied by PEG. With this model, 1%, 2%, and 3% PEG-6000 correspond very closely to ϕ values of 0.05, 0.10, and 0.15, respectively, if the molecular weight of PEG is assumed to be 8000. From the μ_{NI} values we calculate the excluded volume contribution G_{NI} to the free energy of a solution per mole of monomeric GDH.

$$G_{NI} = (M_1/c_t)\ \Sigma \mu_{NI} C_i \qquad (40)$$

where c_t is the concentration of GDH in solution in g/l,

M_1 is the molecular weight of monomeric GDH,

$\mu_{NI}(\phi)$ is a function of ϕ,

$C_i(K)$ is the molar concentration of i-mer species of GDH and is a function of association constant K, and

the sum is taken over all polymeric forms of GDH of significant concentration. Curves of G_{NI} are shown in Figure 28 for [GDH] = 1 mg/ml.

We shall define the enzyme association constant K_1 as that

Figure 27. Nonideal Chemical Potential of GDH (Ordinate) due to Exluded Volume Effects. Phi is the fraction of the total volume occupied by PEG. These results are shown assuming normal end-to-end association (A) and cubic association (B). The cubic form is shown in order to indicate the effects of the large assymetry inherent in the normal form of GDH polymerization on its nonideal chemical potential. The reported results are per mole of polymeric GDH. The equivalent number of moles of monomeric GDH is i. GDH polymer size is given as the number of monomer units per polymer molecule (i).

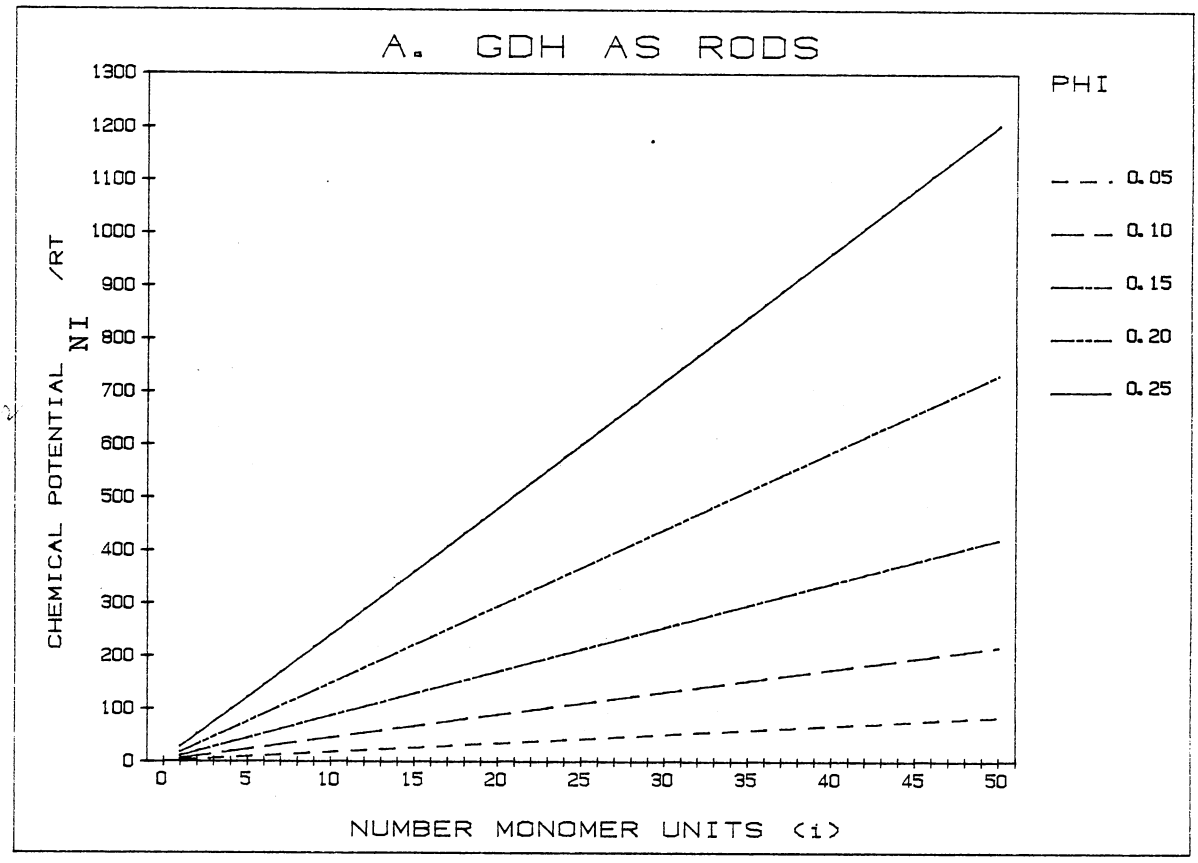
A. GDH AS RODS
CHEMICAL POTENTIAL NI /RT
NUMBER MONOMER UNITS (i)
PHI
0.05
0.10
0.15
0.20
0.25
0
100
200
300
400
500
600
700
800
900
1000
1100
1200
1300
0
5
10
15
20
25
30
35
40
45
50

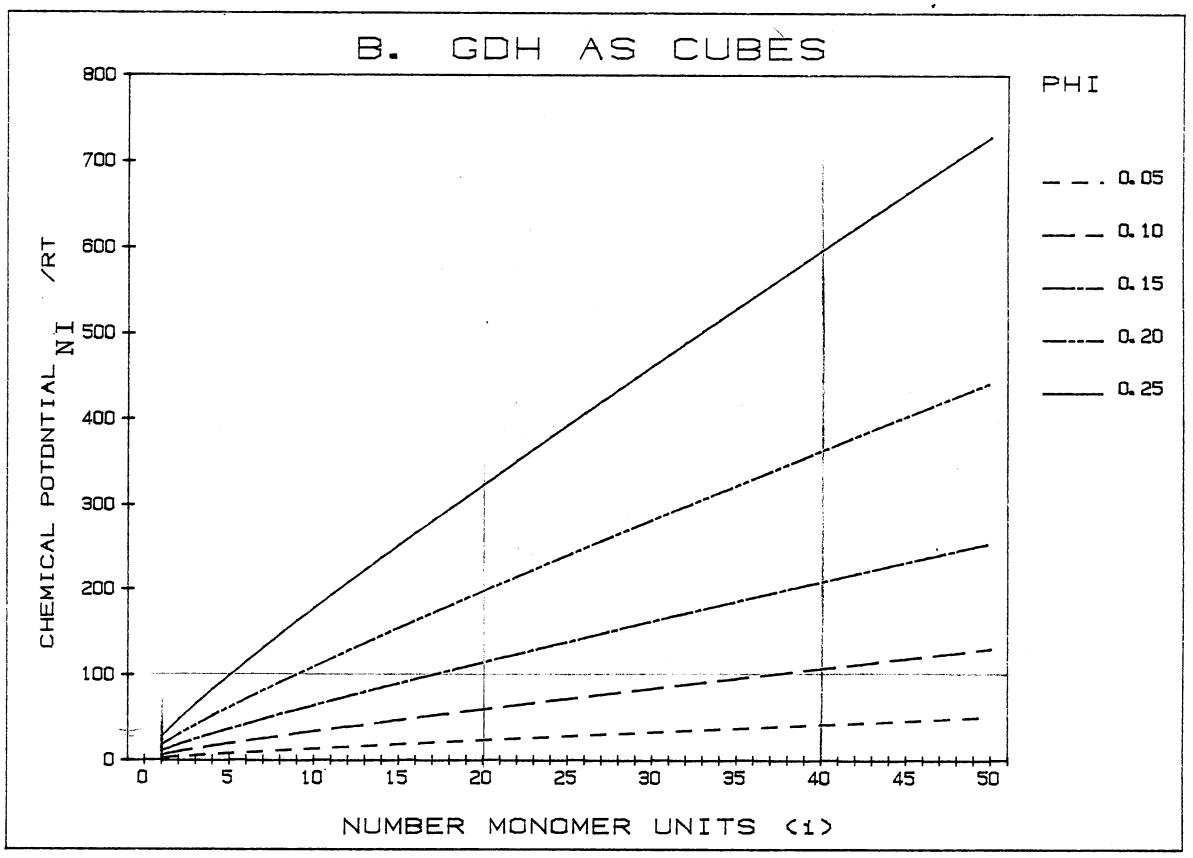
B. GDH AS CUBES
CHEMICAL POTDNTIAL NI /RT
NUMBER MONOMER UNITS (i)
PHI
0.05
0.10
0.15
0.20
0.25
0
100
200
300
400
500
600
700
800
0
5
10
15
20
25
30
35
40
45
50

Figure 28. Nonideal Free Energy per Mole Monomeric GDH. Results are shown for both end-to-end (A) and cubic (B) modes of polymerization. The nonideal free energy is reported as a function of both the GDH association constant, K, and the fraction of volume occupied by background molecules, phi. The molar distribution GDH polymers was calculated assuming that the enzyme concentration was 1 mg/ml. The calculated free energy was then scaled to that appropriate for one mole of GDH.

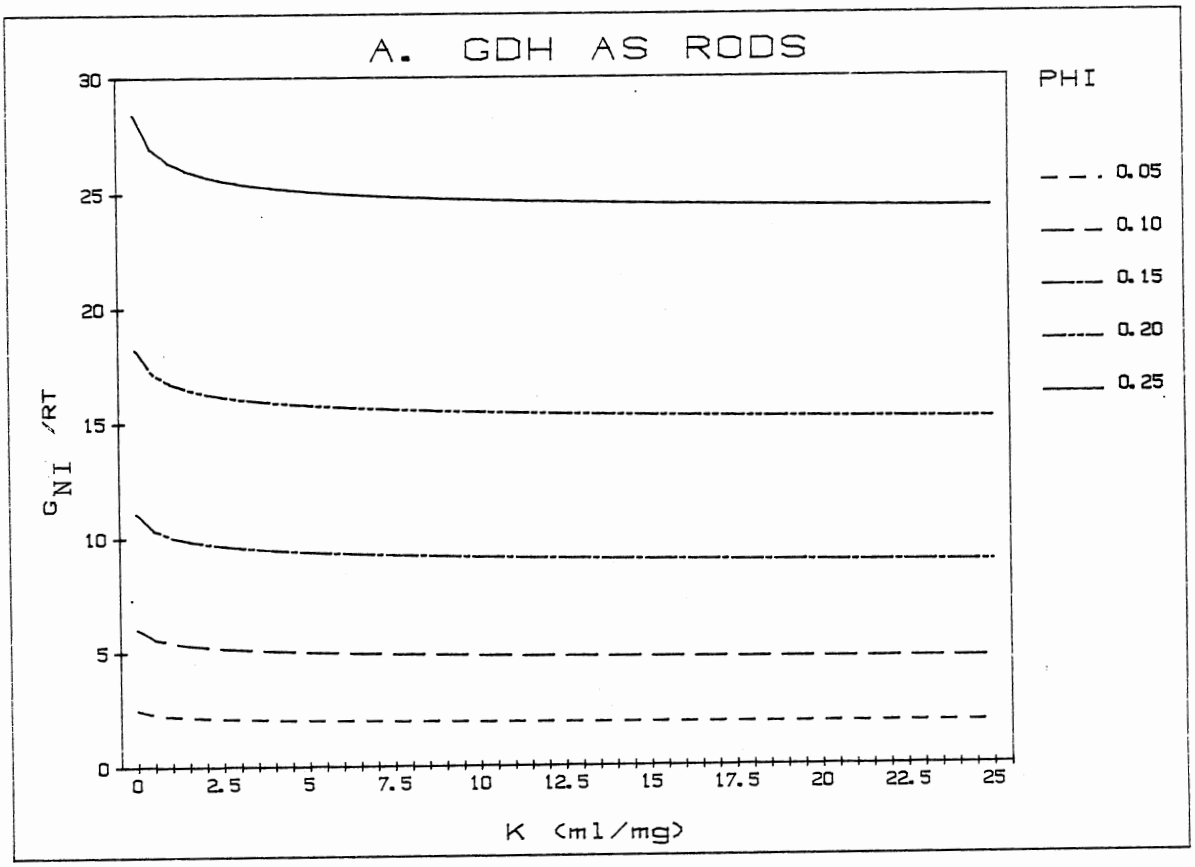
A. GDH AS RODS
PHI
0.05
0.10
0.15
0.20
0.25
G_{NI} /RT
K (ml/mg)
0
2.5
5
7.5
10
12.5
15
17.5
20
22.5
25
30

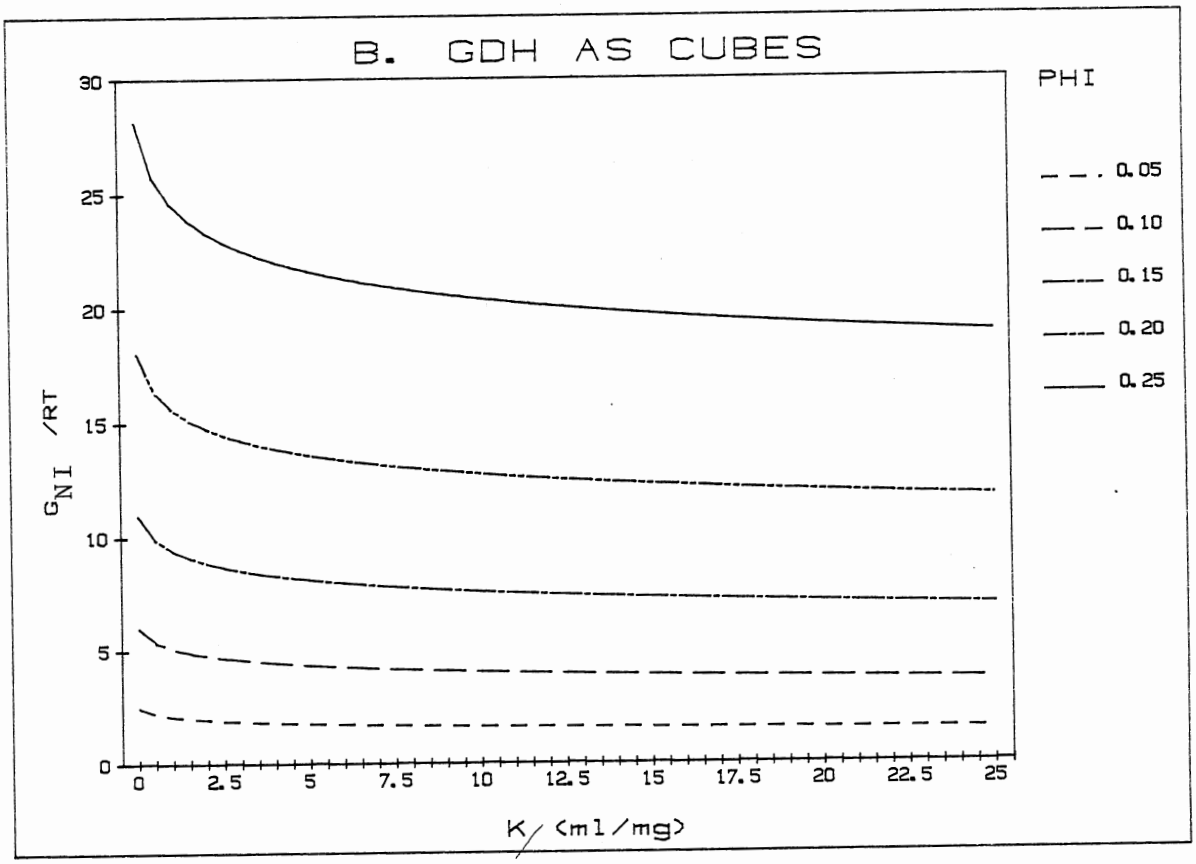
B. GDH AS CUBES
PHI
0.05
0.10
0.15
0.20
0.25
G_{NI} /RT
K (ml/mg)
0
2.5
5
7.5
10
12.5
15
17.5
20
22.5
25
30

characterizing the enzyme association in the absence of PEG. Then the difference $\Delta G_{NI} = G_{NI}(K_2) - G_{NI}(K_1)$ in going from an enzyme association with K_1 to one with K_2 (with $K_2 > K_1$) on any curve is the extent to which the solution can minimize the unfavorable G_{NI} contributed by excluded volume effects upon the addition of PEG by the process of increased GDH association. The values are summarized in Table IV for the conditions 1 mg/ml GDH, 5^{o} C., and varying concentrations of PEG-6000 in standard MOPS buffer. For a given PEG concentration, K_2 and K_1 are the experimentally measured values of the GDH association constant in the presence and absence of PEG, respectively. To evaluate the excluded volume mechanism for PEG enhanced association, we compare these values of ΔG_{NI} to the ideal free energy change (ΔG_I) needed to shift GDH species concentrations from values $C_i(K_1)$ to values $C_i(K_2)$. The distribution $C_i(K_1)$ corresponds to the equilibrium distribution in the absence of PEG. The distribution $C_i(K_2)$, however, is a hypothetical (ideal) non-equilibrium distribution because there can only be one equilibrium distribution $[C_i(K_1)]$, and this distribution must also be independent of other components in an ideal solution. In the absence of PEG, GDH equilibria do adequately follow ideal behavior at these GDH concentrations (1 mg/ml) so the calculation should be realistic in this regard. The working equation for ΔG_I is derived in Appendix F and expressed here as the sum of standard state terms SST and concentration terms, CT,

$$\Delta G_I = SST + CT \tag{41}$$

where

$$SST = CF \times RT\ln\langle K_1^{n-1}[1/mole]^{n-1} \sum_{i=1}^{n-1}(1-i/n)\Delta C_i[moles/l]\rangle \tag{42}$$

TABLE IV

ΔG_I AND ΔG_{NI} FOR THE CHANGE IN GDH ASSOCIATION

[PEG] (% w/v)	ϕ_{PEG}	K 0.5 1/g	$\Delta G_I/RT$	$\Delta G_{NI}/RT$	
0	0.00	2.90			
1	0.05	4.33	0.73	−0.04	−0.0500245
2	0.10	5.66	1.19	−0.17	−0.18017
3	0.15	8.57	1.85	−0.41	−0.460095

ΔG_I is the change in free energy per mole GDH required to move from the particle distribution given by K in the absence of PEG to the K measured in the presence of PEG for a GDH concentration of 1 mg/ml. ΔG_{NI} is the change in the nonideal free energy due to excluded volume effects for an identical change in GDH distribution. ϕ is the fraction of total solution volume occupied by PEG.

$$\Delta C_i = C_i(K''_2) - C_i(K''_1) \tag{43}$$

$CF = M_1/c_t$, the ratio of the enzyme monomer molecular weight and the total enzyme weight concentration, $K''[1/mol_1] = M_1K[1/g]$, and

$$CT = CFxRT \sum_{i=1}^{n} [C_i(K_2)\ln C_i(K_2) - C_i(K_1)\ln C_i(K_1)] \tag{44}$$

The results of these calculations are summarized in Table IV. As a result of these calculations, three major observations can be made.

1. The enhanced association observed for GDH in a solution of PEG is greater than can be ascribed to excluded volume effects.

The decrease in nonideal free energy, ΔG_{NI}, available from the change in K and resulting decrease in the excluded volume effect is much less than that required by the change in GDH particle distribution, ΔG_I (comparison in Table IV). At a constant weight percent polymer, G_{NI} is less for a higher molecular weight polymer than a lower molecular weight one (6). Thus, if PEG exists in an associated form with conditions of these experiments as discussed below, its contribution to excluded volume effects should be even less. If the shift in K cannot be explained in terms of excluded volume effects, what alternatives are possible? The volume occcupied by the polymer acts to decrease the concentration of the water. For our purposes this may be viewed as an effective increase in the concentration of GDH. If such a concentration change was solely responsible for the observed change in the extent of association, then the effective concentrations of GDH would have to be 1.5, 2.0, and 3.0 times as great as the nominal value (1 mg/ml) for 1%, 2%, and 3% PEG, respectively. Such values are unrealistically high. Lerman (40) has shown that the vapor pressure of water undergoes only very slight changes upon the addition of PEG, even at very high PEG

concentrations. This implies that the activity of the water is essentially unchanged by these PEG concentrations.

Another possible factor is the enthalpic contributions to GDH association which play an important role in the self-association of the protein in the absence of polymer. The hard particle model used in calculation excluded volume effects does not consider any contributions from this source.

2. ΔG_{NI} is small because of the open-ended nature of GDH self-association.

The small change in ΔG_{NI} from the enhanced self-association of GDH contrasts with the much larger effects described by Minton for closed enzyme associations such as $2E_1 \rightleftharpoons E_2$ or $4E_1 \rightleftharpoons E_4$. That ΔG_{NI} is small in our case is not due to the end-to-end association of GDH which leads to the production of very asymetric particles, since similiar results are obtained assuming the far more symmetric cubic association. This is illustrated by considering the following scheme

$$2E_1 \rightleftharpoons E_2 \tag{45}$$

for an enzyme the size of GDH in a background of polymer of the size of PEG. Assuming cubic forms for both E_1 and E_2, $\Delta G_{NI}/RT$'s are -1.82 and -4.26 per mole E_1 for the complete conversion of E_1 to E_2 at ϕ's of 0.15 and 0.25, respectively. Even if E_1 and E_2 are modelled as rods undergoing end-to-end association, the corresponding values of $\Delta G_{NI}/RT$ are -1.32 and -2.76.

All of the association steps for GDH may be treated as $E_i + E_1 \rightleftharpoons E_{i+1}$. $\Delta G_{NI}/RT$ per mole E is -0.87, -.52, and -0.24 at a ϕ of 0.15 for i=5, 10, and 25, respectively. To go from one associated state to a more associated state leads to a much smaller reduction in G_{NI} than

does going from an unassociated state to a moderately associated one. This is the basis for the statement above (observation number two).

3. The low solubility of GDH in PEG is probably a result of the small reduction in G_{NI} upon additional association.

Values for G_{NI}/RT for GDH are large and increase rapidly as ϕ is increased (Figure 28). As we have shown above, this free energy cannot be relieved by additional association. However, phase separation may reduce it by two ways:

a) Reduction in the concentration of GDH in solution, and

b) Decreasing the extent of GDH association (since the polymerization is driven by the protein's concentration).

The second factor is only significant if the extent of self-association becomes very small.

Until now our description of exluded volume effects has been confined to PEG-6000 as the added polymer. On the basis of hydrodynamic radii, BSA and PEG-6000 would be expected to have very similar excluded volume effects at equivalent number densities. Thus, 10% BSA and 1.2% PEG-6000 might be expected to have the same effect on GDH. The value of $\bar{s}_{20,w}$ for GDH at 1 mg/ml enzyme is 23.2 S in 10% BSA and 22.9 S in 1% PEG-6000. It would therefore seem likely that excluded volume plays some important role in the enhancement of GDH association. In any case the change in association cannot be ascribed to effects confined to PEG.

A truly accurate estimate of the free energy contribution to excluded volume requires more certainty on molecular dimensions and comformations than is currently available, especially with flexible polymers. However, we have attempted to estimate the maximum excluded volume effects that one could expect. Thus our conclusions should still be valid.

Effect of PEG on the Inhibition of GDH by GDP

To assess the possible effects of PEG on the catalytic properties of GDH, we have measured some of the kinetic constants of GDH reactions in the presence and absence of its allosteric effector GDP. These measurements include the transient-state of GDP inhibition. The inhibitory properties of GDP and GTP on GDH activity have been rather thoroughly investigated (41,42). Inhibition of enzyme activity by these nucleotides occurs in the presence of NADH or NADPH. The binding constant for both nucleotides increases with increasing GDH dissociation. Thus, both nucleotides inhibit GDH association by means of the coupled equilibria of ligand binding and enzyme association. Nucleotide regulation of GDH activity may be important in metabolic control.

Huang and Frieden (43) measured the rate of depolymerization of GDH upon the addition of GDP and NADH by monitoring the decrease in solution turbidity at 310 nm. After the addition of NADH and GDP, the depolymerization of the enzyme appears to proceed by two steps, each of which may be modelled as a first order reaction as shown by Equation 46.

$$E_m \xrightarrow[GDP]{NADH} E'_m \xrightarrow{k_1} E_n \xrightarrow{k_2} E_p \qquad (46)$$

where E'_m represents the enzyme with bound GDP and NADH but prior to any depolymerization, and the subscripts m, n, and p represent the average extent of association of the enzyme, with $m>n>p$.

The second depolymerization step was only observed when NADH, not NADPH, was used. The bimolecular additions of NADH and GDP to the enzyme are far too rapid to be monitored by the stopped-flow methods

employed by them. Therefore Huang and Frieden only measured k_1 and k_2. A conformational change in the enzyme which could be monitored by changes in the absorbance at 365 nm of enzyme-bound NADH accompanied the depolymerization of E_n to give E_p. The depolymerization of E_m' to give E_n is also presumed to be accompanied by a protein conformational change, but no comparable spectrophotometric change has been reported. Therefore, its progress was monitored by measuring intensities of light scattering.

Huang and Frieden did not report any measurements of the enzymatic activities of the transient-state enzyme forms. We performed such kinetic measurements on the inhibition of GDH by GDP using transient- and steady-state portions of the reaction. The effect of PEG on this inhibition was also studied. To simplify analysis, saturating levels of the substrates α-ketoglutarate (7 mM) and NH_4Cl (100 mM) were used. The catalytic reaction could then be treated as a simple, one-substrate reaction with respect to NADH, obeying Michaelis-Menten kinetics. We chose to make our measurements at GDP concentrations sufficiently high that the enzyme was completely dissociated at equilibrium. Therefore the only enzyme form at equilibrium was E_p (monomeric GDH). The reaction was initiated by mixing a solution containing GDH with an equal volume of solution containing substrates (and GDP, if present). All final reaction mixture contained 0.5 mg/ml GDH and 100 μM NADH. Some reaction mixtures contained 1 mM GDP and/or 2% PEG-6000. The rate of NADH oxidation was monitored by measuring the change in absorbance at 365 nm. Data was collected until equilibrium was reached. Adequate fits to the data required three different enzymatically-active forms. A model for such a system is given by equation 47.

$$\begin{array}{ccccc} E_m' + A & \overset{K_{a1}}{\rightleftharpoons} & E_m'A & \xrightarrow{k_{r11}} & E_m' + P \\ \downarrow k_1 & & & & \\ E_n + A & \overset{K_{a2}}{\rightleftharpoons} & E_nA & \xrightarrow{k_{r12}} & E_n + P \\ \downarrow k_2 & & & & \\ E_p + A & \overset{K_{a3}}{\rightleftharpoons} & E_pA & \xrightarrow{k_{r13}} & E_p + P \end{array} \qquad (47)$$

where the E's are the previouly mentioned GDH forms,

A is the substrate NADH,

P is the product NAD^+,

K_{ai} is the Michaelis constant for the substate A with respect to enzyme form E_i, and

k_{rli} is the first-order rate constant corresponding to the rate limiting step in the release of P from E_i.

Such a model allows for, but does not require, different kinetic properties for each of the three forms.

The first 99% of the reaction was fitted to equation 48 (see Appendix G for derivation).

$$dP/dt = k_{r11}E_tAe^{-k_1t}/(K_{a1}+A) + k_{r12}E_tA(1-e^{-k_1t})/(K_{a2}+A) + k_{r13}E_tA(1-e^{-k_2t})/(K_{a3}+A) \qquad (48)$$

Since the reaction in the reverse direction is extremely unfavorable under our experimental conditions, contributions to the progress curves from this source was considered negligible. This was confirmed by minimal changes in the fits to the progress curves if the data at longer reaction times were omitted. Curve fitting was performed on a PDP 11-40 minicomputer using the program Mini-CRICF, a version of CRICF (44) designed to run on minicomputers. The program integrates rate equations

and then fits the parameters of the equation to the supplied kinetic data by nonlinear least squares techniques. The results of these fits are given in Table V.

The constants k_{r11} and K_{a1} were obtained from fitting kinetic measurements performed in the absence of GDP. k_{r13} and K_{a3} were fit to portions of progress curves at which E'_m and E_n were insignificant (long t). Alternatively, k_{r13} and K_{a3} could have been determined from experiments in which the enzyme was pre-incubated with GDP and NADH. All other parameters were obtained by fitting to selected portions of this same progress curve while other parameters were held fixed. Values of k_{r12} and K_{a2} were highly correlated. Only the ratio k_{r12}/K_{a2} could be reliably determined.

The three GDH forms observed in this experiment monitoring enzymatic activity are probably the same forms observed by Frieden by his direct spectral measurements of the rates of depolymerization. The rate constants governing the interconversion of enzymic forms measured here are very similiar to those reported by Frieden for the depolymerization reaction. From the changes in enzymatic activity, k_1 is about 22 s^{-1} and k_2 is about 0.8 s^{-1}. Frieden found k_1 and k_2 to be 20 sec^{-1} and 0.45 sec^{-1}, respectively. His measurements were performed at 10° C in acetate buffer, pH 7.45, while ours were made at 5° C in standard MOPS buffer, pH 7.2.

Although the ratios of the constants governing the catalytic activity for the enzyme forms E_n and E_p, k_{r12}/K_{a2} and k_{r13}/K_{a3}, are very similiar, both enzyme forms were required to obtain a good fit to the progress curves. This means that either:

1) the small differences in constants of E_n and E_p are real

TABLE V

EFFECT OF PEG-6000 ON THE INHIBITION OF GDH BY GDP

CONDITION	[GDP] (mM)	[PEG] (% w/v)	k_{r11} (s^{-1})	K_{a1} (μM)	k_{r11}/K_{a1} ($s^{-1}\mu M^{-1}$)
A	0	0	104.2	42.0	2.48
B	0	2	129.9	46.4	2.80

CONDITION	[GDP] (mM)	[PEG] (% w/v)	k_1 (s^{-1})	k_{r12}/K_{a2} ($s^{-1}\mu M^{-1}$)	k_2 (s^{-1})	k_{r13} (s^{-1})	K_{a3} (μM^{-1})	k_{r13}/K_{a3} ($s^{-1}\mu M^{-1}$)
C	1	0	21.2	0.24	0.85	2.75	11.4	0.24
D	1	2	23.5	0.29	0.79	3.55	13.9	0.26

All solutions contained 0.5 mg/ml GDH, 100 μM NADH, 7 mM α-ketoglutarate, and 100 mM NH_4Cl in standard MOPS buffer. Measurements were made at 5° C.

(otherwise an equally good fit to the data would be obtained with a model using only two enzyme forms, or

2) the third enzyme form is artificially providing additional constants to compensate for systematic error in the data.

A comparison of the kinetic parameters for GDH in the presence and absence of PEG show very little difference. The enzyme appears to be somewhat more active in polymer. However, the difference is not large enough to be of any great consequence. The two rate constants k_1 and k_2 reflecting the two rates of depolymerization show little change upon the addition of PEG to the reaction mixture. Frieden has shown that, even under widely varying differences in the initial and final extent of GDH association, the rate constants governing the two depolymerization steps change very little. The somewhat higher activity of the enzyme in PEG over that in buffer alone does lead to large difference in the concentration of product as a function of time in these experiments.

Kinetic differences may well be larger at sub-saturating levels of GDP and substrate. However more data and more extensive analysis would be required to deal with the transient- and steady-state kinetics of such a system.

CHAPTER IV

SUMMARY AND CONCLUSIONS

In the first chapter I posed several questions to be investigated in the research reported in this thesis. I would like to examine these questions in light of the results contained in Chapter III.

Relationship Between GDH Association and Polymer-Induced Precipitation

Under the experimental conditions employed, only the higher molecular weight PEG's precipitated GDH. Therefore, the discussion of solubility must be confined to the PEG's. For PEG, conditions that promote enzyme self-association also lower the enzyme's solubility in PEG. The inherent ability of PEG to promote GDH association contributes to this lower solubility. The mode of PEG precipitation of the GDH may be through the formation of protein aggregates of such size that they cannot remain in solution. In support of these contentions I would offer the following experimental evidence.

1. Ionic strength and pH conditions known to enhance GDH self-association in the absence of polymer resulted in lower GDH solubility in PEG-6000. Conversely, solution conditions known to decrease the extent of GDH polymerization lead to increases in the solubility of GDH in PEG-6000.

2. For different molecular weight PEG'S, the potency of the PEG in

reducing GDH solubility directly paralleled the increase in GDH association attributable to the PEG at polymer and protein concentrations at which GDH was soluble.

3. At PEG-6000 concentrations near the solubility limit of GDH, large soluble aggregates of the enzyme were observed by static light scattering measurements.

Polymer Effects on GDH Association

The association of GDH was enhanced by the addition of a second polymer if a sufficiently high concentration of the polymer was used. This was true for all the polymers examined (PEG's, BSA, and 9.4k dextran). The order of potency in enhancing GDH polymerization at the same polymer weight concentration was PEG-6000 >> PEG-20000 >> PEG-1000 $\simeq$ BSA > 9.4k dextran. Analysis of the increased polymerization of GDH in PEG-6000 was consistent with changes due to an increase in the stepwise association constant K for GDH, rather than through changes in the mode of GDH association.

Mechanism of Polymer Action

Because of the complex behavior of GDH precipitation as a function of PEG concentration, we were unable to measure a single constant describing the thermodynamic interaction between PEG and GDH as has been done for other protein-PEG combinations. We demonstrated that, although the solubility of some of the GDH-PEG solutions did not change with time, these solutions were not at thermodynamic equilibrium. The calculation of the interaction constant between PEG and protein from solubility data requires that the solution be at equilibrium.

Excluded volume effects were insufficient to explain the enhanced association of GDH in PEG-6000. However, such effects probably play an important role. At low PEG concentrations (e.g., less than 2%) where segment overlap between PEG molecules is negligible, BSA and PEG-6000 are likely to have approximately equal excluded volumes per mole. Excluded volume theory then predicts that they should exert the same effect due to their volume on a second macromolecule in solution. In fact, when the polymers are compared on the basis of number rather than weight concentration, their ability to enhance the polymerization of GDH is equal. Since there is little, if any, similarity in the chemical properties of these two polymers, it is difficult to imagine alternative molecular forces contributing to the GDH-polymer incompatibility.

The low solubility of GDH in PEG's can at least qualitatively be explained by excluded volume effects. The large value of G_{NI} for GDH due to PEG's excluded volume cannot be effectively reduced by increasing the extent of GDH polymerization. Since this free energy can be totally alleviated by the precipitation of the enzyme, the low solubility of GDH is reasonable.

PEG Effect on the Inhibition of GDH by GDP

No significant changes were observed in the various kinetic constants governing the inhibition of GDH by GDP upon the addition of PEG-6000. However, because we used saturating concentrations of GDP, we did not measure the kinetic constant most likely to be affected by the addition of the polymer. This constant, K_I, governs the inhibition of the enzyme at subsaturating levels of GDP. K_I is known to be a function of the extent of GDH polymerization. Since PEG enhances the association

of the enzyme, we would expect K_I to increase accordingly. Such an increase in the extent of association is not reflected in the constants governing the rates of isomerization and depolymerization of the enzyme. It seems likely that any kinetic changes resulting from the polymer action on GDH are not due to direct polymer-induced conformational changes on any enzymic species, but are instead a result of the same protein-protein interactions that exist in the absence of polymer. That is to say, the kinetic consequences of polymer effects are the indirect result of facilitating the formation of enzyme complexes, rather than the direct result of polymer-protein interaction.

Metabolic Significance of GDH-Polymer Interactions

Up to this point I have not proposed any major consequences *in vivo* for the effects of polymers observed on GDH *in vitro*. Certainly what follows is mostly conjecture. However, there is enough experimental evidence in favor of the following role for GDH to merit at least some discussion.

GDH is found in the mitochondrial matrix at concentrations in the range of 10-20 mg/ml. This is more than sufficient to produce extended aggregation of the enzyme, especially when one considers the high polymer (macromolecular) concentration in the matrix. In fact, GDH may exist primarily as precipitated enzyme *in vivo* (1). The ammonium sulfate precipitate of GDH has been shown to be organized into superstructures including sheets and several different types of tubes (45). The basic unit of all of these structures is the linear polymer chain observed in solution. These superstructures may also exist *in vivo*. As we have previouly discussed, GDH is known to associate with a

number of other enzymes resulting in changes in their kinetic behavior. I would suggest that GDH may form an underlying structure to which many mitochondrial enzymes are associated, forming mitochondrial "particles" containing some of the enzymes of the Krebs cycle and related metabolic pathways. Such complexes, like the pyruvate dehydrogenase complex or those involved in fatty acid synthesis and degredation, could have overall properties significantly different than those of any single enzyme. Such an arrangement would allow substrate molecules to pass from one protein to another in an efficient manner. Coupling of this type might produce reaction rates in vivo far more rapid than predicted from in vitro studies, especially for enzymes with substrates at low intracellular concentrations. The discrepancy between the observed turnover of molecules in the Krebs cycle and that predicted on the basis of the substrate and enzyme concentrations thought to exist in the mitochondrial matrix may be the result of large enzymic complexes (46).

REFERENCES CITED

1. Srere, P. A. (1980) Trends Biochem. Sci. 5, 120-121.

2. Minton, A. P. (1981) Biopolymers 20, 2093-2120.

3. Yoshida, A. (1966) J. Biol. Chem., 241, 4966-4976.

4. Fulton, A. (1982) Cell, 30, 345-347.

5. Cohen, C., Caspar, D. L. D., Johnson, J. P., Nauss, K., Margossian, S. S., and Parry, D. A. D (1972) Cold Springs Harbor Symp. Quant. Biol. 37, 287-297.

6. Loewy, A. G. and Siekevitz, P. (1968) in Cell Structure and Function, 2nd Ed., Holt, Rinehard, and Winston, New York.

7. Herzog, W., and Weber, K. (1978) Eur. J. Biochem., 91, 249-254.

8. Fenton, J. W. II, and Fusco, M. J. (1974) Thrombosis Res., 4, 809.

9. Halper, L. A., and Srere, P. A. (1977) Arch. Bioch. Biophys., 184, 529-534.

10. Backman, L., and Johansson, G. (1976) FEBS Letters, 65, 39-43.

11. Bosca, L., Aragon, J. J., and Sols, A. (1982) Fed. Proc., 41, 1398.

12. Clarke, F. M. and Masters, C. J. (1975) Biochim. Biophys. Acta, 381, 37-46.

13. DeDuve (1972) in Structure and Function of Oxidation-Reduction Enzymes, Akeson and Ehrenberg, ed. pp. 715-728.

14. Fahien, L. A., and Kmiotek, E. (1979) J. Biol. Chem., 254, 5983-5990.

15. Albertson, P. (1971) Partition of Cell Particles and Macromolecules, Wiley-Interscience, New York, NY.

16. Miekka, S. I., and Ingham, K. C. (1978) Arch. Bioch. Biophys., 191, 525-536.

17. Miekka, S. I., and Ingham, K. C. (1981) Arch. Bioch. Biophys., 203, 630-641.

18. Lee, J. C. and Lee, L. L. Y. (1981) J. Biol. Chem. 256, 625-631.

19. Atha, D. H. and Ingham, K. C. (1981) J. Biol. Chem., 256, 12108-12117.

20. Goldin, B. R. and Frieden, C. (1971) Current Topics in Cellular Regulation, 4, p. 77, Herecker, B. L. and Stadtman, E. R., eds., Academic Press

21. Christopherson, R. I. and Jones, M. E. (1979) Anal. Biochem., 100, 184-187.

22. Olson, J. A. and Anfisen, L. B. (1972) J. Biol. Chem., 197, 67-79.

23. Coleman, R. F. and Frieden, C. (1966) J. Biol. Chem, 241, 3652-3660.

24. Chervenka, C. H. (1970) A Manual of Methods for the Analytical Ultracentrifuge, Spinco Division of Beckman, Inc., Palo Alto, CA.

25. Nichol, L. W., Ogston, A. G., and Preston, B. N. (1967) Biochem. J., 102, 407-416.

26. Tanford, C. (1961) Physical Chemistry of Macromolecules, p. 358, Wiley, New York

27. Aaron, S. H. and Lou, R. L. H. (1954) J. Polymer Sci., 14, 29-36.

28. Tanford, C. (1961) Physical Chemistry of Macromolecules, pp. 197-210, Wiley, New York

29. Tanford, C. (1961) Physical Chemistry of Macromolecules, p. 392, Wiley, New York

30. Edmond, E. and Ogston, A. G. (1970) Biochem. J. 117, 85-89

31. Edmond, E. and Ogston, A. G. (1968) Biochem. J., 109, 569-576.

32. Markau, K., Schneider, J., and Sund, H. (1971) Eur. J. Biochem., 24, 393-400.

33. Kirkwood, J. G. and Goldberg, R. J. (1950) J. Chem. Phys., 18, 61-67.

34. Jullien, M. and Thusius, D. (1976) J. Mol. Biol., 101, 397-416.

35. Tanford, C. (1961) Physical Chemistry of Macromolecules, p. 342, Wiley, New York

36. Valentine, R. (1968) in Precongress Abstracts of the Fourth European Congress of Electron Microscopy, Boeciarelli, ed., 2, p. 3, Rome.

37. Tanford, C. (1961) Physical Chemistry of Macromolecules, pp. 372-374, Wiley, New York

38. Reisler, E. and Eisenberg, H. (1970) Biopolymers, 9, 877-889.

39. Ifflaende, U., Markau, K., and Sund, H. (1974) Eur. J. Biochem., 49, 555-563.

40. Lerman, L. S. (1973) in Physico-Chemical Properties of Nucleic Acids, Duchesne, J., ed., pp. 59-76, Academic Press, London, England.

41. Frieden, C. and Colman, R. (1967) J. Biol. Chem., 242, 1705-1715.

42. Frieden, C. in Roles of Nucleotides for the Function and Conformation of Enzymes, H. Kalcker, ed., p. 184, Munskegaard, Copenhagen.

43. Huang, C. Y., and Frieden, C. (1969) Proc. Nat. Acad. Sci., 64, 338-344.

44. Chandler, J. P. and Spivey, H. O. (1972) Comput. Biomed. Res., 5, 515-534.

45. Josephs, R., Eisenberg, H., and Reisler, E. (1972) in Protein-Protein Interactions, Jaenicke, R. and Helmreich, E., ed., pp. 57-90, Springer-Verlang, New York.

46. Srere, P. A. (1976) in Gluconeogenesis: Its Regulation in Mammalian Species, Hanson, R. W. and Mehlman, M. A., eds., pp. 153-161, Wiley-Interscience, NY

47. Baily, F. E. Jr., and Callard, R. W. (1959) J. Appl. Polymer Sci., 1, 56-62.

48. Harned, H. S. and Owen, B. B. (1950) The Physical Chemistry of Electrolytic Solutions, 2nd Ed., pp. 397-400, Reinhold, New York

49. Tanford, C. (1961) Physical Chemistry of Macromolecules, pp. 343-344, Wiley, New York

50. Tanford, C. (1961) Physical Chemistry of Macromolecules, p. 196, Wiley, New York

51. Tanford, C. (1961) Physical Chemistry of Macromolecules, pp. 390-392, Wiley, New York

52. Alexandrowicz, A. (1959) J. Polymer Sci., 40, 107-112.

53. Polson, A. (1977) Prep. Biochem., 7, 129-154.

54. Klaarner, P. E. O. and Ende, H. A. (1975) in Polymer Handbook, 2nd Ed., Brandrup, J. and Immergut, E. H., ed., 4, p. 81, Wiley, New York

55. Tanford, C. (1961) Physical Chemistry of Macromolecules, p. 194, Wiley, New York

56. Pike, E. R. (1981) in Scattering Techniques Applies to Supramolecular and Nonequilibrium Systems, Chen, S.-H., Chu, B., and Nossal, R., ed., pp. 179-200, Plenum Press, New York

57. Frost, A. A. and Pearson, R. G. (1961) Kinetics and Mechanism, 2nd Ed., pp. 166-167, Wiley, New York

APPENDIX A

EFFECT OF PEG-6000 ON THE pH OF BUFFERED SOLUTIONS

The interaction of PEG with salts in aqueous solution is very complex. One of the effects observed from these interactions is the separation of the solution into an aqueous PEG phase and an aqueous salt phase if the salt concentration is sufficiently high (47). The ability of different salts to cause such phase separation is not correctly predicted by the Debye-McAuly equation which describes the effect of salts on the activity coefficient of a neutral molecule in solution (48). The strength of the interaction between salt and PEG is somewhat anion-specific, and is reminiscent of the classic "Hofmeister Series" for the salting out of proteins (47).

I would like to discuss a different, although probably related, phenomenon. Addition of PEG to some buffer solutions changes the measured pH of the buffer. The pH of MOPS, phosphate, and pyrophosphate buffers as a function of buffer and PEG-6000 concentration is shown in Figure 29. The corresponding results for citrate buffer are shown in Figure 30. The concentrations of the buffer components in the Figures 29 and 30 are the concentrations for the solutions containing PEG, rather than the concentrations of buffers to which PEG was subsequently added. Therefore the pH changes cannot be attributed to dilution of the buffer by the addition of PEG. There is no obvious relationship between

the anionic buffer species used and the observed pH changes with the addition of PEG to the solution. I will therefore content myself with making a few observations about these observed pH changes in the buffers that we examined.

1. For phosphate and citrate buffers (Figures 29 and 30), the amount of the pH change upon the addition of a fixed concentration of PEG is almost identical for different buffer concentrations. This rules out the possibility of the pH change being attributable to small amounts of basic impurities in the PEG.

2. The amount of pH change in the buffer by PEG does not correlate with the ability of the buffer to induce aqueous phase separation of the PEG and buffer component. For pyrophosphate (Figure 29 C), the pH dependence of the buffer on PEG concentration is minimal. Yet this was the only PEG-buffer pair in which phase separation was observed in the range of PEG and buffer concentrations used.

3. The amount of change in the buffer pH upon the addition of PEG does not depend on the charge on the buffer's anionic component. Three citrate buffers were prepared, covering different pH ranges. In these different ranges, the predominant species in solution went from H_3Citrate and H_2Citrate$^-$ for the data shown in Figure 30 (Citrate I) to HCitrate^{-2} and Citrate^{-3} (Citrate III). Yet the effect of PEG concentration on pH was essentially the same for all three pH ranges studied.

Because we did not wish to deal with the added complexity of these pH shifts in our studies on polymer effects, MOPS buffer proved to be a good choice. For a number of studies in the literature other buffers have been used with PEG. For many buffers, this leads to the necessity

Figure 29. Effect of PEG-6000 on the pH of MOPS, Phosphate, and Pyrophosphate Buffers. The pK_a of MOPS is 7.20. The pK_{a2} of orthophosphate is 7.21. The pK_{a3} of pyrophosphate is 6.68.

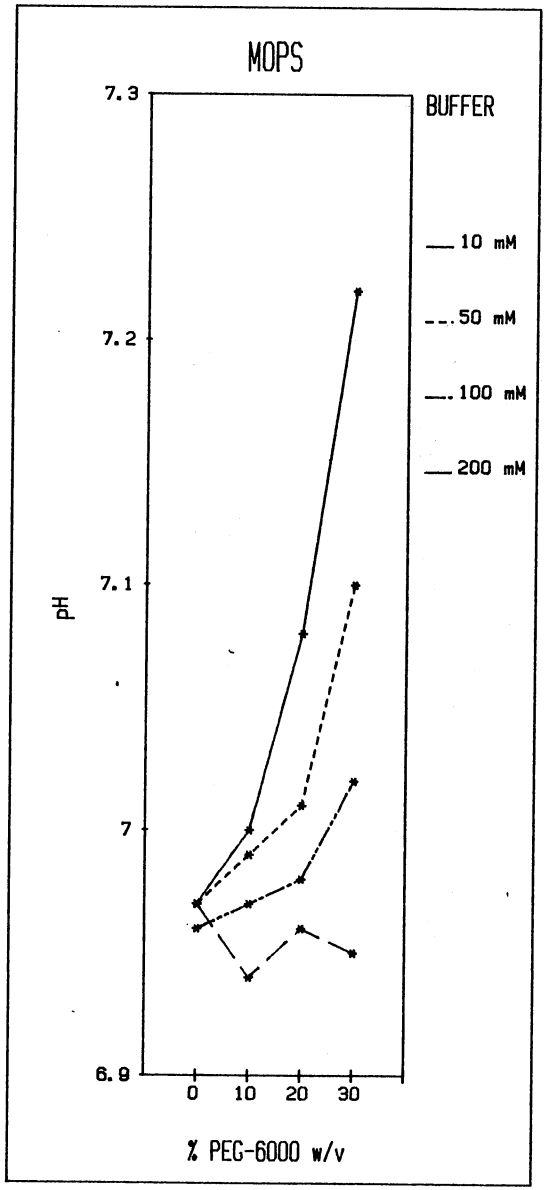
MOPS
BUFFER
10 mM
50 mM
100 mM
200 mM
pH
7.3
7.2
7.1
7
6.9
0
10
20
30
% PEG-6000 w/v

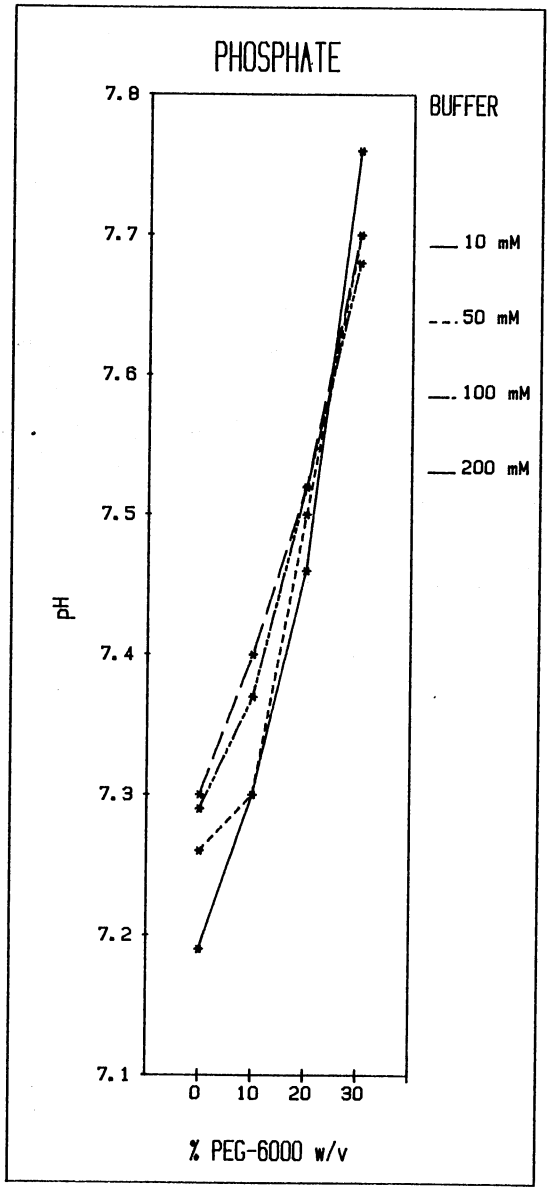
PHOSPHATE
BUFFER
10 mM
50 mM
100 mM
200 mM
pH
7.8
7.7
7.6
7.5
7.4
7.3
7.2
7.1
0
10
20
30
% PEG-6000 w/v

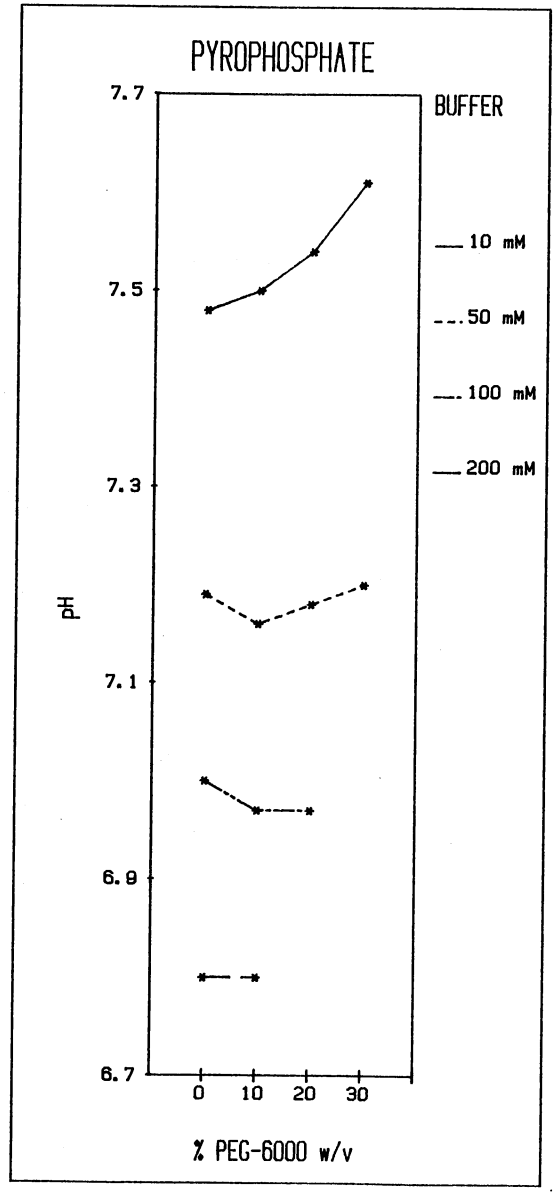
PYROPHOSPHATE
BUFFER
10 mM
50 mM
100 mM
200 mM
pH
7.7
7.5
7.3
7.1
6.9
6.7
0
10
20
30
% PEG-6000 w/v

Figure 30. Effect of PEG-6000 on the pH of Citrate Buffers. The three conditions shown correspond roughly to three different buffering regions of citrate (pK_a's of 3.06, 4.74, and 5.40, respectively).

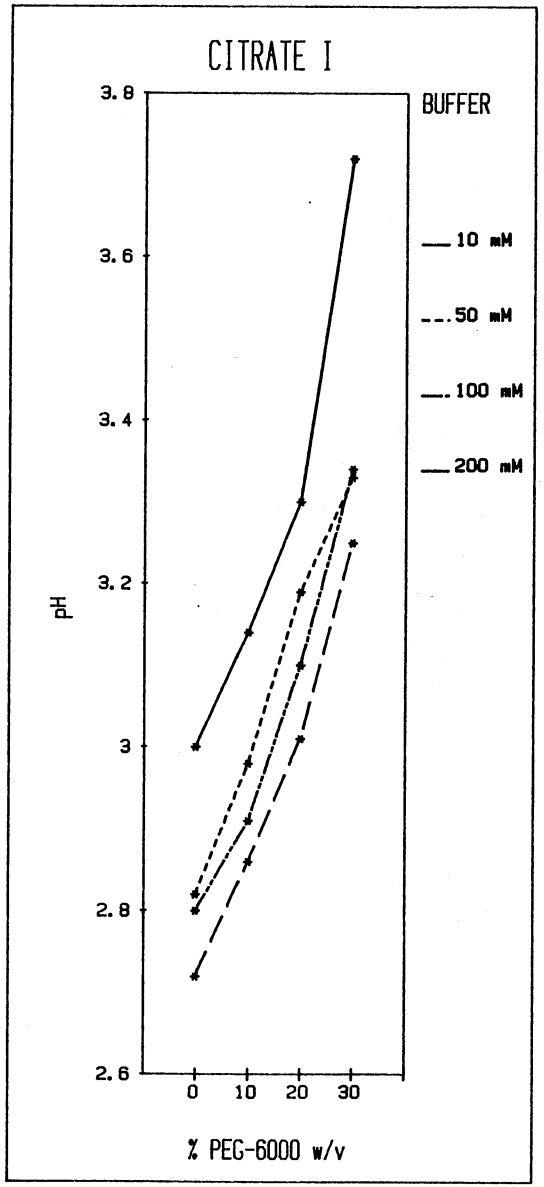
CITRATE I
BUFFER
10 mM
50 mM
100 mM
200 mM
pH
3.8
3.6
3.4
3.2
3
2.8
2.6
0
10
20
30
% PEG-6000 w/v

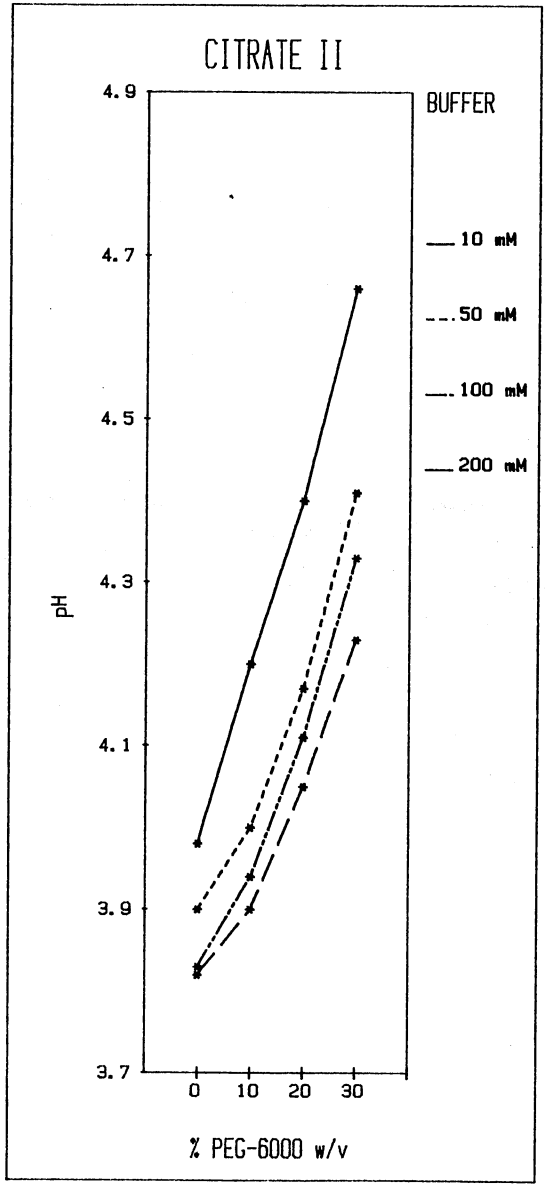
CITRATE II
BUFFER
10 mM
50 mM
100 mM
200 mM
pH
4.9
4.7
4.5
4.3
4.1
3.9
3.7
0
10
20
30
% PEG-6000 w/v

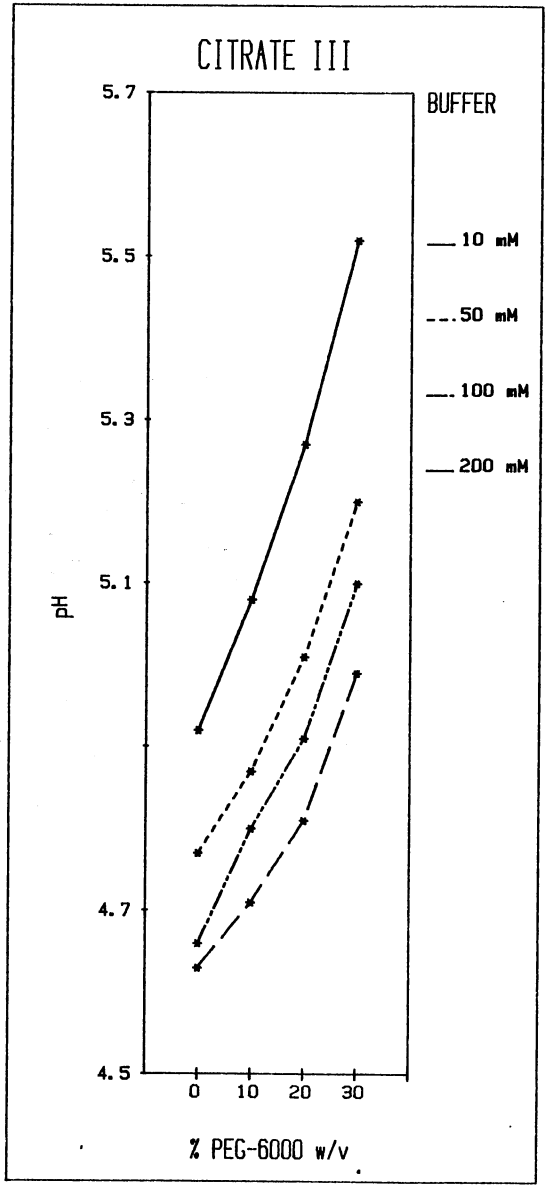
CITRATE III
BUFFER
10 mM
50 mM
100 mM
200 mM
pH
5.7
5.5
5.3
5.1
4.7
4.5
0
10
20
30
% PEG-6000 w/v

of adjusting the pH of many different samples, or (as may happen in some cases) ignoring the affect of such pH changes and the accompanying changes in ionic strength. However, since both of these conditions can strongly effect the properties of PEG-protein solutions, it is important to use appropriate controls or avoid these PEG-buffer effects.

APPENDIX B

KINEMATIC VISCOSITIES OF POLYMERS

IN STANDARD MOPS BUFFER

TABLE VI

KINEMATIC VISCOSITIES OF POLYMERS
IN STANDARD MOPS BUFFER

[Polymer]	PEG-1000	PEG-6000	PEG-20000	BSA	9.4k dextran
0	1.58	1.58	1.58	1.58	1.58
1		1.97	2.21		
2		2.42	3.15		
2.5				1.75	
3		2.94	4.35		
4		3.55	5.93		
5	2.22	4.27	7.88	1.96	2.47
6		5.01	10.58		
7		5.83	13.29		
8		6.90	17.29		
9			21.94		
10	3.03	9.02	28.13	2.58	3.95
12	3.43				
14	3.88				
15		17.25			6.39
16	4.39				
18	4.96				
20	5.75	30.12			10.26

Viscosities are in centipoise.

APPENDIX C

DETERMINATION OF R_e FOR PEG-6000

When calculating the excluded volume effect of PEG-6000 on GDH, we need to know the molecular dimensions of both GDH and the PEG. The dimensions of GDH in solution are well established. However, some difficulties arise in measuring the dimensions of PEG. Since PEG is a random coil polymer, its dimensions are a function of a number of factors including the nature of the solvent and temperature. It is therefore important to measure the dimensions of the polymer in the system to be studied.

A random coil polymer molecule at sufficiently dilute concentration may be treated as an equivalent hard sphere with radius R_e. The value of R_e depends on the experimental technique used to study the polymer. In the case of transport methods, however, the relationship of these different R_e's to the polymer's radius of gyration, R_G, are known. R_e is equal to kR_G, where k is a constant dependent on the transport method used. The best theoretical estimates for values of k for several different transport methods are summarized in Table VII.

It is important to distinguish between the R_e's measured by transport processes and those measured by equilibrium methods. Let us first consider transport processes. PEG is a random coil in which, for hydrodynamic purposes, the solvent in the very interior of the coil is presumed to be trapped and indistinguishable from solvent inherently

TABLE VII

Calculated Values of R_e

Calculated From	Experimental Method	Symbol	k (R_e/R_G)	Dependence on MW	R_e (nm)	R_G (nm)
Intrinsic Viscosity [η]	viscosity Increments	$R_{e,\eta}$	0.875	$M^{1/3}$	3.04	3.47
Frictional Coefficient f	Sedimentation Velocitiy	$R_{e,f}$	0.665	M	1.94	2.92
Second Virial Coefficient B	Light Scattering	R_e^*	0.85	$M^{2/3}$	2.94	3.46

bound to the polymer. Solvent which lies further away from the center of the polymer coil (e.g., outside the radius of gyration) becomes progressively less restricted as the segment density decreases. The polymer and trapped solvent may be treated as a hard sphere with an equivalent radius R_e, where R_e reflects the physical dimensions of the polymer molecule (49). However, the concept of an equivalent sphere in the treatment of equilibrium processes is somewhat different and more complex (28). Let us refer to the radius of this sphere as R_e^*. R_e^* represents the radius of a spherical volume from which other polymer molecules are excluded by the presence of a first molecule. In an equilibrium measurement, this "physical excluded volume" causes the second virial coefficient B to become positive, where B = 0 for an ideal solution. Thus the physical exluded volume and R_e^* are simply calculated from the B value obtained from a thermodynamic equilibrium measurement if no other factors are contributing to the B coefficient (50). In this case, $R_e^* = 0.85\ R_G$ for a polymer with a random distribution of segments. However, interactions between polymer segments, relative to segment-segment interactions can also contribute to B and give thermodynamically "effective excluded volumes" and effective R_e^* values considerably different from the physical values, especially if the solvent is a "poor" one for the polymer (28). The second virial coefficient may be measured from the dependence of such properties as osmotic pressure and light scattering intensity on the concentration of the polymer.

In our treatment of the excluded volume effect due to PEG on GDH, we feel that R_e is a better approximation of the physical dimensions of the polymer than is R_e^*, since R_e^* reflects polymer-polymer interactions

that may not be functions of molecular size. However, both values are in good agreement for this system (see Table VII).

Intrinsic Viscosity

It has been shown that the intrinsic viscosity, $[\eta]$, is related to R_e by Equation 1 (51).

$$[\eta] = 10\pi N_A (R_{e,\eta})^3/(3M_w) \quad (1)$$

where N_A is Avagodro's number, and

M_w is the weight-average molecular weight.

By simple rearrangement we get

$$R_{e,\eta} = \langle 3[\eta]M_w/(10\pi N_A)\rangle^{1/3} \quad (2)$$

The viscosity data in Appendix B which were used to correct sedimentation velocity values were also used to calculate $[\eta]$. For the measured value of $[\eta]$=22.2 g/cc and the reported M_w value of 8000 for PEG-6000 (52), R_e was calculated to be 3.04 nm from Equation 2.

Diffusion Coefficient

As discussed in Appendix E, dynamic light scattering (DLS) may be used to determine the diffusion coefficient of a macromolecule. The property actually measured, Γ, is related to D by the following equation:

$$\Gamma = q^2 D \quad (3)$$

where q is the scattering vector (see p. 80).

$$D = K_B T/f \quad (4)$$

where K_B is Boltzmann constant,

T is the temperature in degrees K, and

f is the frictional coefficient for the polymer.

We also know that, for flexible polymers,

$$f = 6\pi\eta R_{e,f} \tag{5}$$

where η is the kinematic viscosity of the solution.

By substituting 5 into 4 and rearranging, we find that D is related to R_e as follows:

$$R_{e,f} = K_B T/6\pi\eta D \tag{6}$$

However, Γ may reflect properties of the macromolecule other than translational diffusion. Γ was 20800, 20300, and 23600 for 1%, 2%, and 3% PEG at 5^o in standard MOPS buffer using an incident beam with a wavelength of 5145 A. The viscosity differences between the three solutions are very large. Therefore, the fact that the measured Γ values were nearly independent of η would lead one to believe that the property measured was not diffusion. Instead, it is probably motion of the segments in the polymer. This would depend on the microscopic viscosity in the area immediately surrounding the polymer, which is relatively independent of the macroscopic change in viscosity that occurs as the polymer concentration is raised. Therefore, we have not calculated R_e from DLS data.

Sedimentation Velocity

The equation for sedimentation velocity is

$$s = M_w(1-\bar{v}\rho)/(N_A f) \tag{7}$$

where $\bar{v}$ is the partial specific volume of the polymer, and

ρ is the solvent density.

By substituting in the known relationship for f,

$$s = M_w(1-\bar{v}\rho)/(N_A 6\pi\eta R_{e,f}) \tag{8}$$

where η is now the true viscosity instead of the kinematic viscosity. By simple rearrangement we get

$$R_{e,f} = M_w(1-\bar{v}\rho)/(N_A 6\pi s_{20,w}) \quad (9)$$

Polson (53) has found the $s_{20,w}$ of 6000 M_w PEG equals 0.49 S. The value of $\bar{v}$ is 0.837. Therefore $R_{e,f}$ is 1.76 nm.

Polson's measurements were made on PEG having a M_w of 6000, in contrast to my measurements on PEG-6000 which has a M_w of 8000 (52). PEG's under a molecular weight of 20000 show very little dispersity, so that all molecular weight averages are very similiar. Thus the $s_{20,w}$ of PEG-6000 can be estimated from the $s_{20,w}$ of Polson's measurements from the approximation

$$s_2 = s_1(M_2/M_1)^{2/3} \quad (10)$$

This gives an estimated value of 0.59 S for PEG-6000, or $R_{e,f}$ equal to 1.94 nm. This is equivalent to an $R_{e,\eta}$ of 2.55 nm. While such a value is somewhat less than the comparable value actually calculated from viscosity increments, it still is in rather good agreement.

Static Light Scattering (Second Virial Coefficient)

Light scattering data is often analyzed by the equation

$$Kc/R_\theta = 1/M_w + 2Bc + 3Dc^2 + \ldots \quad (11)$$

where K is a well-known collection of universal and system constants,

c is the solute concentration in g/l,

R_θ is Rayleigh's ratio at angle θ, and

B and D are the 2nd and 3rd virial coefficients, respectively.

The light scattering intensity of 1%, 2%, and 3% PEG-6000 in standard MOPS buffer at 5 deg was found to be independent of angle and concentration of PEG. $10^6/R_\theta$ was 9.04, 8.02, and 8.34 for 1%, 2%, and

3% PEG solutions, respectively. For such concentration independence, one might think that the 2nd term in equation 3 predominates; that is,

$$Kc/R_\theta = 2Bc \tag{12}$$

By simple rearrangement

$$B = K/(2R_\theta) \tag{13}$$

Using a light source with a wavelength of 632.8 nm, an angle of observation of 90^o, and the known refractive index increment of PEG of 0.137, K is equal to 6.79×10^{-8} for our measurements (25). The average value of B calculated from K and the measured values for R_θ for the three PEG solutions is 4.0×10^{-3}. This compares favorably with the values of 4.0×10^{-3} determined by Alexandrowicz (52) through combined osmotic pressure and light scattering studies, and $4.7 \pm 0.5 \times 10^{-3}$ by Ogston (25) using sedimentation equilibrium. K/R_θ for all three PEG solutions which we studied was approximately 8.0×10^{-3}. This is very close to the value extrapolated to zero PEG concentration by Alexandrowicz (9.9×10^{-3}), although it does not explain the lack of polymer concentration dependence. For a solution in which long range attractive and repulsive forces may be ignored, excluded volume dictates the magnitude of B from which it has been shown (50) that

$$B = 16\pi N_A (R_e^*)^3/(3M_w^2) \tag{14}$$

This yields a value of 2.94 nm for R_e^*, in excellent agreement with $R_{e,\eta}$.

However there is a major difficulty with the above treatment of the light scattering data. To determine B in this fashion requires other terms in the virial expansion to be negligible (either individually or as an algebraic sum). If we assume that $1/M_w$ is no more than 20% of Bc for c = 10 g/l, then M_w must be at least 125000. Plots of Kc/R_{90} vs. c

(Equation 11) by Alexandrowicz were nonlinear for PEG concentrations less than 50 g/l. He obtained a value of 30,000 by extrapolation along the linear portion of the curve corresponding to higher concentrations, and a value of 8000 from the intercept extrapolated from values below 50 g/l PEG. The concentration of my PEG samples fell in this lower range. However, Alexandrowicz's experiments were performed at room temperature, where PEG-PEG interactions seem to be less than those at lower temperatures. In any case the aberrant light scattering behavior of PEG observed here is not without precedent. In fact, excluded volume theory predicts that self-association of the polymer would be favored at higher polymer concentrations. The PEG may be acting as if it were of much higher molecular weight than one would normally assume. Alternatively contributions from higher order terms in the virial expansion may account for the odd behavior. Unfortunately M_w appears in all equations used to calculate the various values of R_e. Therefore it is important to accurately measure M_w by a less ambiguous method.

The molecular weight of the polymer can be calculated from its sedimentation and diffusion coefficients by the use of the following equation:

$$M = (s_o RT)/[D_o(1-\bar{v}\rho)] \qquad (15)$$

From the estimate of s_o=0.59 from above, the literature value of 10.4×10^{-7} cm^2/s for D_0 for PEG with a molecular weight of 8800 (54), and the known values for the other constants, M is 8500. This is very close to the value of 8000 used throughout this thesis. Therefore, the behavior observed with static light scattering is most likely due to contributions from higher order virial terms for the PEG solution rather than polymer associaion alone. Physically these virial terms may

reflect the combination of changes in polymer conformation and intermolecular interactions that occur as the polymer concentration increases. Since a significant overlap of polymer segments between different polymer molecules might occur with PEG concentrations as low as 2%, such a combination of effects are not unreasonable. Furthermore, increased intermolecular interactions might lead to thermodynamically compensating changes in polymer conformations under these conditions. For example, extensive polymer segment overlap would be expected to greatly reduce the excluded volume that exists in the absence of this overlap (55).

Because of these uncertainties, we trust R_e values obtained from transport measurements more. A summary of the different values calculated for R_e and R_G by the different methods is given in Table VII. Values of R_G are included solely to provide an easy comparison of the results obtained from different experimental methods.

APPENDIX D

THE SOLUBILITY OF INDIVIDUAL ENZYME SPECIES IN A POLYMERIZING ENZYME AS PRECIPITATING CONDITIONS ARE ACHIEVED

We consider an "open-ended" polymerizing enzyme like GDH and assume: that association equilibria between all polymeric species are achieved; and that when the solution becomes saturated with enzyme, an equilibrium between solution and a single solid phase precipitate exists. If we slowly add enzyme to a solution starting with an initially low and totally soluble enzyme concentration, then the weight concentration of all GDH forms present increases. At some point the solution becomes saturated with respect to one of the species. It is very unlikely that more than one enzyme species would become saturated at the same time, since this would require two or more solubility conditions to be the same except for microscopic differences. This is unlikely because the concentration of each enzyme species is in general different as required by the distribution function (Equations (6) and (7), and Figure 17, pp.69-71). Addition of more enzyme results in the precipitation of the saturated species, leaving its concentration and therefore the concentration of all other enzyme species unchanged at equilibrium.

Even if PEG is present in the solution, the effect of incrementing GDH concentration is much the same. At some point, one GDH form reaches

the limits of its solubility. We then conclude, as stated on p. 31, that at fixed PEG concentrations only one enzyme species is at its solubility limit as total enzyme concentration is increased. Thus, in spite of the complexity of enzyme concentration dependent association, a classical single solubility limit should be achieved with such enzymes; i.e., its solubility should be independent of the total enzyme concentration.

Now let us consider what happens to GDH solubility as we move from low PEG concentrations to higher ones. With high PEG concentrations, the solubility limit with respect to the total concentration of GDH in solution is lower than in the absence of PEG. This is apparently for two reasons. The first reason is that PEG inherently lowers the solubility of proteins, especially for larger ones. Also, the addition of PEG shifts the association of GDH such that the concentration of the more polymerized enzyme forms is higher than the concentration of the same species would be in a solution in which PEG was absent. Hence the solubility limit of such an enzyme form is reached at a lower total concentration of GDH. At low PEG concentrations, the solubility of the enzyme is high enough to require high total enzyme concentrations for saturation of the solution. This causes the formation of large enzyme species, whose solubility in PEG is inherently much lower than that of small forms. The situation is quite different at high PEG concentrations. Here the concentration of GDH in the saturated enzyme solution is quite low, and is in fact too low to promote extensive polymerization of the enzyme. However, the PEG concentration is now high enough that these less polymerized forms now have low solubility limits. Equation 2, p. 28 was derived assuming only one protein species

in the solution phase. In general (and certainly so for excluded volume effects), the β coefficient in Equation 2 would be different for each different protein species that is in solution equilibrium. Since we expect different GDH enzyme species to become insoluble as PEG concentration is varied, we would not expect this enzyme to obey Equation 2. This is the conclusion made on p. 28.

We have also derived the above conclusion mathemetically. The above descriptions, however, are considered easier for the reader to follow. They also provide additional insight and intuition beyond what is readily obtained from the more formal mathematical proof.

APPENDIX E

METHODS OF ANALYSIS FOR DYNAMIC LIGHT SCATTERING DATA

Dynamic light scattering measurements monitor scattered light intensities from a small volume of sample illuminated with a laser beam. Sufficient time resolution is used to characterize the rates of fluctuations in the concentrations of the macromolecules in the small volume. These concentration fluctuations are characterized by corresponding fluctuations in the scattering intensity, I. Small molecules can diffuse more rapidly than larger ones. Thus concentration fluctuations (and the corresponding intensity fluctuations) of the smaller molecules in the volume element are more rapid. We may define an autocorrelation function, $g(\tau)$, which reflects how rapidly these intensity fluctuations occur. Let us consider the scattering intensity $I(t)$ at time time t and the intensity at some time $t+\tau$. The autocorrelation function of the scattering intensity is then defined as

$$g(\tau) = \lim_{T\to\infty} (1/T) \int_0^T i(t)i(t+\tau)dt \qquad (1)$$

where τ is the correlation time, and

T is the total time over which the correlation is calculated. Physically, the autocorrelation function represents how quickly the positions of the macromolecules become uncorrelated with (i.e., randomized with respect to) their positions at time = 0. For a single

macromolecular species the autocorrelation function is a single exponential with a decay constant

$$g^2(\tau) = 1 + ce^{-2q^2D\tau} \tag{2}$$

where $g^2(\tau)$ is the normalized autocorrelation function of the scattered light at time τ,

c is an experimental constant; $0<c<1$

q is the scattering wave vector (see p. 80), and

D is the particle translational diffusion coefficient.

For polydisperse solutions with distributions which are approximated well by continuous functions

$$g^2(\tau) = 1 + c[\int_0^\infty G(\Gamma)e^{-\Gamma\tau}d\Gamma]^2 \tag{3}$$

where $G(\Gamma)$ represents the distribution function of decay rates Γ. The value of Γ is equal to q^2D for a solution containing only one macromolecule undergoing diffusion.

The above integral has the form of a Laplace transform. Thus to describe $G(\Gamma)$ requires determining the Laplace inversion of the data. However, the inversion of an equation of this type is unstable; that is, a minor pertubation in the data can lead to large changes in the solution. If the form of $G(\Gamma)$ is known, then the inversion is often greatly simplified. Unfortunately in many cases this information is not available.

For this reason polydisperse solutions have been primarily analyzed by the method of cumulants, in which

$$\overline{\Gamma} = \int G(\Gamma)\Gamma d\Gamma \tag{4}$$

$$\mu_i = \int(\Gamma-\overline{\Gamma})^i G(\Gamma)d\Gamma \tag{5}$$

where $\overline{\Gamma}$ is the intensity weighted average of Γ, and

μ_i is the i^{th} moment of the distribution.

In this technique, $g^2(\tau)$ is fit to the equation

$$g^2(\tau) = 1+ce^{<-\Gamma\tau+\mu_2\tau^2/2! - \mu_3\tau^3/3! + (\mu_4-3\mu_2^2)\tau^4/4! + \ldots>} \quad (6)$$

Dynamic light scattering cannot provide data of sufficient quality to evaluate terms past μ_3.

A major drawback of the cumulant method of analysis is its inability to resolve much useful information about a bimodal distribution. Such a distribution was encountered in our studies on the effect of polymers on GDH self-association. For this reason the method of analysis developed by Pike et al (56) was chosen. $G(\Gamma)$ is approximated by the band-limited function, $\overline{G}(\Gamma)$. From this a new function, $\zeta(\ln \Gamma)$, is defined such that

$$\zeta(\ln \Gamma)\, d(\ln \Gamma) = \overline{G}(\Gamma)d\Gamma \quad (7)$$

This new function has the following properties:

1. $\zeta(\ln \Gamma)$ can only be known for points $\ln \Gamma_n$, $\ln \Gamma_{n+1}$, etc., separated by at least π/w_{max} where

$$w_{max} \simeq (2/\pi)\ \ln((\sqrt{\pi})/\text{noise}) \quad (8)$$

where noise is the sum of the squared deviations from the experimentally measured $g(\tau)$ and the ideal $g(\tau)$.

2. $\zeta(\ln \Gamma)$ can be reconstructed from these points by the following interpolation formula:

$$\zeta(\ln \Gamma) = \sum_{n=1}^{N} \zeta(\ln \Gamma_n)(a)(\sin b/b) \quad (9)$$

where $a = \sqrt{\ln(\Gamma/\Gamma_n)}$ and

$b = w_{max}a$

When actually fitting the data, values of $G(\Gamma)$ are measured at a spacing such that

$$G(\Gamma) = \sum_{n=1}^{N} a_n \sigma(\Gamma-\Gamma_n) \text{ with } \Gamma_n = \Gamma_1 \exp(n\pi/w_{max}) \tag{10}$$

where σ is the delta function.

The coefficients a_n are obtained by minimizing the function

$$[\sum_{j=1}^{m} \langle g^2(\tau)_j - (\sum_{n=1}^{N} a_n \exp(\Gamma_n \tau_j))^2 \rangle]^2 \tag{11}$$

with respect to the a_n's.

Sornette and Ostowsky[1] recommend using data over a wide range of correlation times (τ). Because of limitations inherent in the autocorrelor used, this required matching of data gathered using different values of the correlation time. Typically, 4 to 5 different data sets were fit simultaneously.

Data fitting was performed on a PDP 11/40 minicomputer using the program CORFIT written by this author. This program allows the selection of several functions to be fit, including a simple sum of exponentials, the cumulant method, the histogram method employed by Chu, and Pike's delta function method. Either heterodyned of homodyned data can be fit, as well as data containing a base line. The user has the option of employing either the Gauss-Newton or Marquardt method of weighted nonlinear least square parameter estimation.

---

[1] Personal communications.

APPENDIX F

DERIVATION OF ΔG_I, CHAPTER III

The open-ended association of GDH can be represented by

$$E_1 \overset{K_1 E_1}{\rightleftharpoons} E_2 \overset{K_1 E_1}{\rightleftharpoons} E_3 \cdots E_i \overset{K_1 E_1}{\rightleftharpoons} E_{i+1} \cdots E_n \qquad (1)$$

for n species. Species beyond E_n may be considered to exist at negligible concentrations. We shall consider the two conditions 1) GDH solution at equilibrium with a distribution of enzyme species $C_i(K_1)$ consistent with an association constant K_1, and 2) the same solution with GDH species at concentrations $C_i(K_2)$. Although this solution is not at equilibrium, $C_i(K_2)$ values are those that would exist at equilibrium if the association constant were K_2 instead of K_1. The solutions are considered ideal with sufficient accuracy. Then using subscripts 1 and 2 (e.g. $C_{i,2}$) to denote molar concentrations of each polymer species and corresponding chemical potentials μ_i for the conditions 1 and 2,

$$\Delta G_I = CF \sum_{i=1}^{n} [\mu_{i,2} C_{i,2} - \mu_{i,1} C_{i,1}] \qquad (2)$$

molar conc.

where $CF = MW_{mon}/c_t$, the ratio of monomer molecular weight to the total weight concentration of GDH.

Since $\mu_i = \mu_i^o + RT \ln C_i$, equation 2 becomes

$$\Delta G_I = CF \sum_{i=1}^{n} \mu_i^o (C_{i,2} - C_{i,1}) + CF \times RT \sum_{i=1}^{n} (C_{i,2} \ln C_{i,2} - C_{i,1} \ln C_{i,1}) \qquad (3)$$

$$= SST + CT$$

that is the sum of standard state terms SST and concentration terms CT. The standard state terms μ_i^o are independent of C_i and thus no second subscript is needed on them. The CT term can be calculated from equations 6 and 7, page 69, but we need to express the μ_i^o terms in SST as functions of known constants, including the association constant K_1 corresponding to the equilibrium distribution $C_{i,1}$. We start by rewriting SST as

$$SST = CF \sum_{i=1}^{n} \mu_i^o \Delta C_i \tag{4}$$

where $\Delta C_i = C_{i,2} - C_{i,1}$.

We eliminate ΔC_n from equation 4 by the relation

$$\Delta C_n = -\sum_{i=1}^{n-1} i\Delta C_i/n \tag{5}$$

which follows from the conservation equation, total concentration equals $\sum_{i=1}^{n} iC_i$. This procedure introduces differences, $\mu_i^o - \mu_n^o$, which we utilize below. Thus,

$$SST = CF\left[\sum_{i=1}^{n-1} (\mu_i^o \Delta C_i) - \mu_n^o \sum_{i=1}^{n-1} i\Delta C_i/n\right] \tag{6a}$$

$$SST = CF[(\mu_1^o - \mu_n^o/n)\Delta C_1 + (\mu_2^o - 2\mu_n^o/n)\Delta C_2 + \ldots +$$

$$(\mu_{n-1}^o - (n-1)\mu_n^o/n)\Delta C_{n-1}] \tag{6b}$$

The general term in equation 6 is

$$T_i = (\mu_i^o - i\mu_n^o/n)\Delta C_i \tag{7}$$

Next we express all μ_i as functions of μ_1 and $RT\ln K_1 = \rho$. This is done by equating the free energies of products and reactants in equation 1. That is,

$$\mu_2 = \mu_1 + \mu_1, \text{ which gives}$$

$$\mu_2^o = 2\mu_1^o - \rho \tag{8}$$

and

$$\mu_3 = \mu_2 + \mu_1, \text{ which gives}$$

$$\mu_3^o = \mu_2^o + \mu_1^o - \rho, \text{ which from equation 8 gives}$$

$$\mu_3^o = 3\mu_1^o - 2\rho$$

In this way, the general term can be shown to be

$$\mu_i^o = i\mu_1^o - (i-1)\rho \tag{9}$$

Elimination of μ_i^o and μ_n^o from equation 7 by means of equation 9 gives

$$T_i = (RT\ln K_1)\Delta C_i(n-i)/n \tag{10}$$

Summation of these terms gives

$$SST = CF(RT\ln K_1)\sum_{i=1}^{n-1}(n-i)\Delta C_i/n \tag{11}$$

from which we can write equation 3 as

$$\Delta G_I = RT[\ln K_1(\sum_{i=1}^{n-1}(n-i)\Delta C_i/n) + \sum_{i=1}^{n}(C_{i,2}\ln C_{i,2} - C_{i,1}\ln C_{i,1})]MW_{mon}/c_t \tag{12}$$

Equation 12 is the working equation used in the section referencing this appendix.

APPENDIX G

DERIVATION OF THE RATE EQUATION DESCRIBING THE OXIDATION OF NADH BY GDH ASSUMING THREE DIFFERENT ENZYMATICALLY ACTIVE FORMS

Let us begin with equation 46 of Chapter III describing the depolymerization of GDH upon the addition of GDP:

$$E_m \xrightarrow[GDP]{NADH} E_m' \xrightarrow{k_1} E_n \xrightarrow{k_2} E_p \qquad (1)$$

where the nature of the individual enzyme forms has been discussed in the body of the text. Since the interconversion of E_m to E_m' is so rapid, we may ignore this step. Then, if we allow for potentially different kinetic properties for each of the remaining enzyme forms (E_m', E_n, and E_p), we can model the overall reaction for the oxidation of NADH to NAD^+ by the following scheme:

$$\begin{array}{ccccc} E_m' + A & \overset{K_{a1}}{\rightleftharpoons} & E_m'A & \xrightarrow{k_{r11}} & E_m' + P \\ \downarrow k_1 & & & & \\ E_n + A & \overset{K_{a2}}{\rightleftharpoons} & E_nA & \xrightarrow{k_{r12}} & E_n + P \\ \downarrow k_2 & & & & \\ E_p + A & \overset{K_{a3}}{\rightleftharpoons} & E_pA & \xrightarrow{k_{r13}} & E_p + P \end{array} \qquad (2)$$

where the E's are the previouly mentioned GDH forms,

A is the substrate NADH,

P is the product NAD^+,

K_{ai} is the Michaelis constant for the substrate A with respect to E_i, and

k_{rli} is the first-order rate constant for the rate limiting step in the release of P from E_i.

Such a model allows for, but does not require, different kinetic properties for each of the three forms. The model ignores back flux from P. Since the GDH reaction is highly irreversible in the direction shown and with the experimental conditions used, the model should be adequate for most of the progress curve.

Let us consider the concentrations of the various enzyme forms as a function of time, assuming that at time zero all of the enzyme is in form E_m'. Let us equate E_0 to the initial concentration of E_m'. Assuming first order kinetics for both depolymerization steps of the enzyme as found experimentally, the concentrations of E_m', E_n, and E_p as a function of time are given by the following equations describing consecutive first order reactions (57):

$$E_m' = E_0 e^{-k_1 t} \tag{3}$$

$$E_n = E_0 k_1 (e^{-k_1 t} - e^{-k_2 t})(k_2 - k_1) \tag{4}$$

$$E_p = E_0 [1 + (k_2 e^{-k_1 t} - k_1 e^{-k_2 t})/(k_1 - k_2)] \tag{5}$$

These simplify greatly if, as expected, $k_1 >> k_2$. Then the concentrations of the respective enzyme forms are given by

$$E_m' = E_0 e^{-k_1 t} \tag{6}$$

$$E_n = E_0 (e^{k_2 t} - e^{-k_1 t}) \tag{7}$$

$$E_p = E_0 (1 - e^{-k_2 t}) \tag{8}$$

For each of the enzyme forms E_i the rate of product formation $(dP/dt)_i$ is given by

$$(dP/dt)_i = k_{r1i}E_iA/(K_{ai}+A) \quad (9)$$

The overall reaction rate is the sum of the rates for each individual form. Therefore, from Equations 6 through 9, we get the rate equation for the conversion of NADH to NAD^+:

$$dP/dt = k_{r11}E_tAe^{-k_1t}/(K_{a1}+A) + k_{r12}E_tA(1-e^{-k_1t})/(K_{a2}+A) + k_{r13}E_tA(1-e^{-k_2t})/(K_{a3}+A) \quad (10)$$

VITA 2

James Richard Appleman

Candidate for the Degree of

Doctor of Philosophy

Thesis: EFFECT OF POLYMERS ON PHYSICAL AND KINETIC PROPERTIES OF GLUTAMATE DEHYDROGENASE FROM BOVINE LIVER

Major Field: Biochemistry

Biographical:

Personal Data: Born in Woodward, Oklahoma, September 21, 1956, the son of Dr. and Mrs. R. E. Appleman.

Education: Graduated from Tonkawa High School, Tonkawa, Oklahoma, in May, 1974; received the Associate of Science degree from Northern Oklahoma College in 1975; received the Bachelor of Science degree from Oklahoma State University in 1978; completed requirements for the Doctor of Philosophy degree at Oklahoma State University in July, 1983.

Professional Experience: Graduate research assistant, Department of Biochemistry, Oklahoma State University, 1978-1983; graduate teaching assistant, Department of Biochemistry, Oklahoma State University, 1980.